LEMING

Progress report

A. Antognini[*], E. Dourassova[‡], K. Kirch[*], D. Goeldi,
A. Soter[†], D. Taqqu, R. Waddy[‡], P. Wegmann[‡], V. Vojtech[§], J. Zhang[‡]
Institute for Particle Physics and Astrophysics, ETH Zurich, 8093 Zurich, Switzerland

M. Bartkowiak, K. Jefimovs, A. Knecht, G. Lospalluto[‡], R. Scheuermann
Paul Scherrer Institute, 5232 Villigen-PSI, Switzerland

F. Wauters
Johannes Gutenberg University of Mainz, 55122 Mainz, Germany

Muonium - probing the SM and beyond

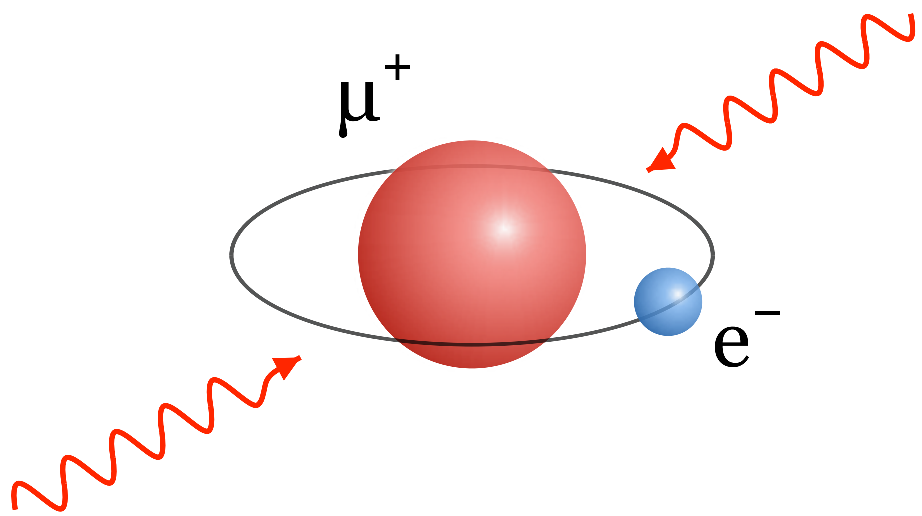

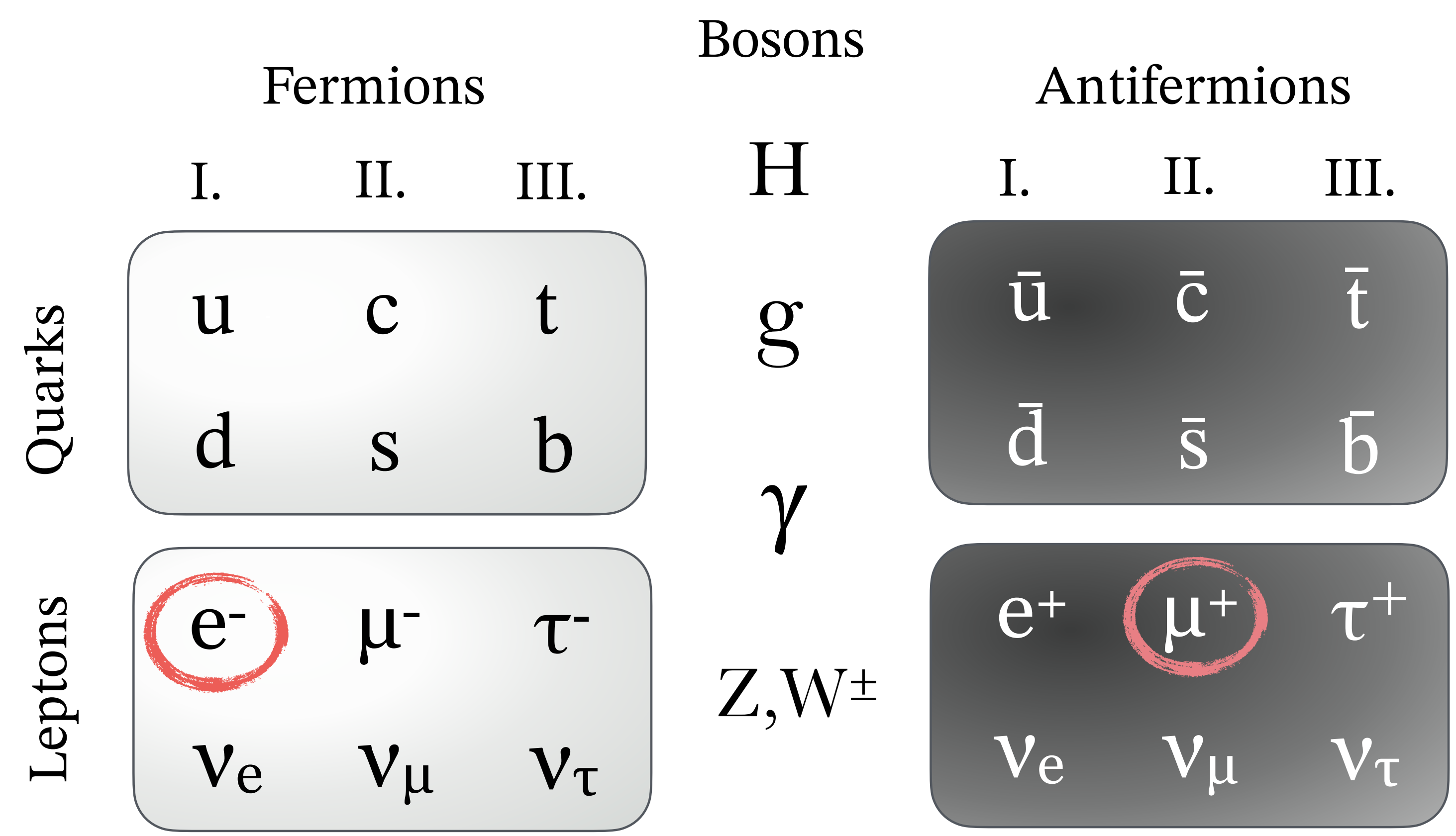

Laser Spectroscopy

Purely **leptonic** exotic atom, dominated by QED effects:

- Fundamental constants (m_μ , μ_μ , R_∞)
- Test of bound-state QED & symmetries (q_μ / q_e)
- Effects on other precision experiments, e.g. muon *g-2*

$$E(1s-2s) \simeq \frac{3}{4} q_e q_\mu R_\infty \left(1 - \frac{m_e}{m_\mu}\right) + \mathrm{QED} + \ldots$$

Muonium - probing the SM and beyond

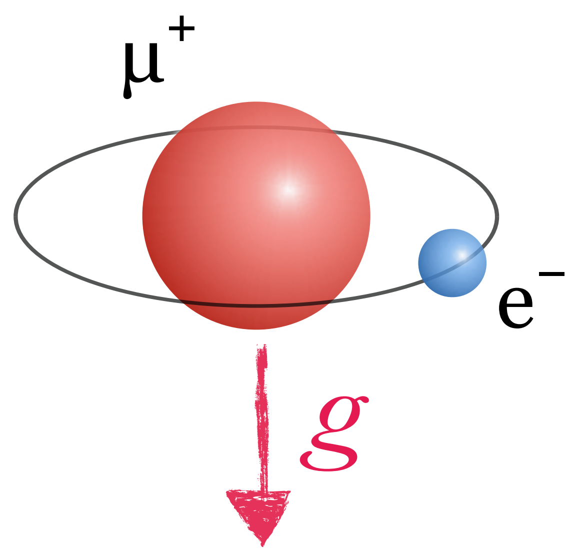

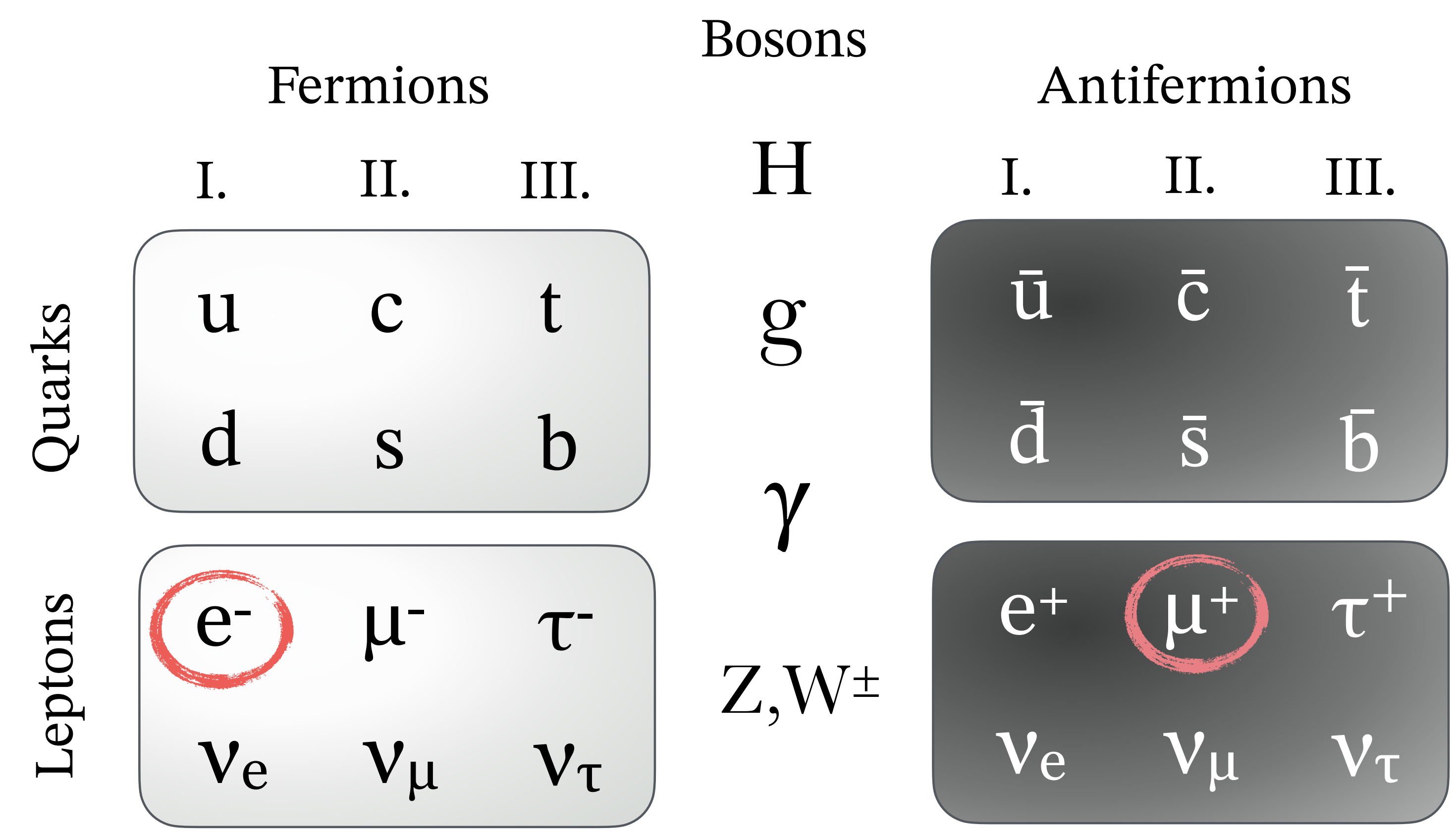

Free fall of Mu

Test of the Weak Equivalence Principle by measuring the coupling of gravity to:

- **fundamental parameters** of SM, in the absence of masses generated by the strong interaction
- **second generation** (anti)fermions of the SM - only possible probe of this sector

Muonium - probing the SM and beyond

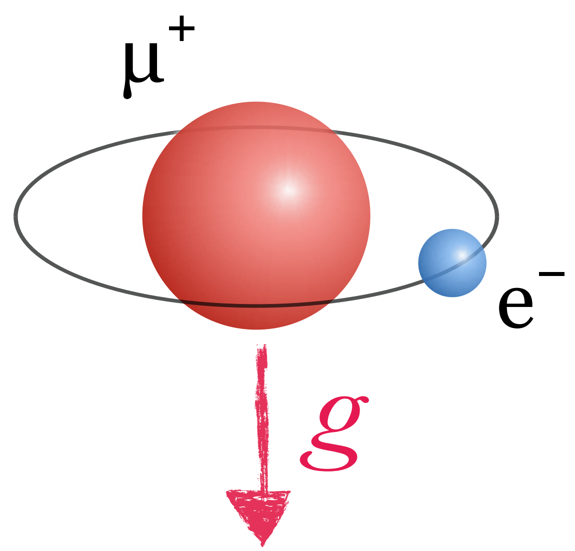

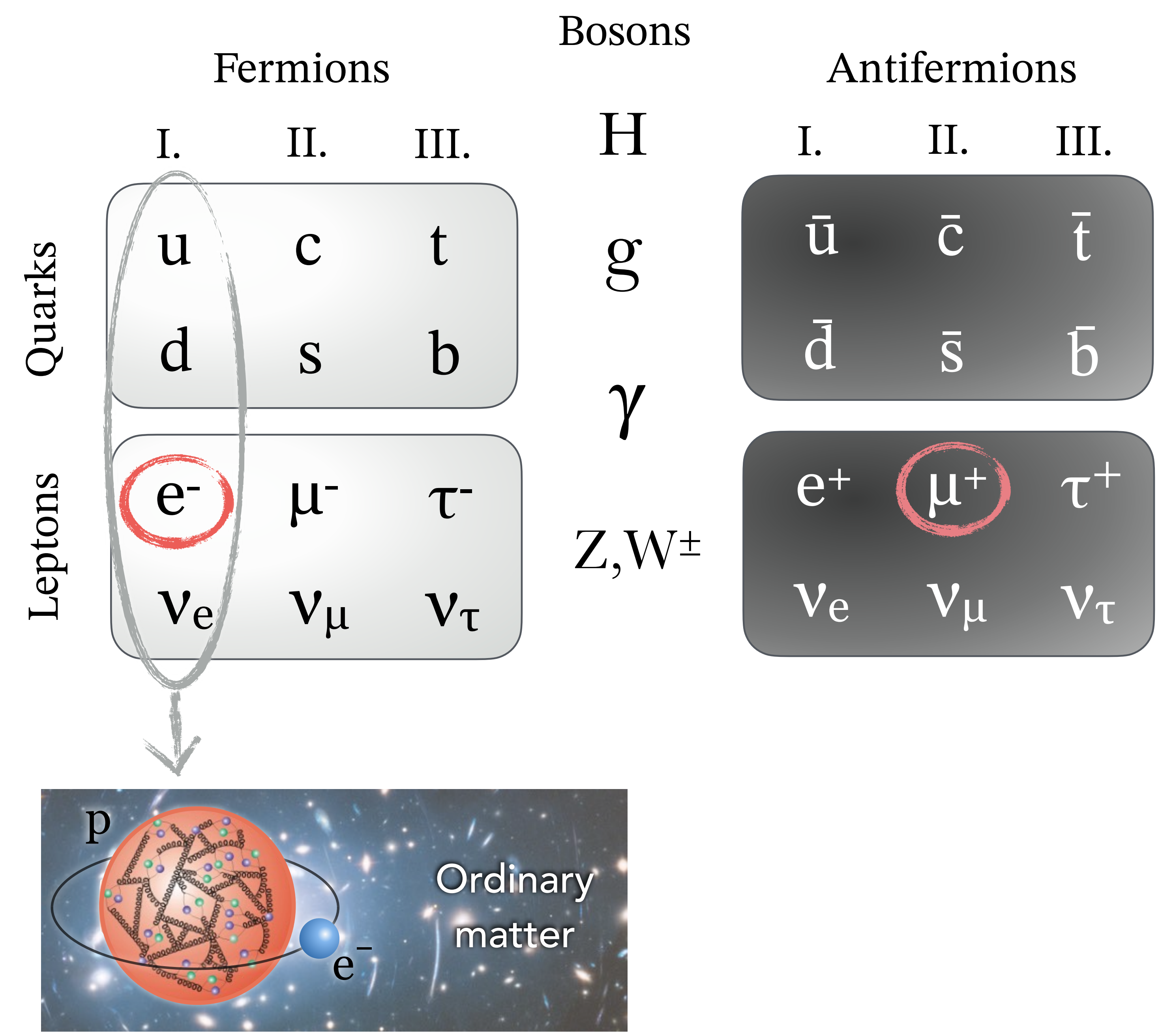

Free fall of Mu

Test of the Weak Equivalence Principle by measuring the coupling of gravity to:

- **fundamental parameters** of SM, in the absence of masses generated by the strong interaction
- **second generation** (anti)fermions of the SM - only possible probe of this sector

Muonium - probing the SM and beyond

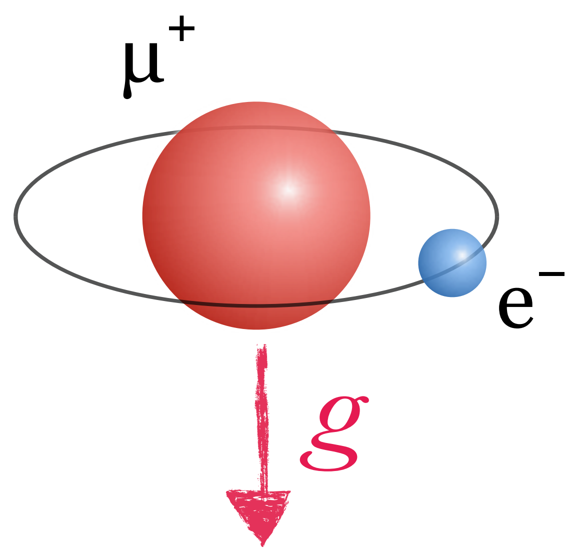

Free fall of Mu

Test of the Weak Equivalence Principle by measuring the coupling of gravity to:

- **fundamental parameters** of SM, in the absence of masses generated by the strong interaction
- **second generation** (anti)fermions of the SM - only possible probe of this sector

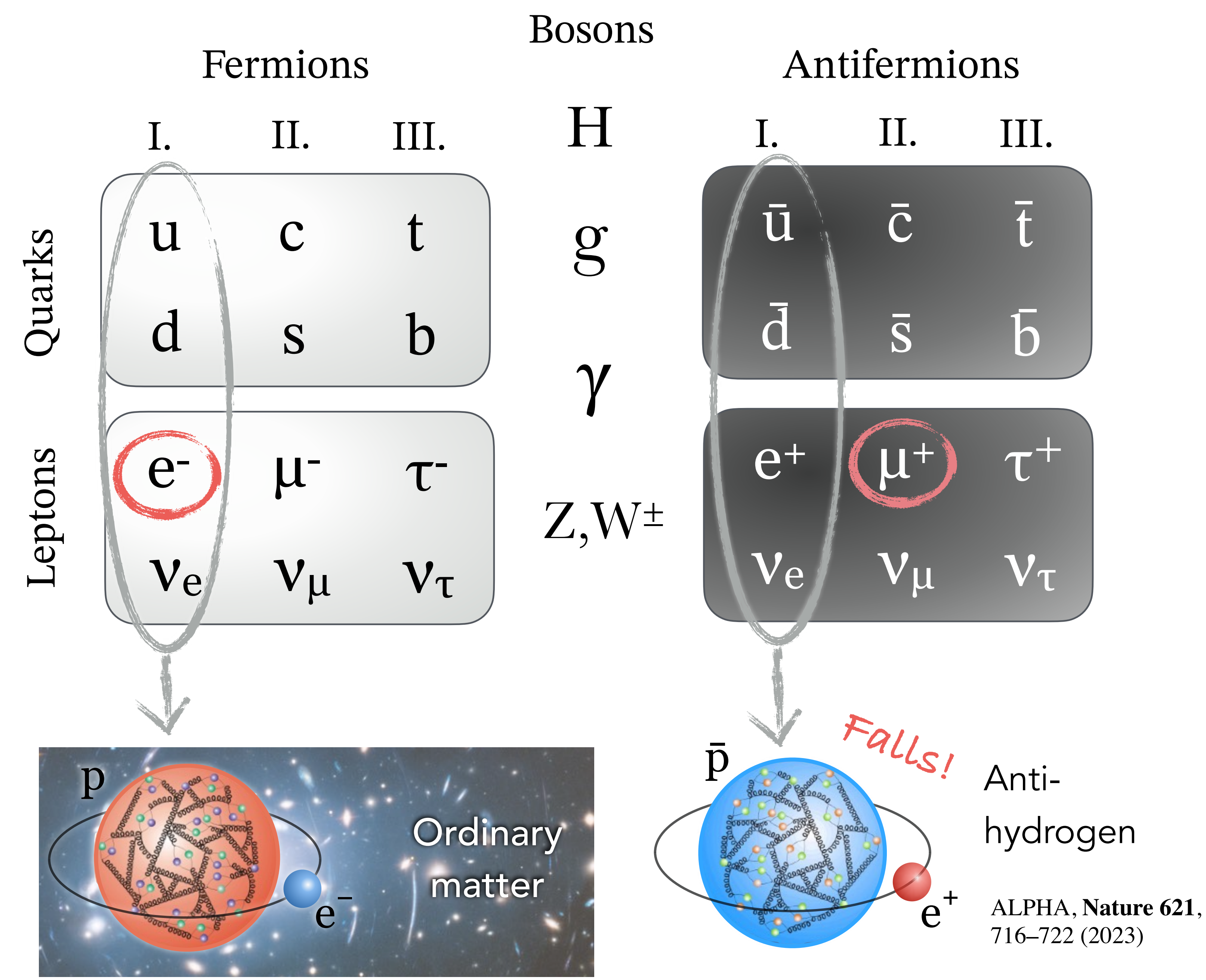

Muonium - probing the SM and beyond

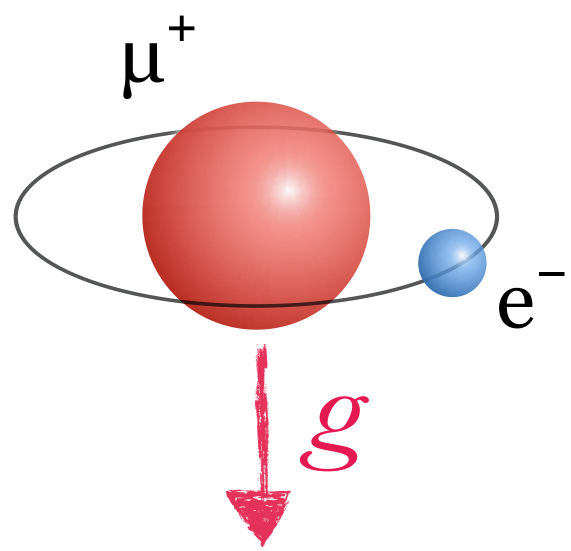

Free fall of Mu

Test of the Weak Equivalence Principle by measuring the coupling of gravity to:

- **fundamental parameters** of SM, in the absence of masses generated by the strong interaction
- **second generation** (anti)fermions of the SM - only possible probe of this sector

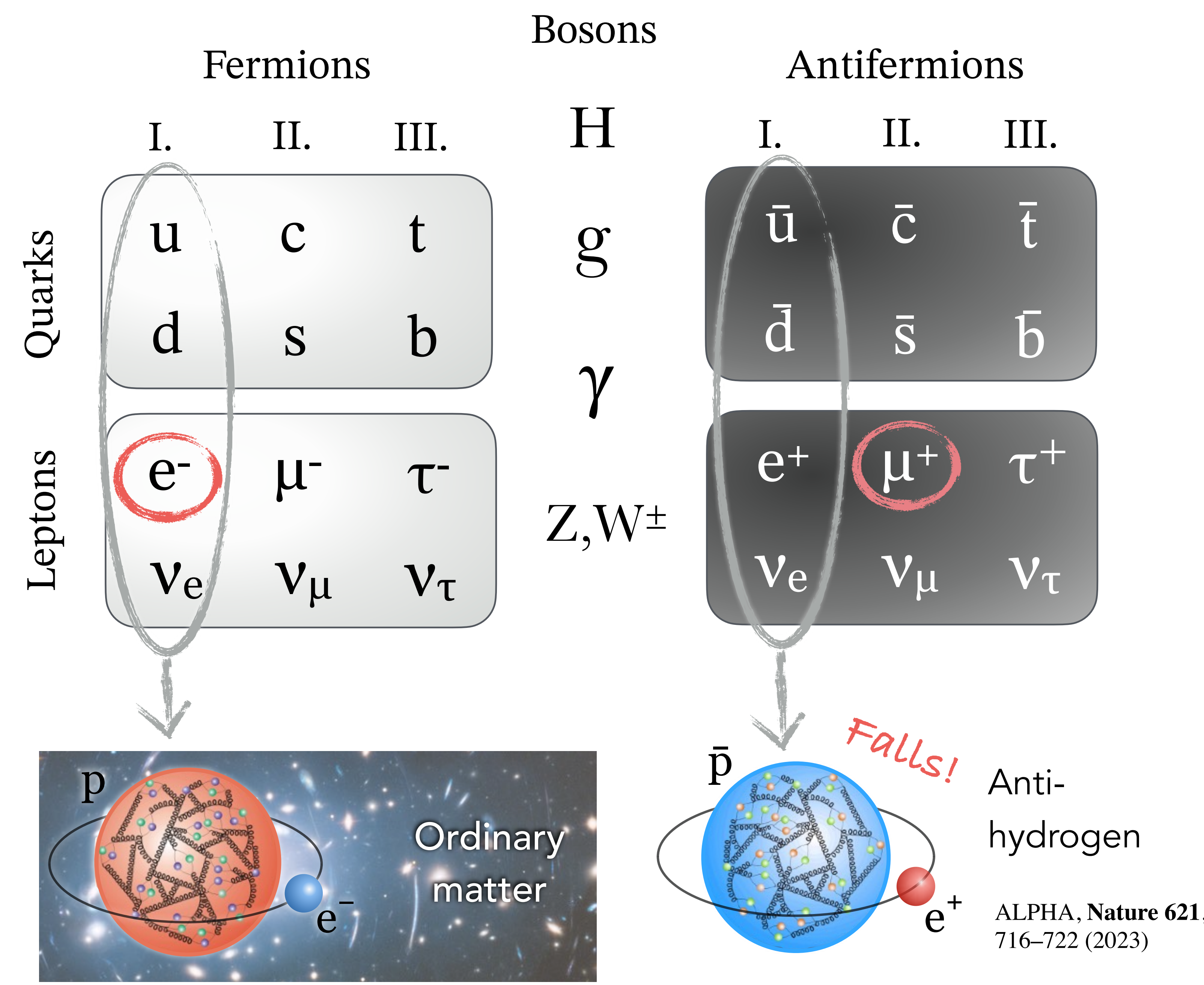

Hadron mass

~1% valence quark
99% strong interaction

Muonium mass

Binding E

μ^+ mass: 105.6583745(24) MeV/c
e^- mass: 0.5109989461(31) MeV/c²

Muonium - probing the SM and beyond

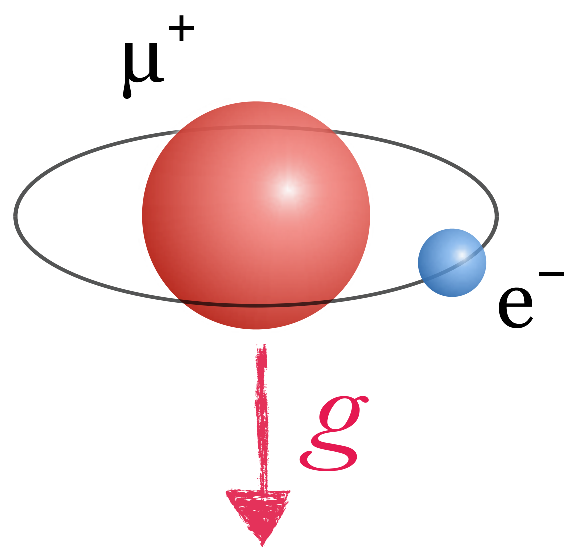

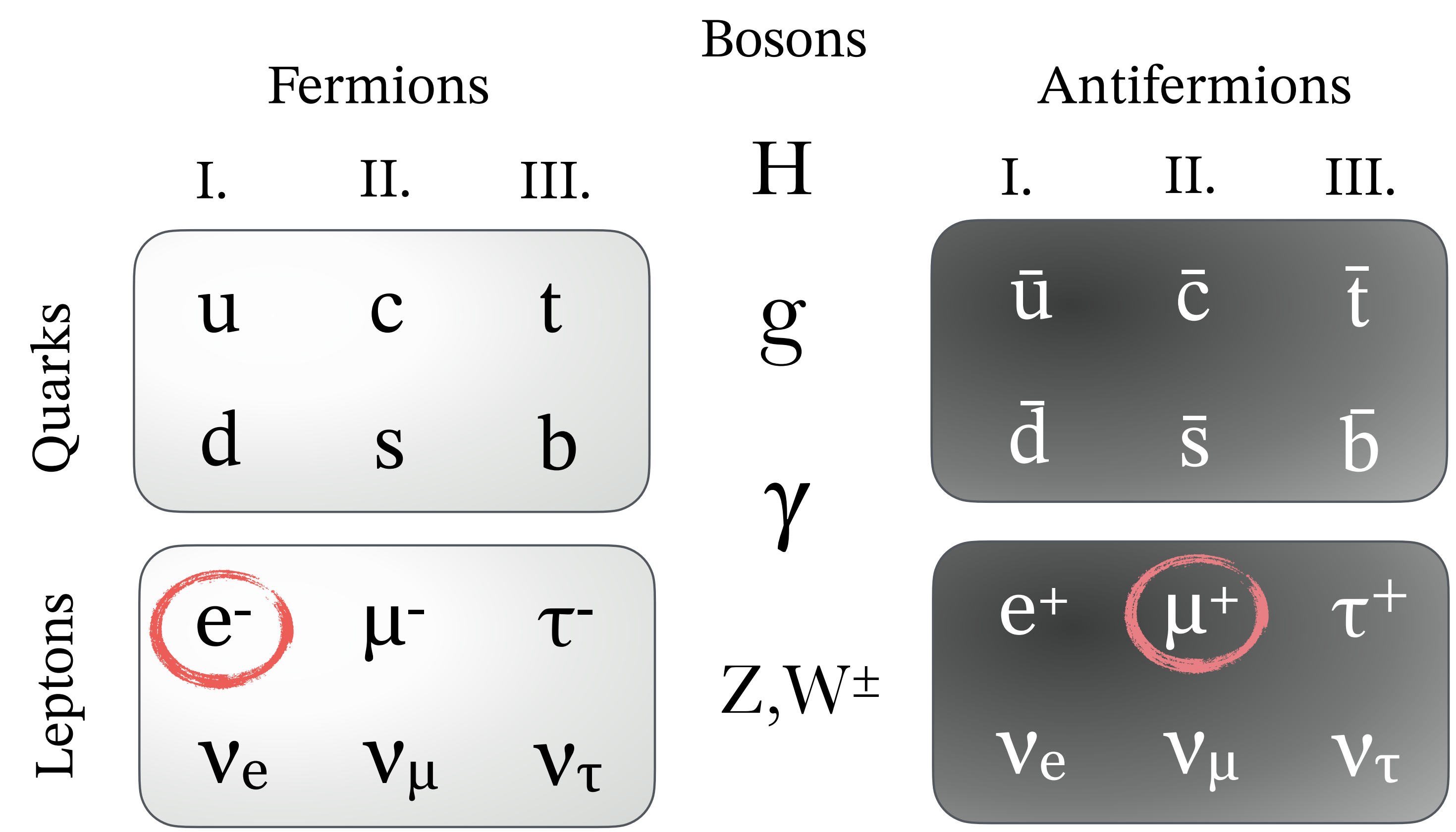

Free fall of Mu

Test of the Weak Equivalence Principle by measuring the coupling of gravity to:

- **fundamental parameters** of SM, in the absence of masses generated by the strong interaction
- **second generation** (anti)fermions of the SM - only possible probe of this sector

- Possibility to test for flavour-dependent new interactions

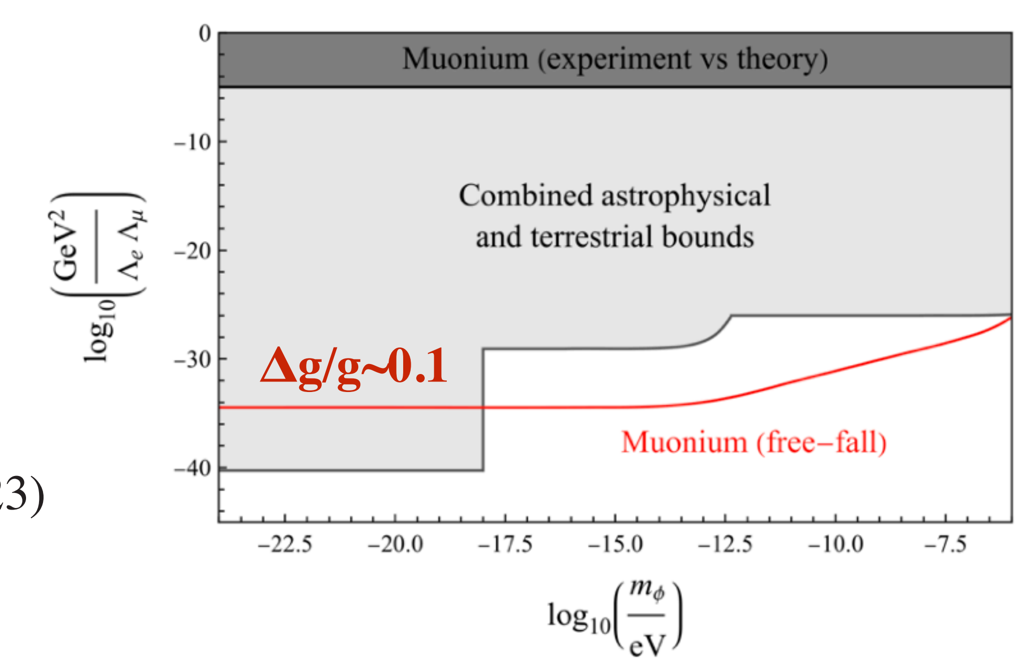

Y. Stadnik PRL 131, 011001 (2023)

The challenges of measuring Mu gravity

Not possible with conventional Mu sources

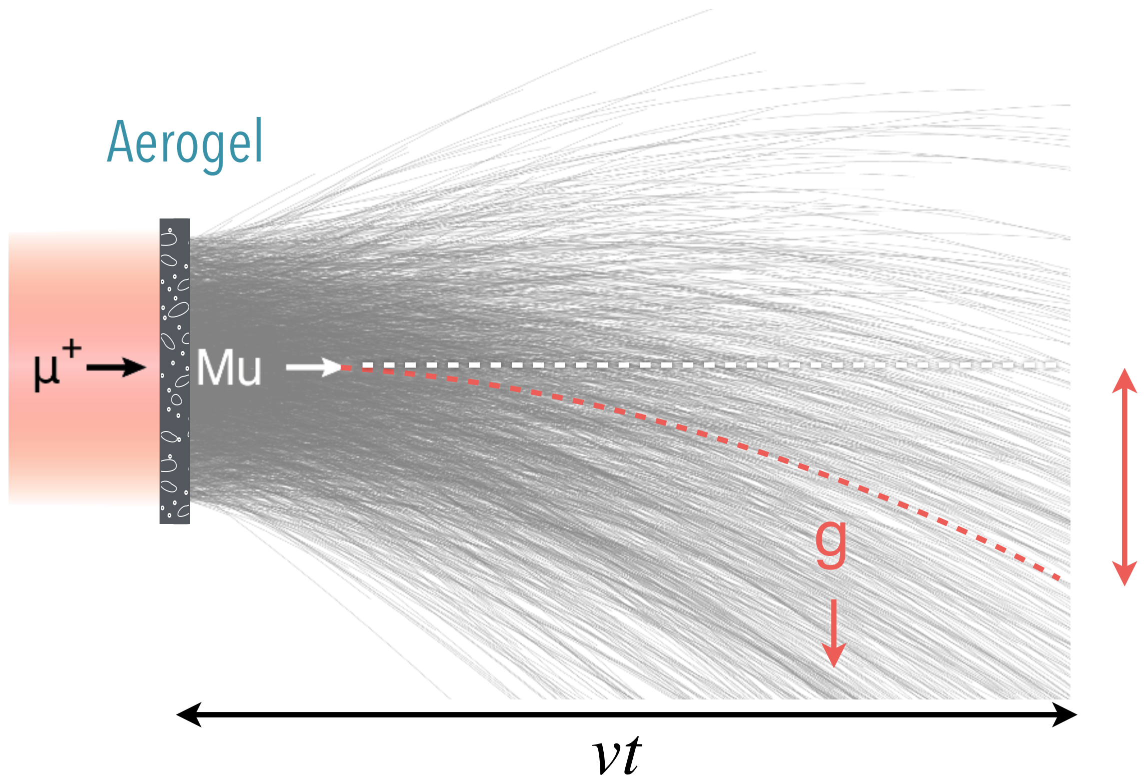

Mu lifetime of 2.2 μs

$$\Delta x = \frac{1}{2} g t^2 < 1 \text{ nm}$$

The challenges of measuring Mu gravity

Not possible with conventional Mu sources

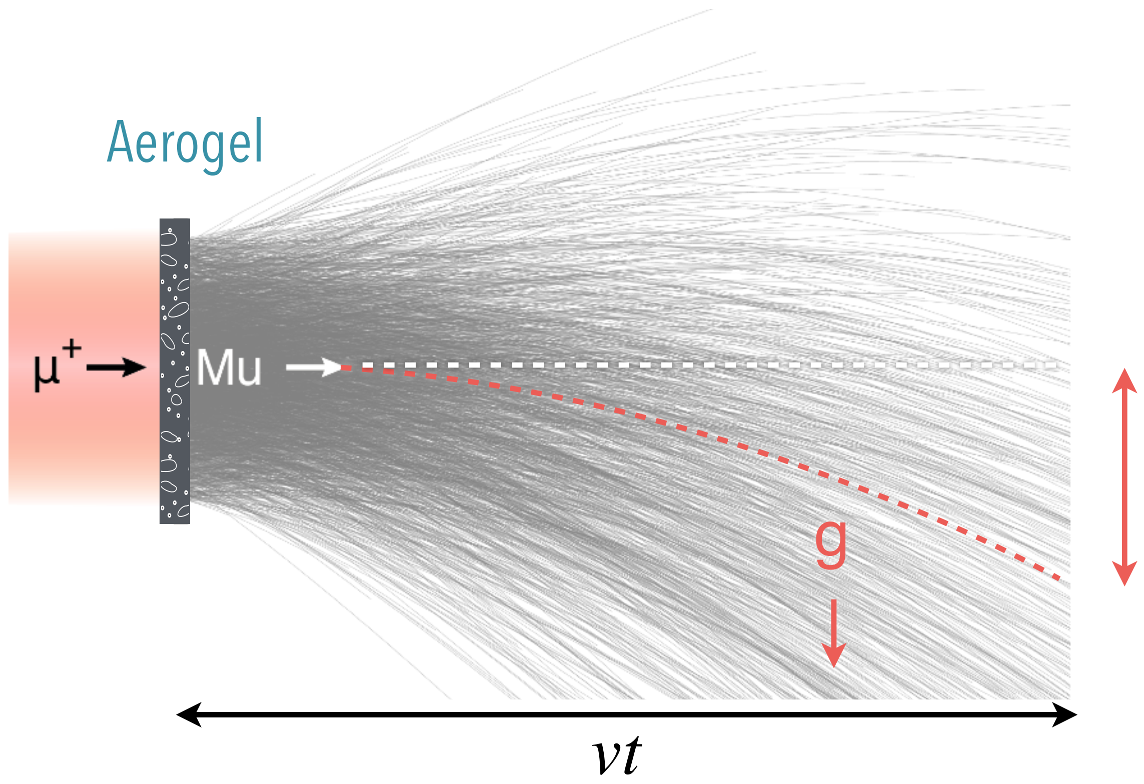

Mu lifetime of 2.2 μs

$$\Delta x = \frac{1}{2} g t^2 < 1 \text{ nm}$$

Why it might be possible with LEMING

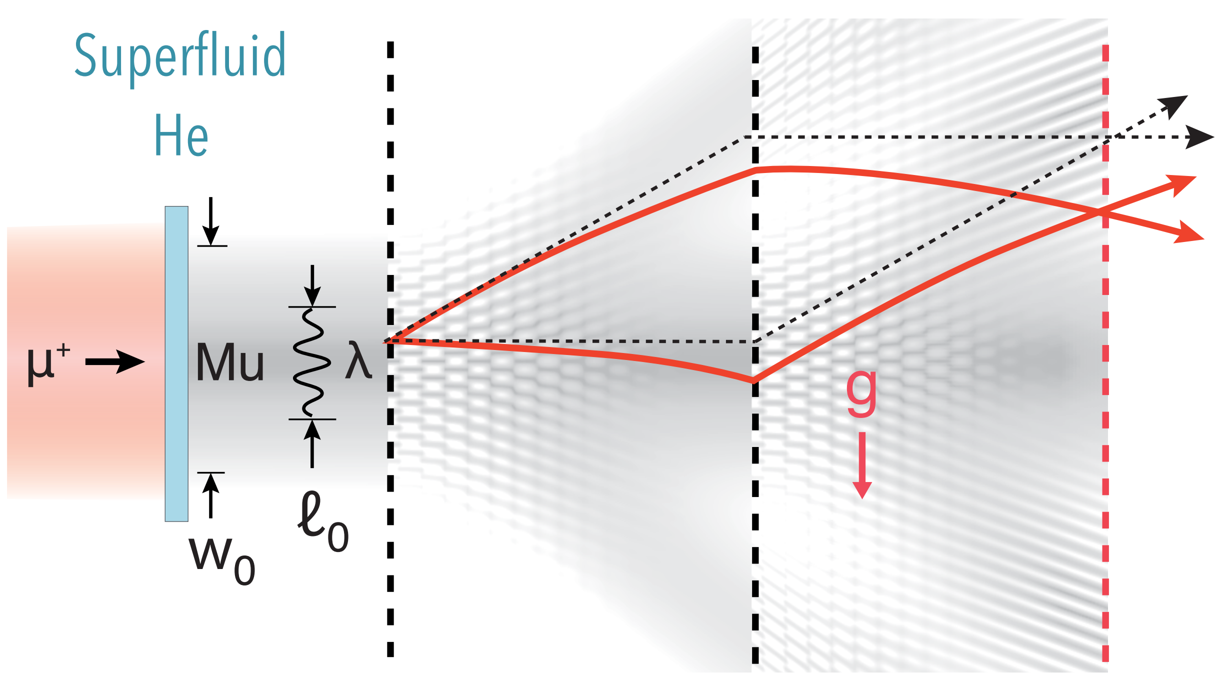

We developed a novel Mu beam amenable to interferometry

First synthesis of superthermal muonium from SFHe

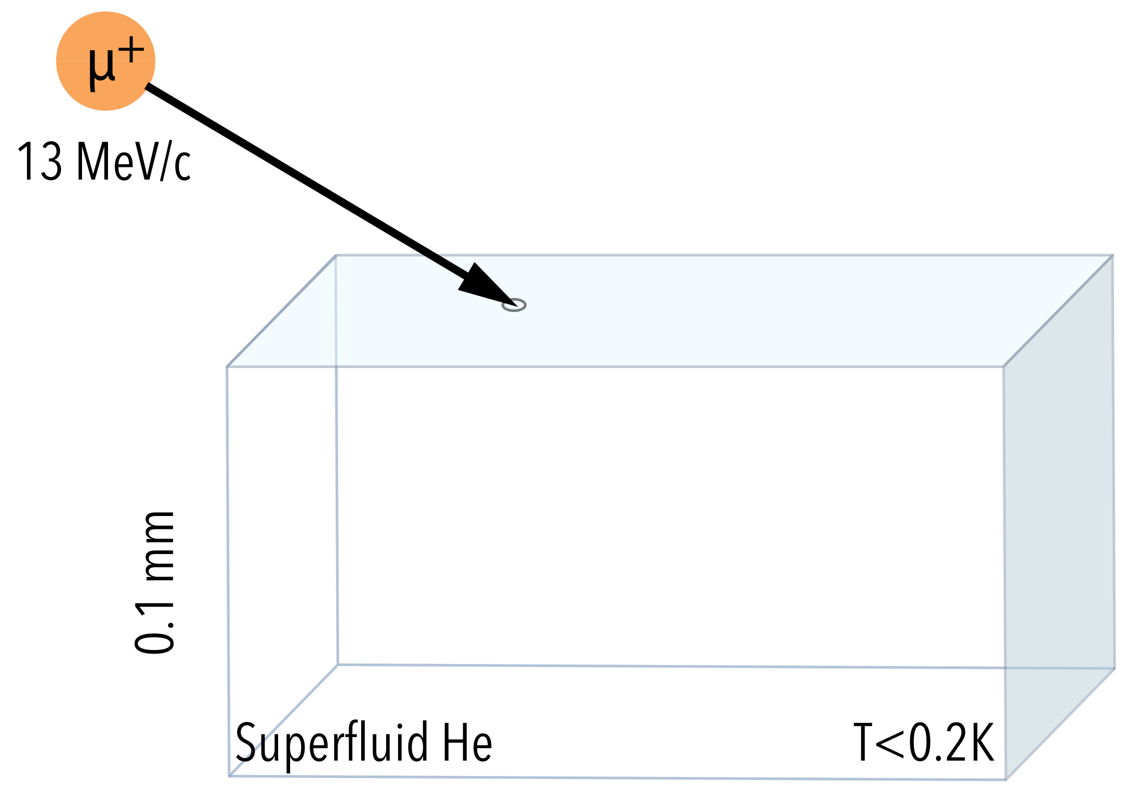

Our reported success in 2022 BVR:
Relies on 4 previously unknown physics process in SFHe:

(1) Mu stop and recombination $p \approx 70\,\%$

First synthesis of superthermal muonium from SFHe

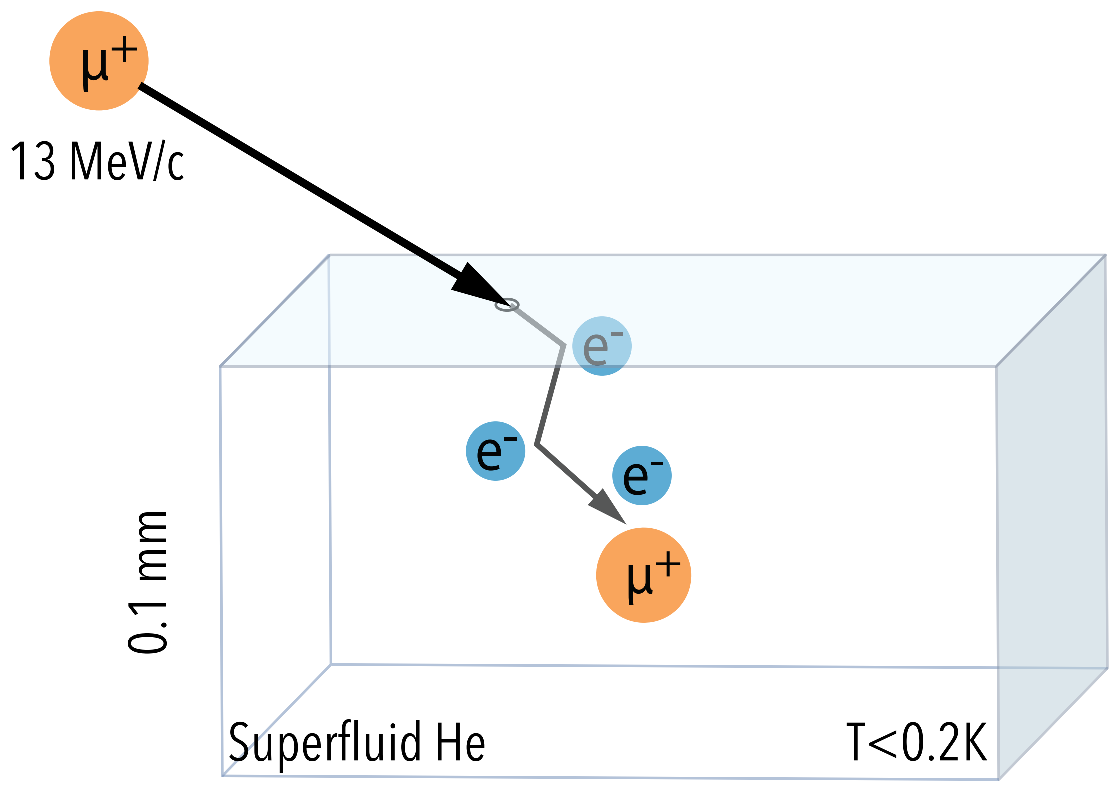

Our reported success in 2022 BVR:
Relies on 4 previously unknown physics process in SFHe:

(1) Mu stop and recombination $p \approx 70\,\%$

Our reported success in 2022 BVR:
Relies on 4 previously unknown physics process in SFHe:

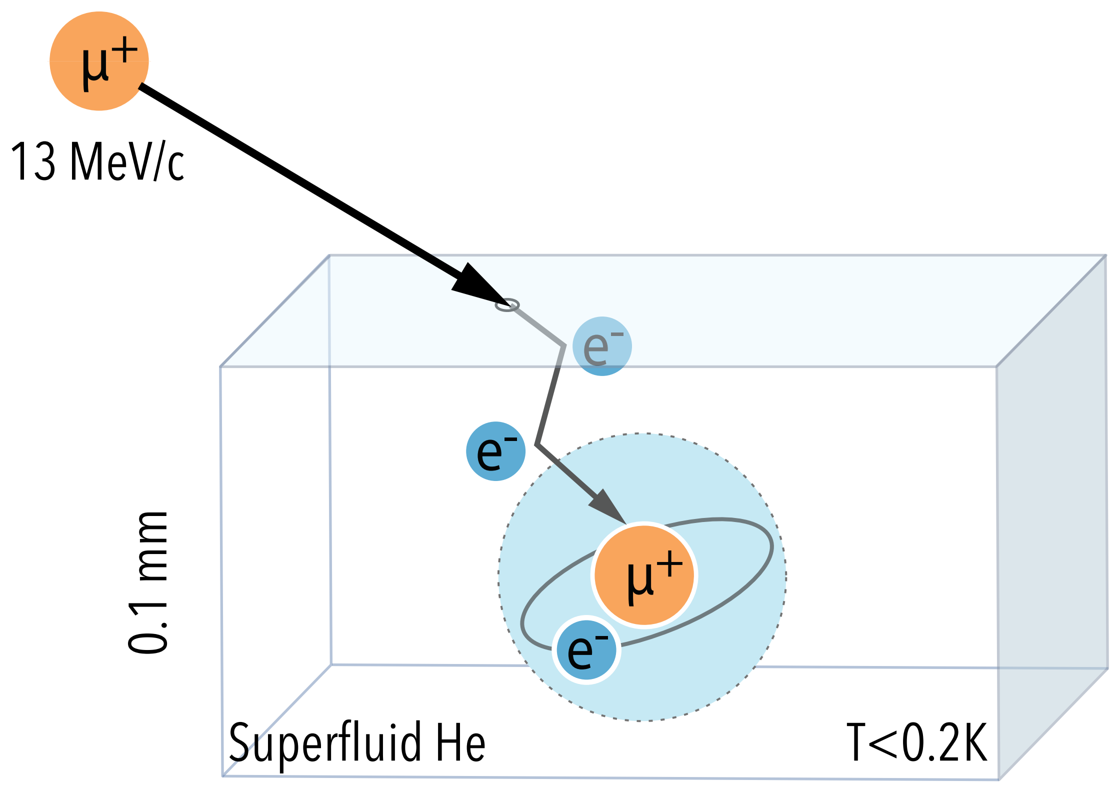

(1) Mu stop and recombination $p \approx 70\,\%$

First synthesis of superthermal muonium from SFHe

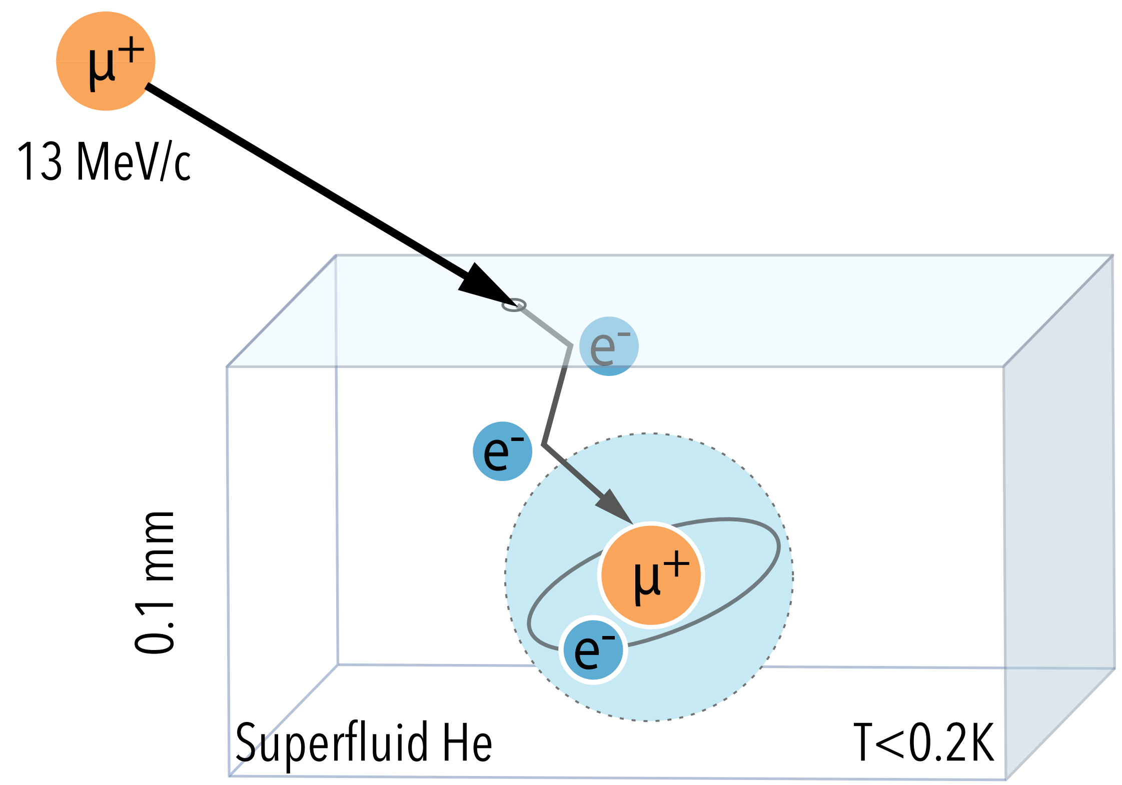

Our reported success in 2022 BVR:
Relies on 4 previously unknown physics process in SFHe:

(1) Mu stop and recombination $p \approx 70\,\%$

(2) Thermalization below the *roton gap*, $v_L \approx 60$ m/s

First synthesis of superthermal muonium from SFHe

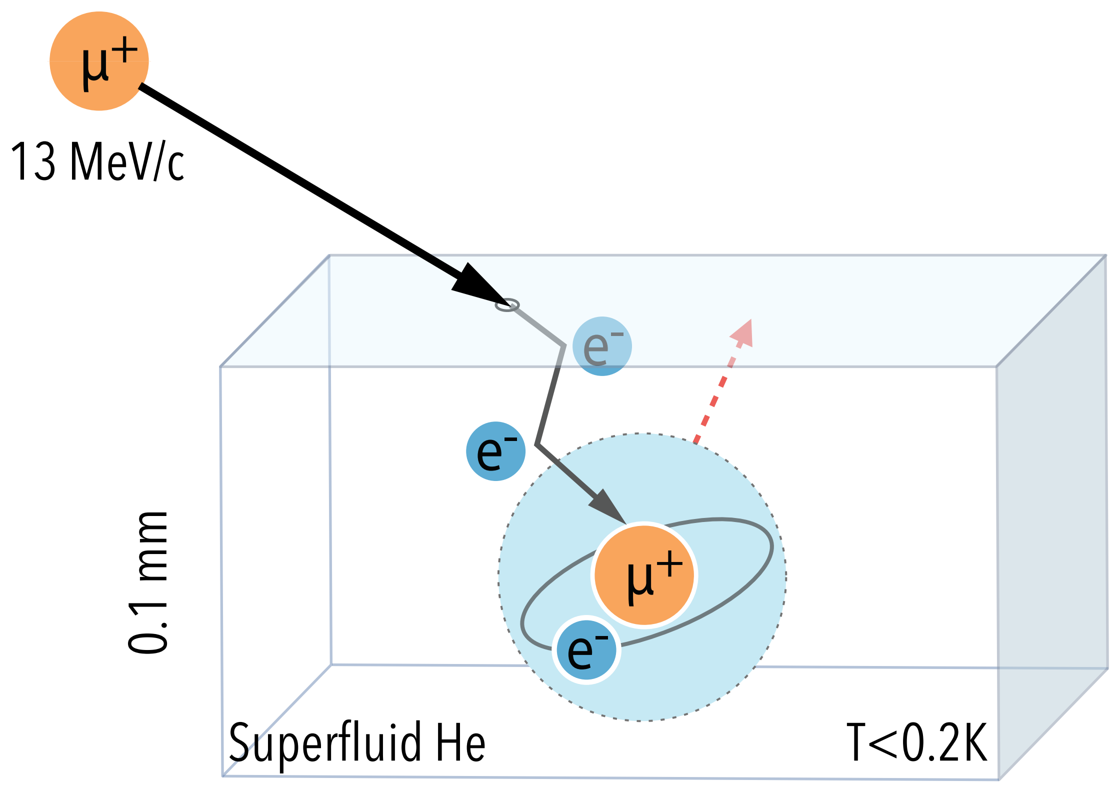

Our reported success in 2022 BVR:
Relies on 4 previously unknown physics process in SFHe:

(1) Mu stop and recombination $p \approx 70\,\%$

(2) Thermalization below the *roton gap*, $v_L \approx 60$ m/s

(3) Ballistic diffusion (no collisions), $\tau_d \approx 1\ \mu s$ * to surface

*other atoms don't do this. Clue for exception: antiprotonic helium in SFHe

A. Soter et al., Nature 603, 411–415 (2022)

First synthesis of superthermal muonium from SFHe

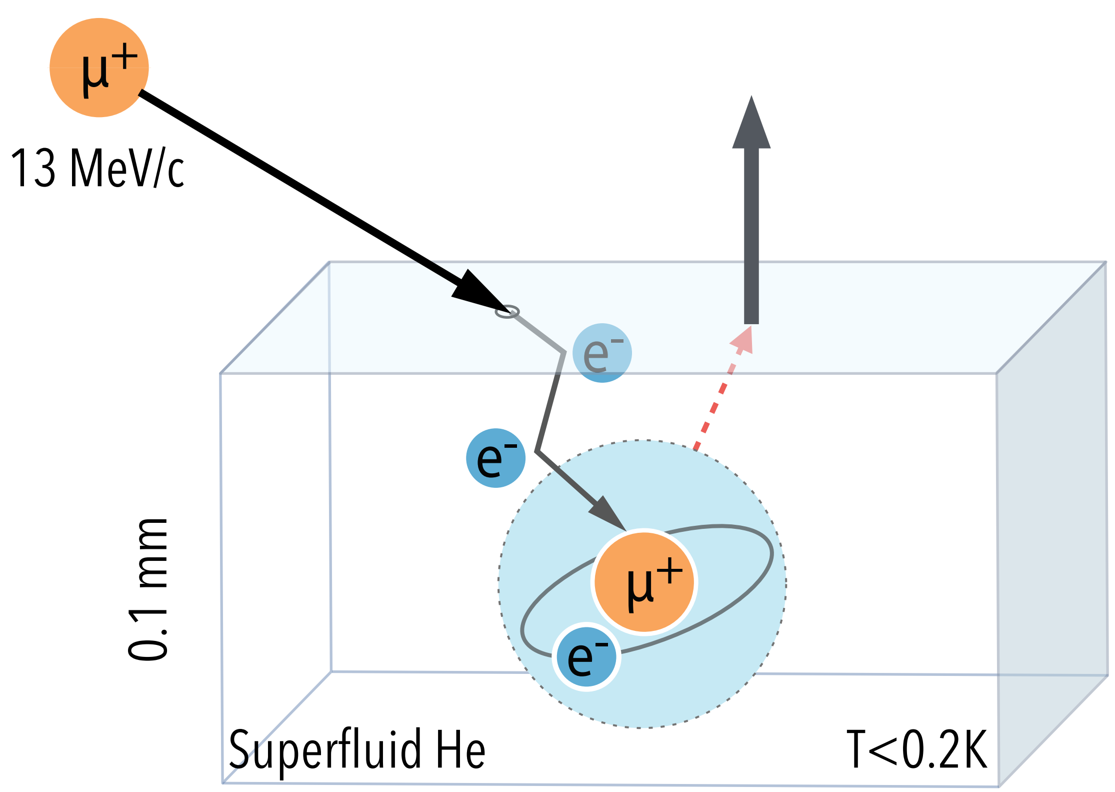

Our reported success in 2022 BVR:
Relies on 4 previously unknown physics process in SFHe:

(1) Mu stop and recombination $p \approx 70\,\%$

(2) Thermalization below the *roton gap*, $v_L \approx 60$ m/s

(3) Ballistic diffusion (no collisions), $\tau_d \approx 1\ \mu$s * to surface

(4) Ejection in the surface normal, due to the large positive chemical potential

*other atoms don't do this. Clue for exception: antiprotonic helium in SFHe

A. Soter et al., Nature 603, 411–415 (2022)

First synthesis of superthermal muonium from SFHe

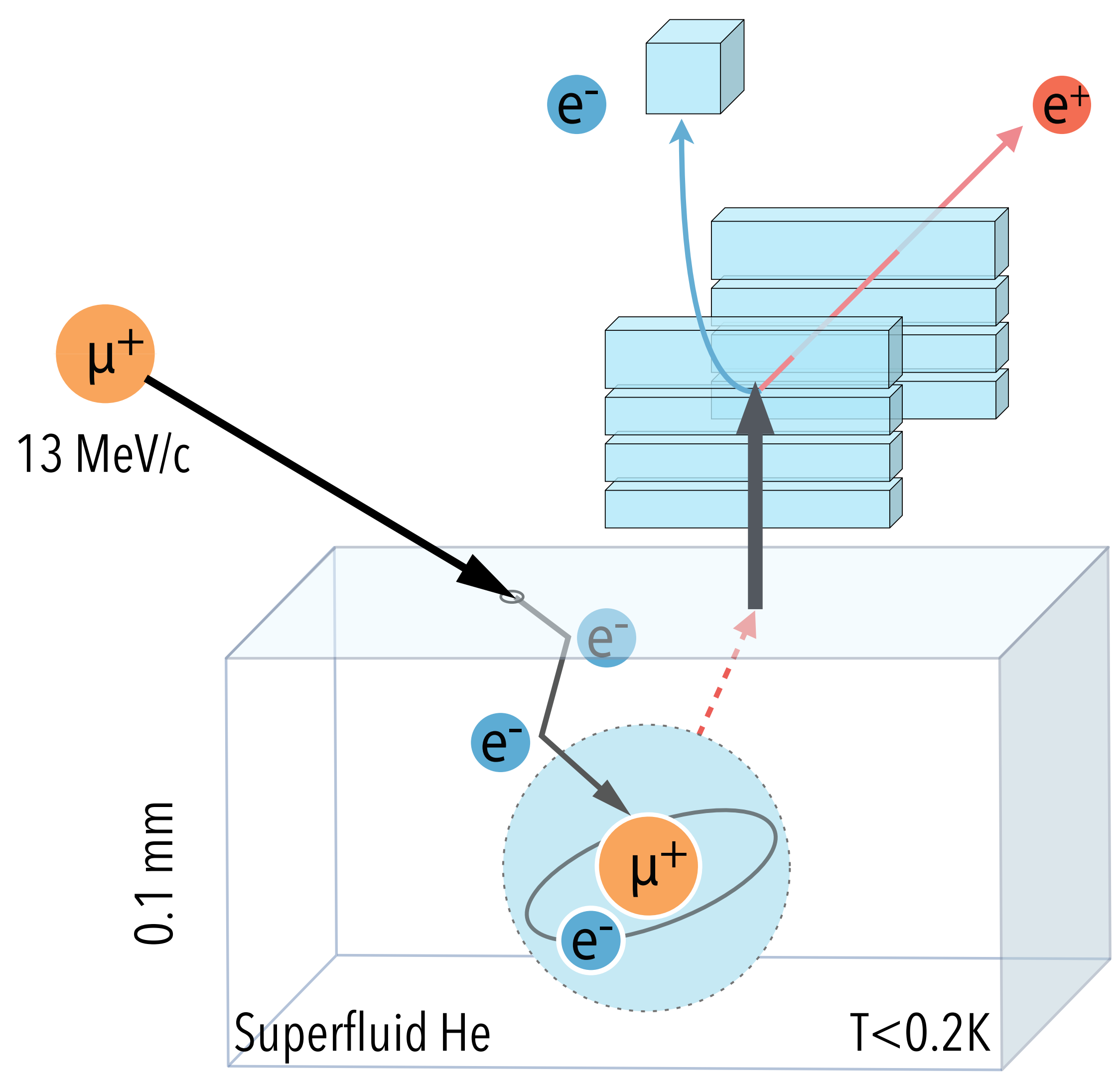

Our reported success in 2022 BVR:
Relies on 4 previously unknown physics process in SFHe:

(1) Mu stop and recombination $p \approx 70\,\%$

(2) Thermalization below the *roton gap*, $v_L \approx 60\ \mathrm{m/s}$

(3) Ballistic diffusion (no collisions), $\tau_d \approx 1\ \mu\mathrm{s}$ * to surface

(4) Ejection in the surface normal, due to the large positive chemical potential

*other atoms don't do this. Clue for exception: antiprotonic helium in SFHe

A. Soter et al., Nature 603, 411–415 (2022)

Characterisation of the superthermal Mu beam

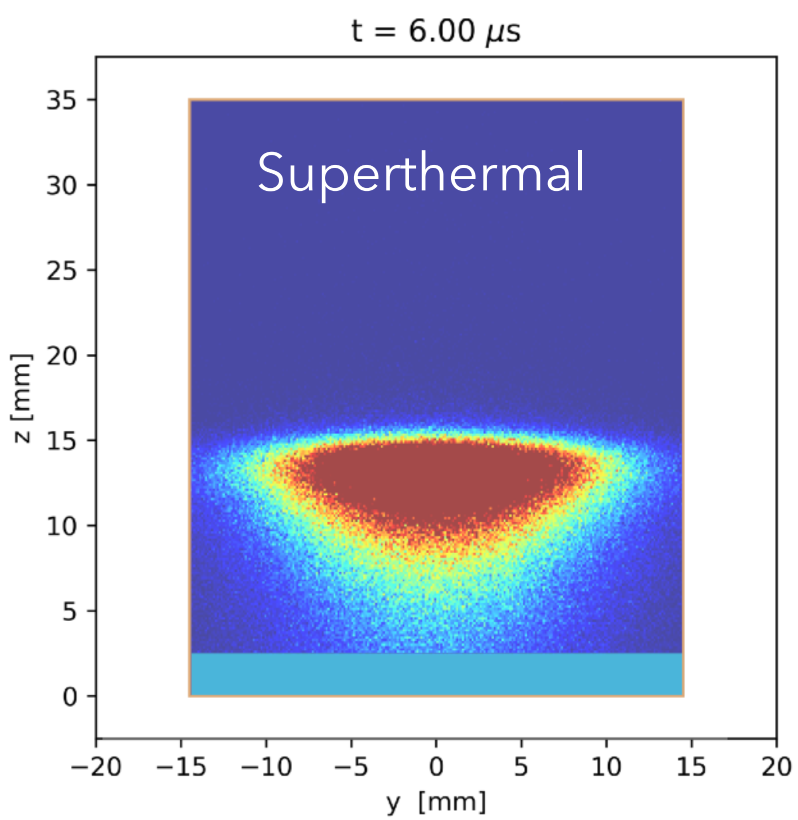

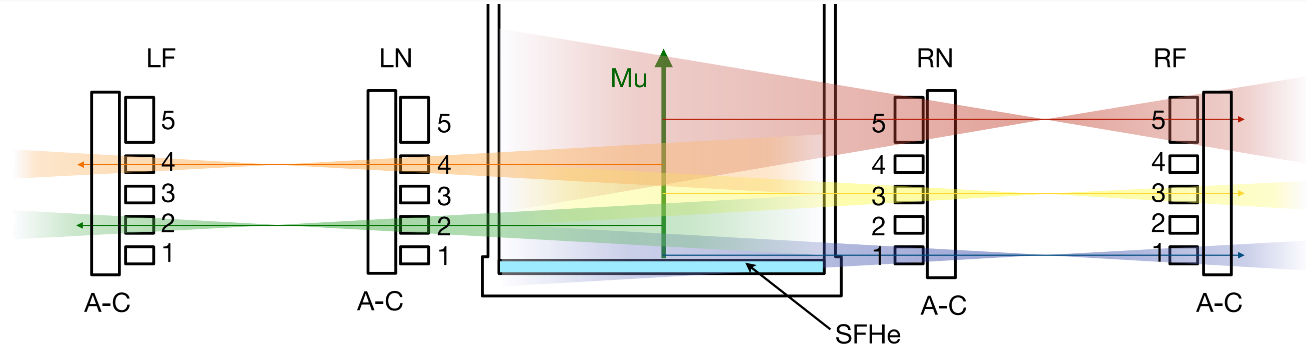

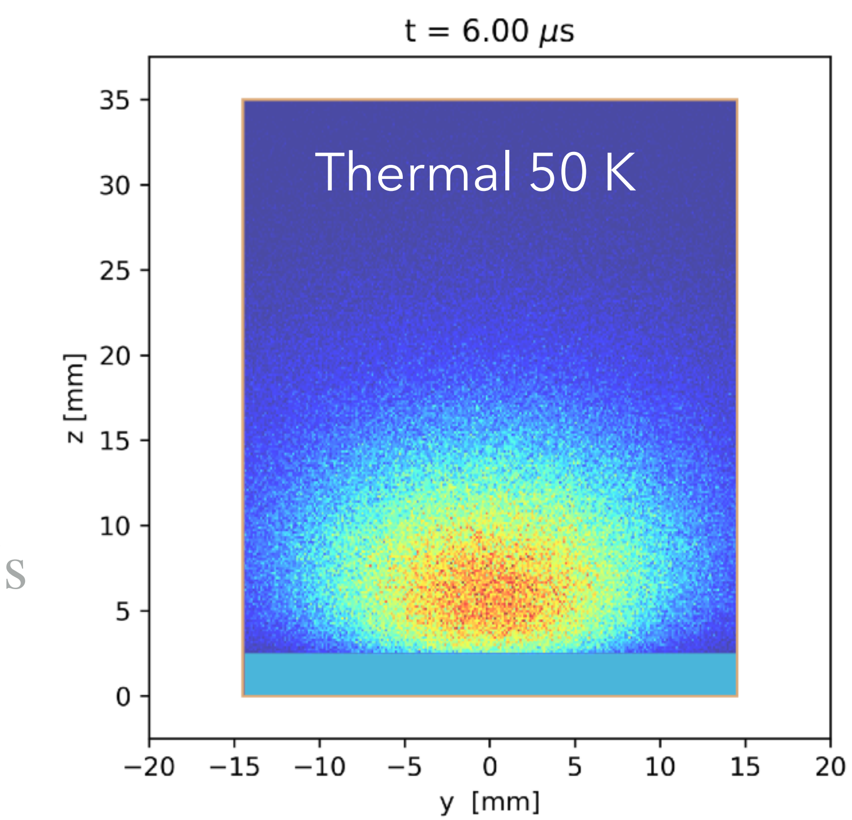

- **Lowest velocity** Mu source $v_x \approx 2175\ \mathrm{m/s}$
- **Narrowest** longitudinal distribution: $\sigma_{v_x} \approx 70\ \mathrm{m/s}$
- **High yield** similar to the best 300 K sources $R(\mu^+ \rightarrow \mathrm{Mu_{vac}}) = 10\,\%$

Reconstructed velocity distribution

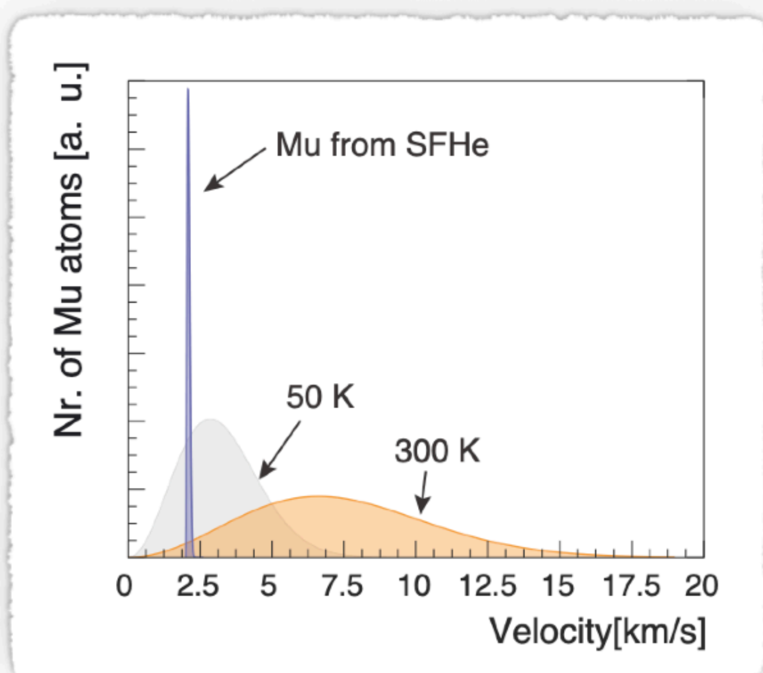

Time spectra of fly-by

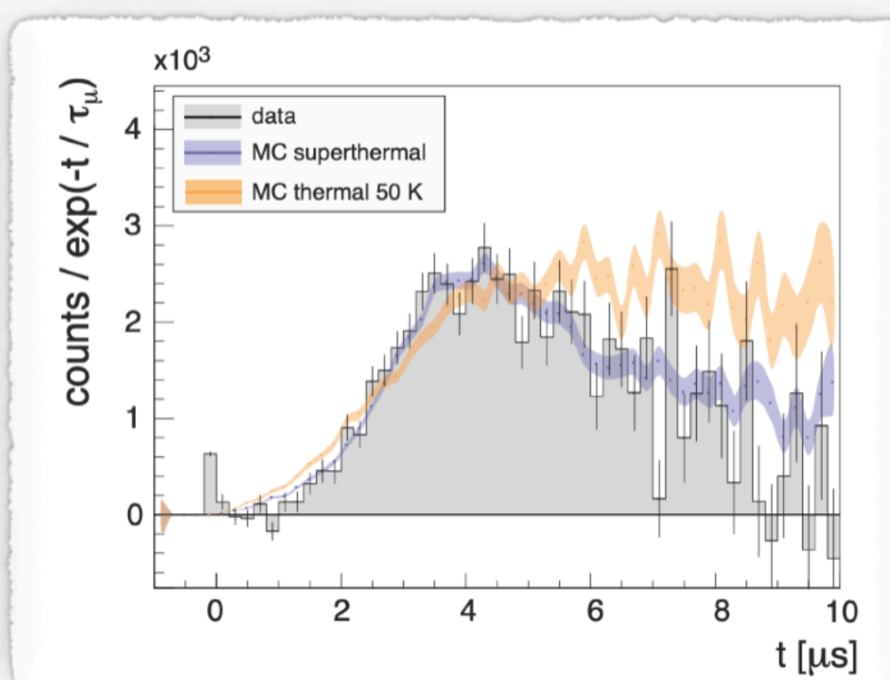

Time spectra of target emission

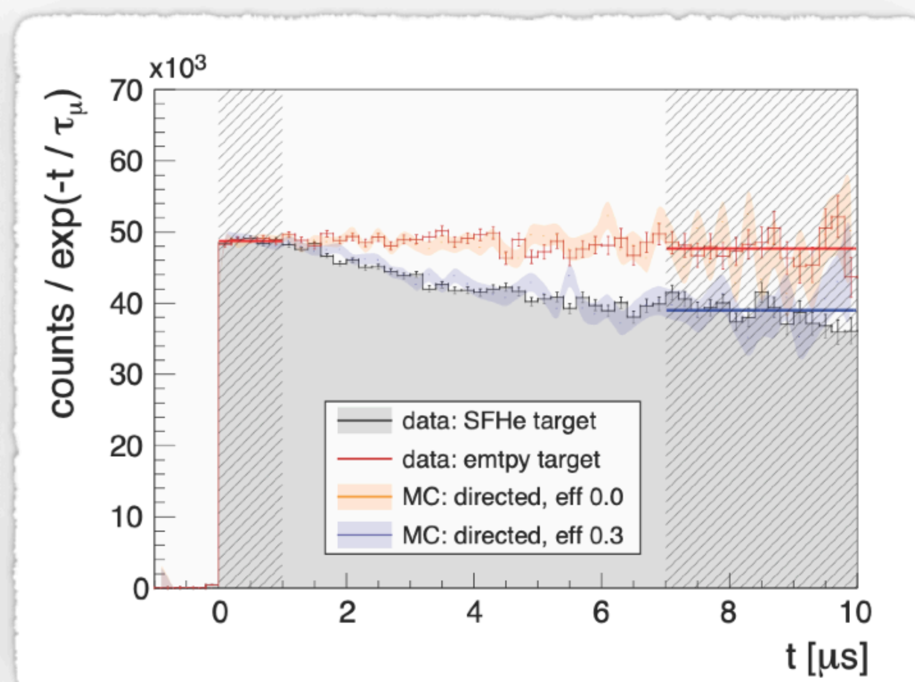

Characterisation of the superthermal Mu beam

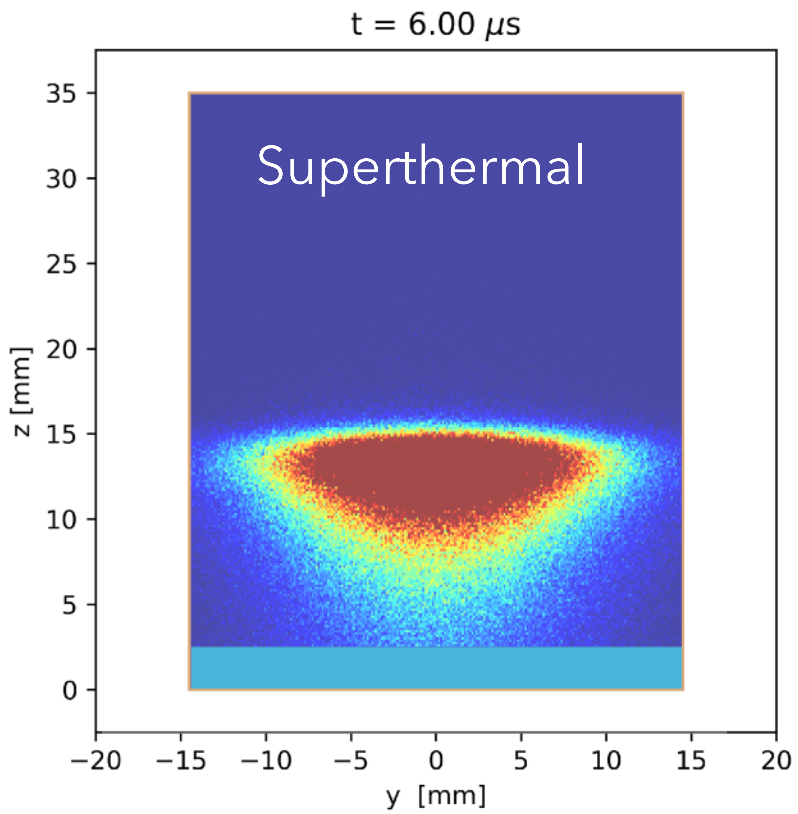

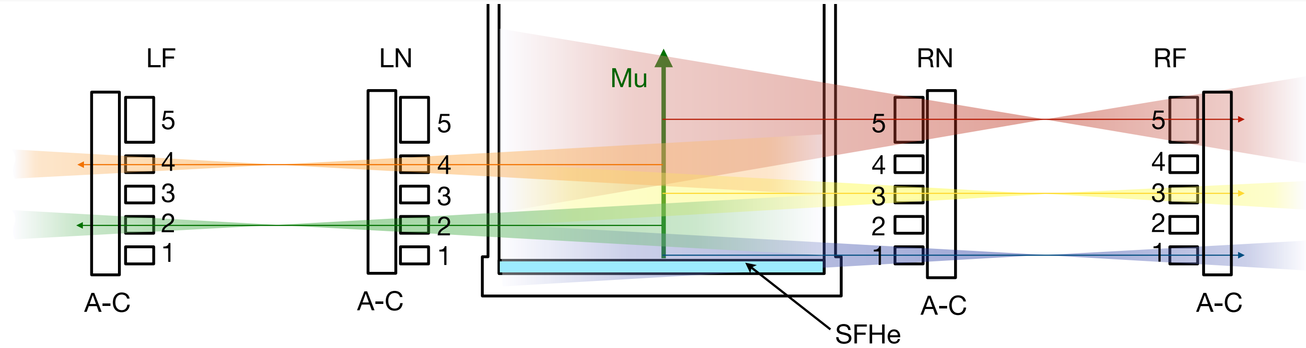

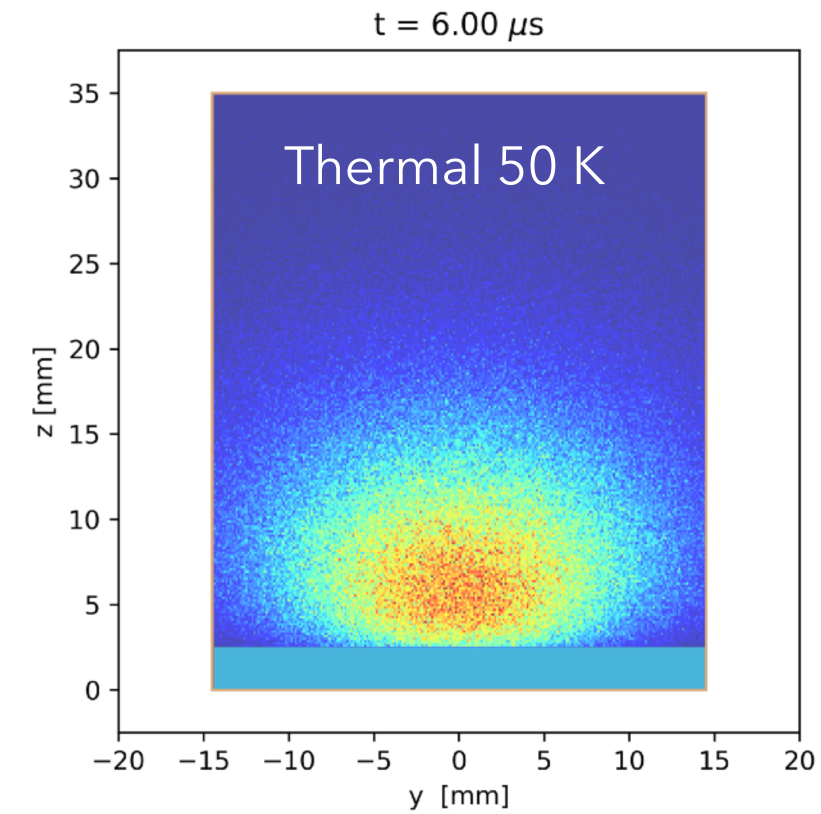

- **Lowest velocity** Mu source $v_x \approx 2175\ \mathrm{m/s}$
- **Narrowest** longitudinal distribution: $\sigma_{v_x} \approx 70\ \mathrm{m/s}$
- **High yield** similar to the best 300 K sources $R(\mu^+ \to \mathrm{Mu_{vac}}) = 10\,\%$

Reconstructed velocity distribution

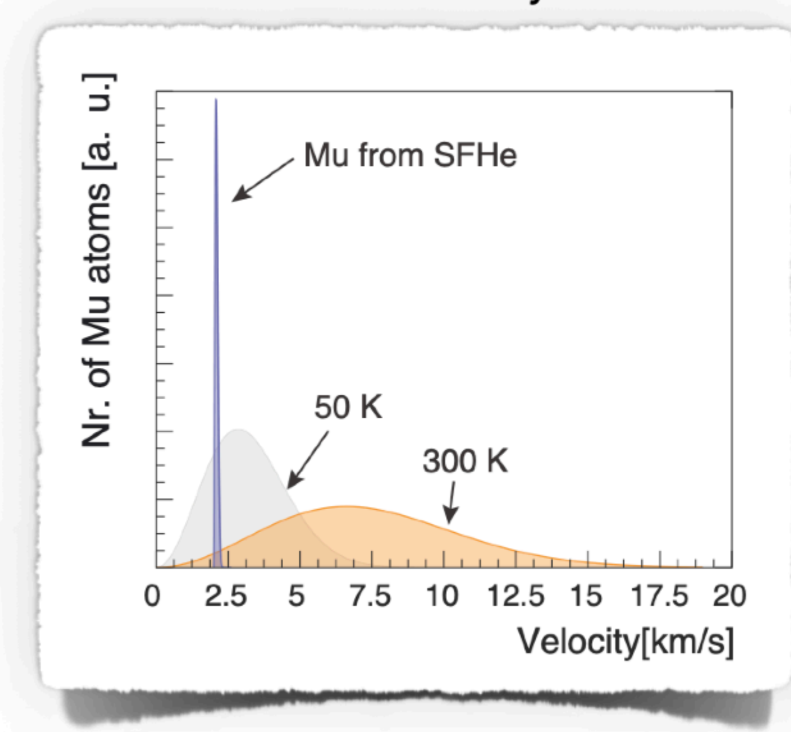

Time spectra of fly-by

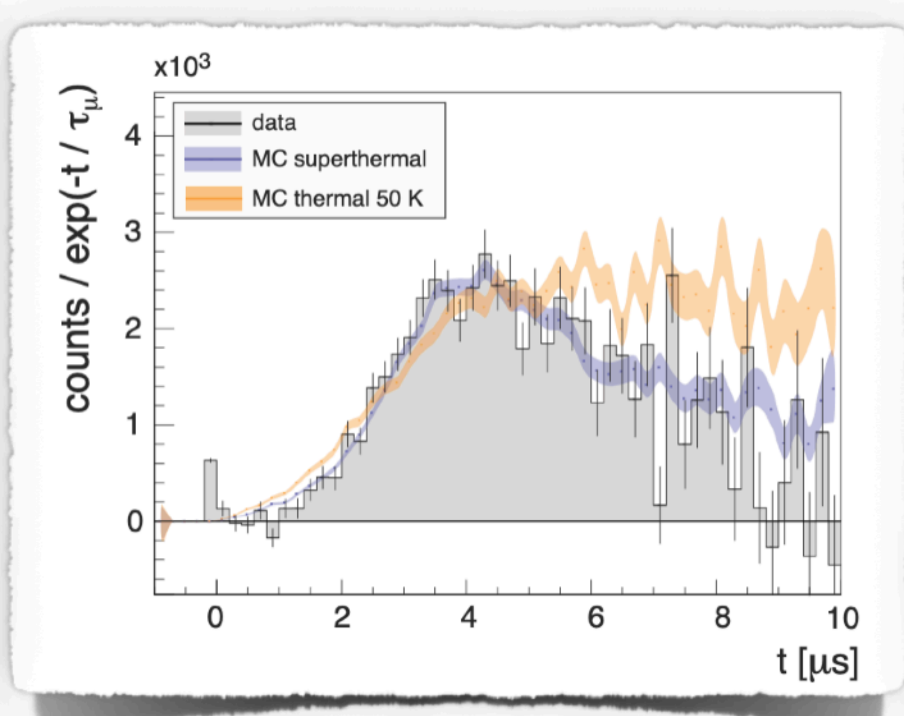

Time spectra of target emission

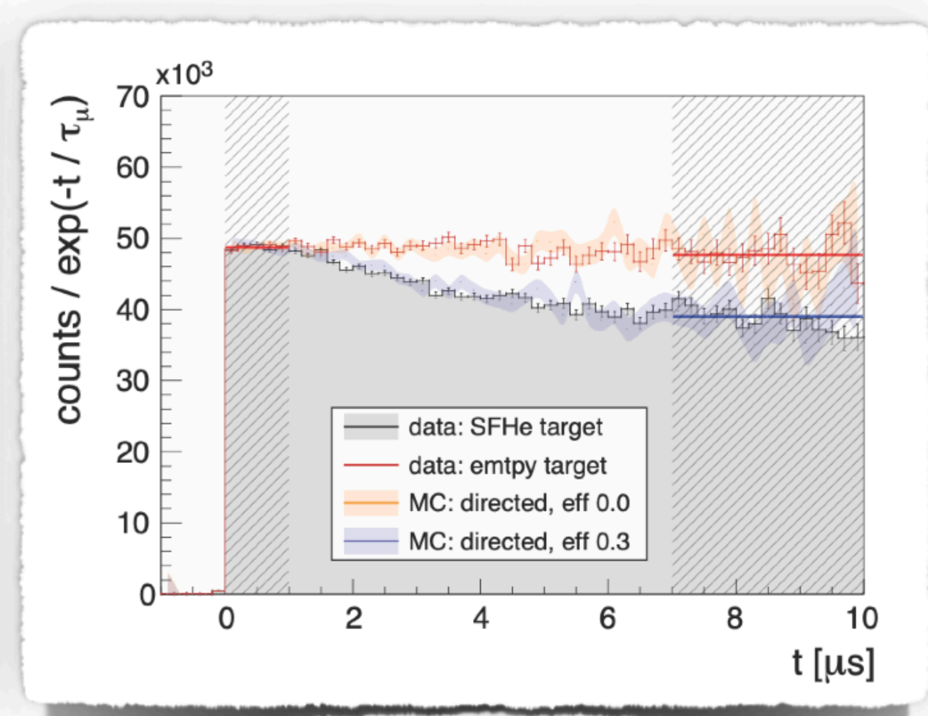

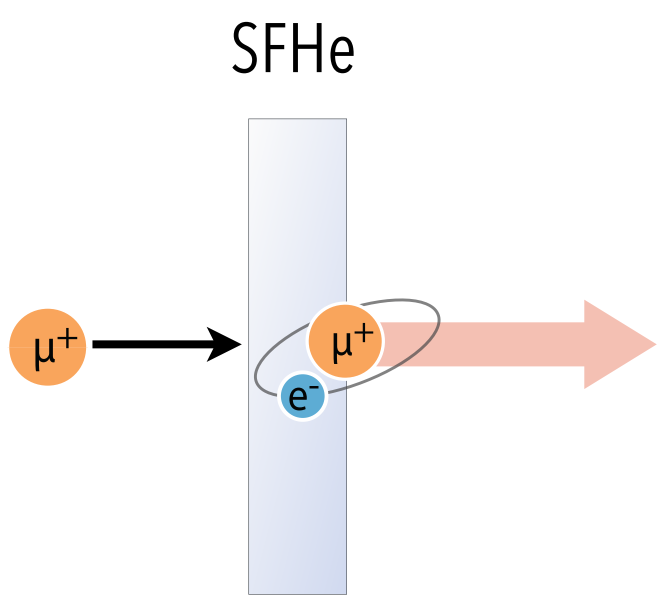

Horizontal cold Mu beam

Atomic mirror / Microfluidic target

Overview of LEMING

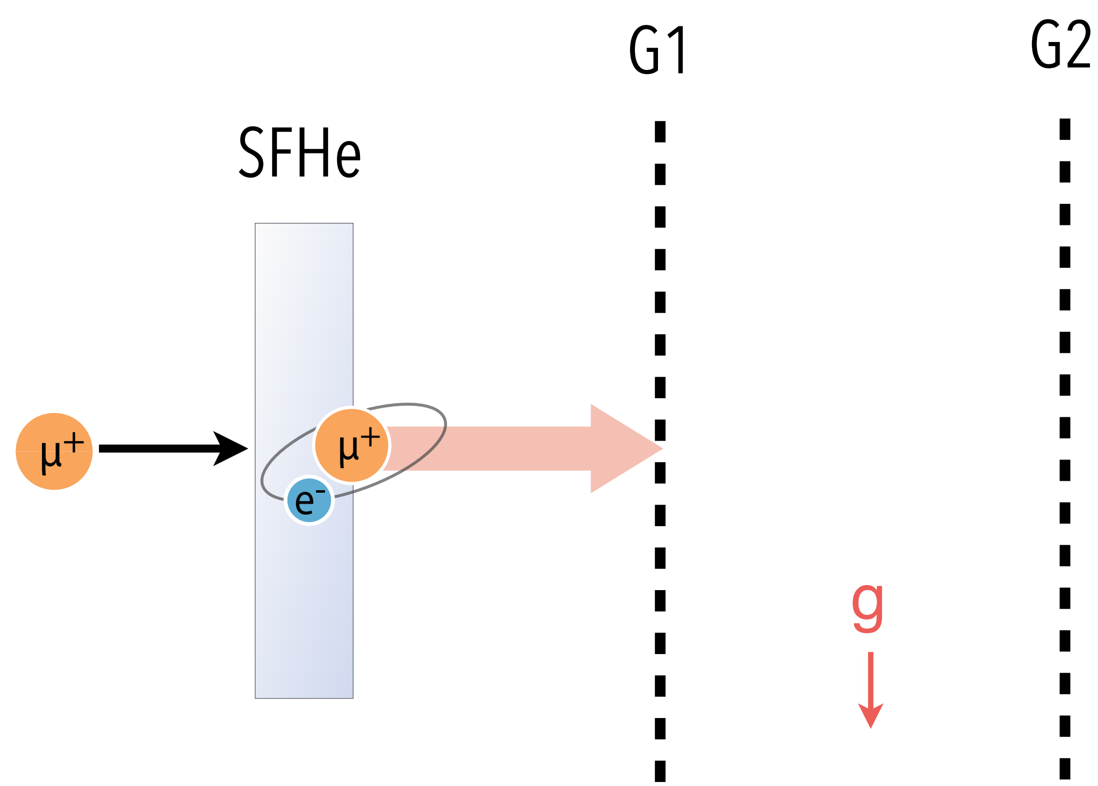

Horizontal cold Mu beam

Atomic mirror / Microfluidic target

Interferometer

G1, G2 and mask M

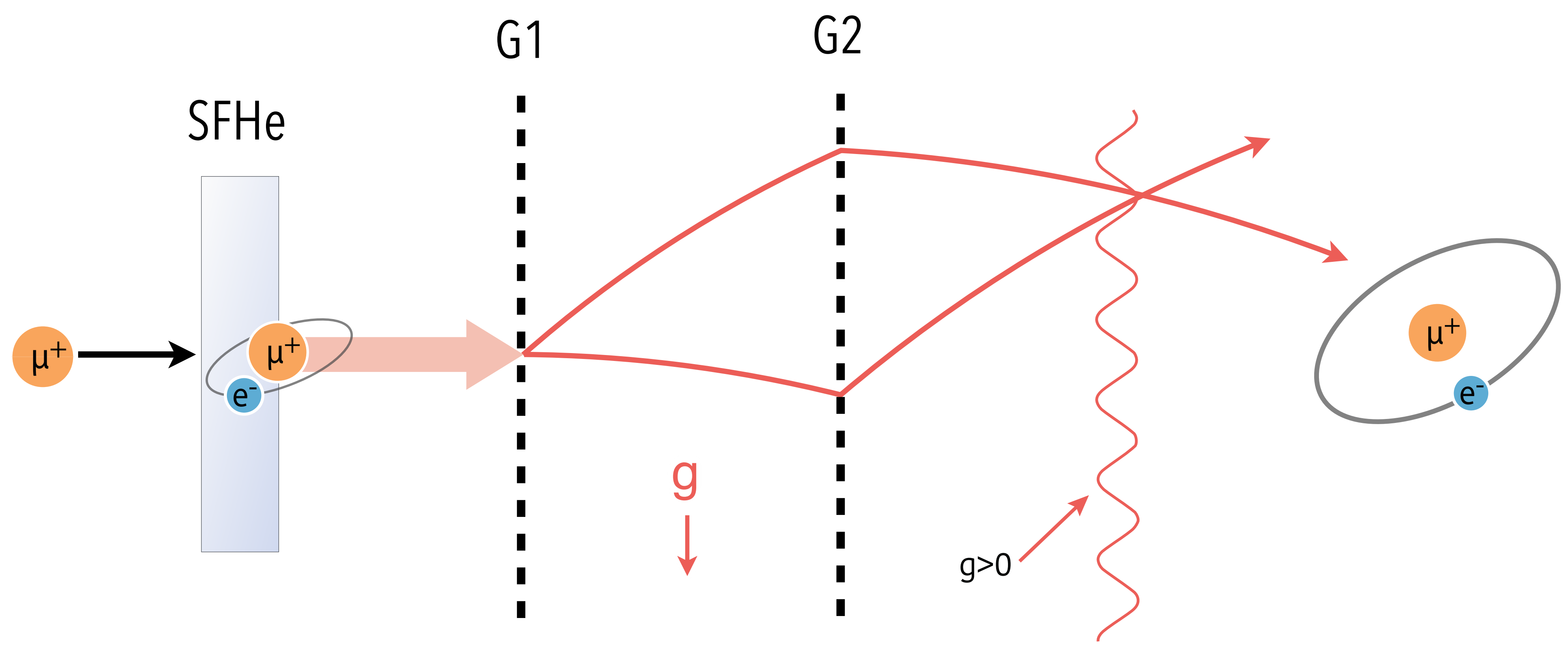

Horizontal cold Mu beam

Atomic mirror / Microfluidic target

Interferometer

G1, G2 and mask M

Overview of LEMING

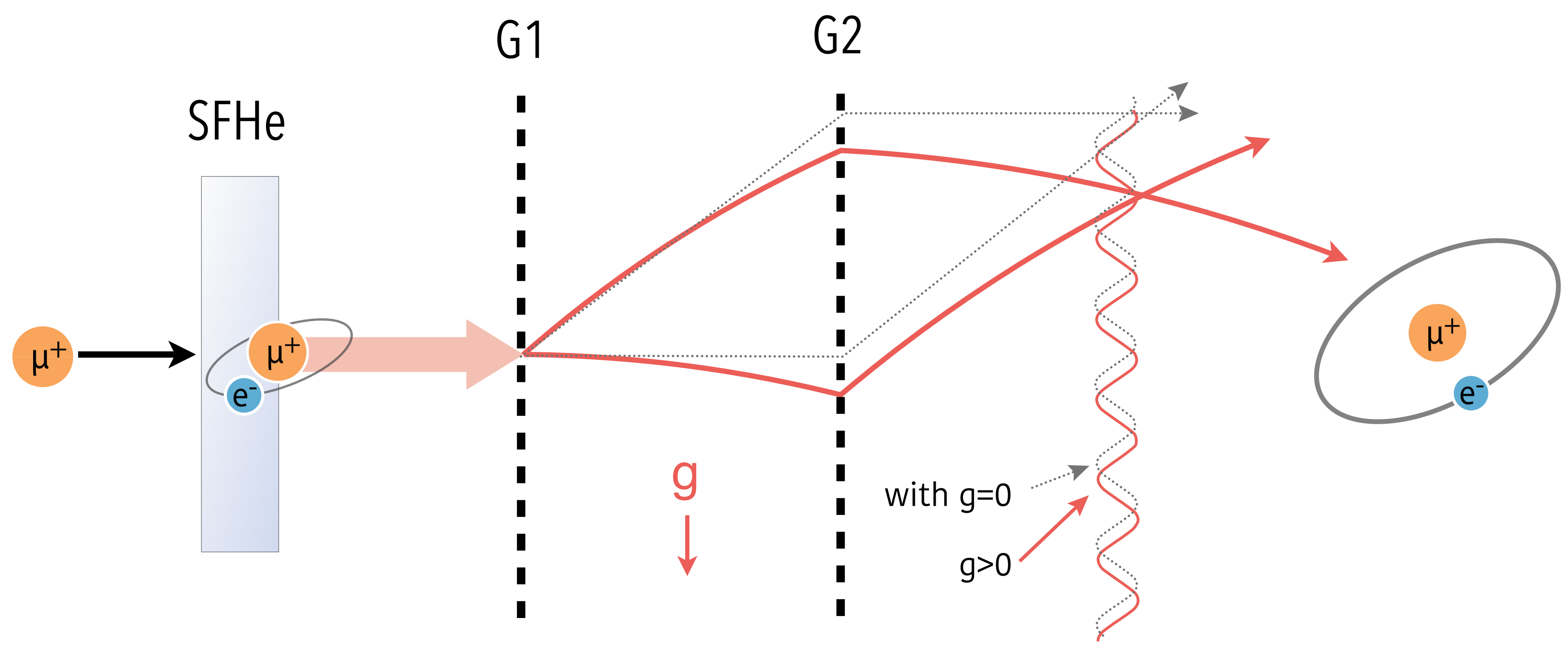

Horizontal cold Mu beam

Atomic mirror / Microfluidic target

Interferometer

G1, G2 and mask M

Overview of LEMING

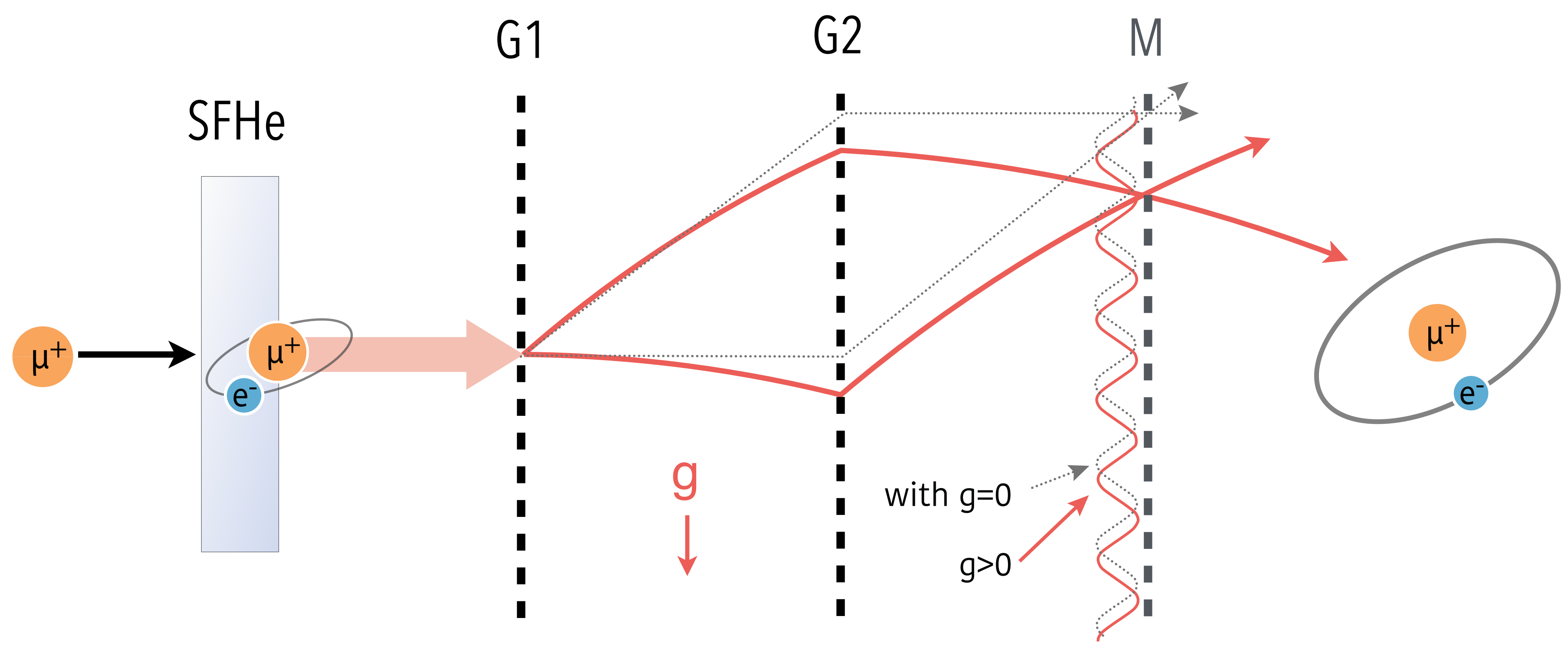

Horizontal cold Mu beam

Atomic mirror / Microfluidic target

Interferometer

G1, G2 and mask M

Overview of LEMING

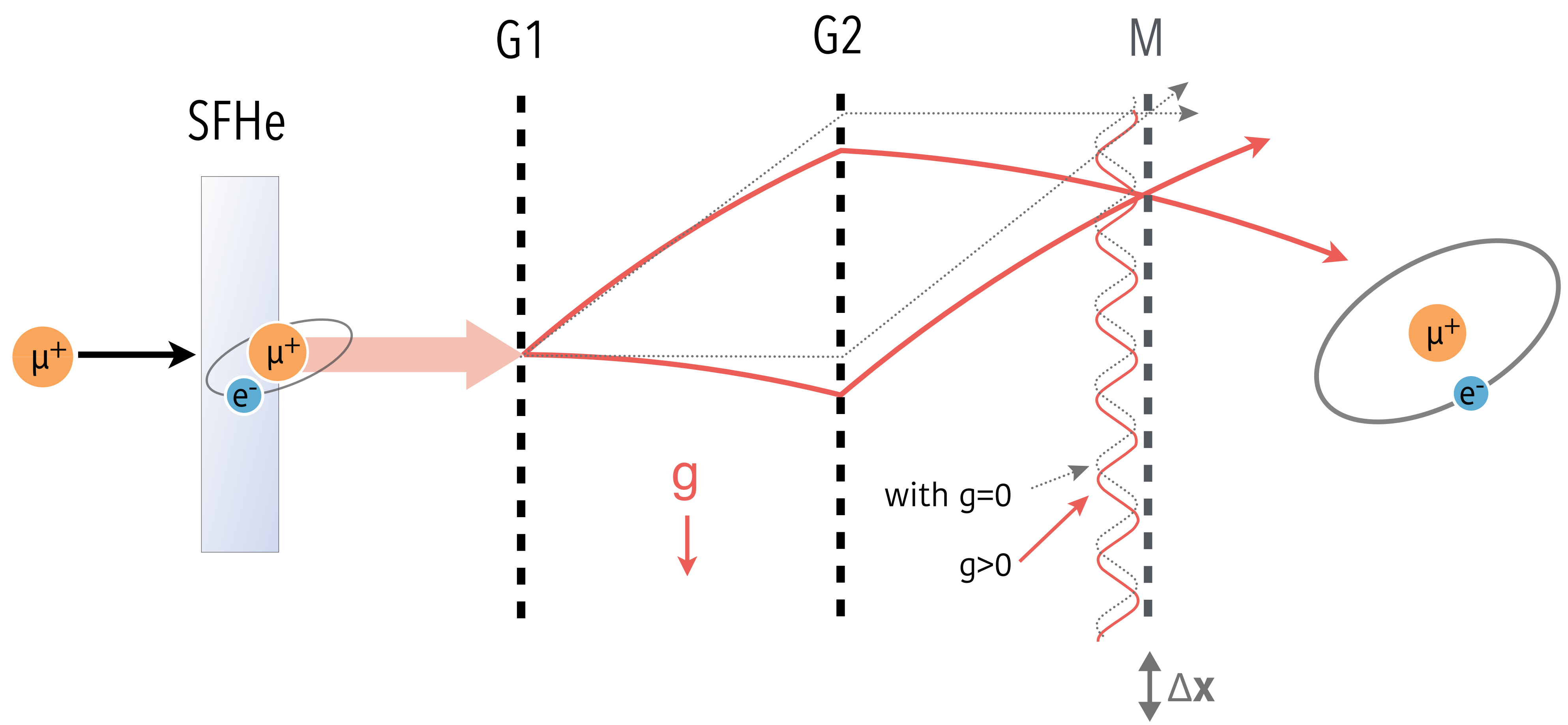

Horizontal cold Mu beam

Atomic mirror / Microfluidic target

Interferometer

G1, G2 and mask M

Overview of LEMING

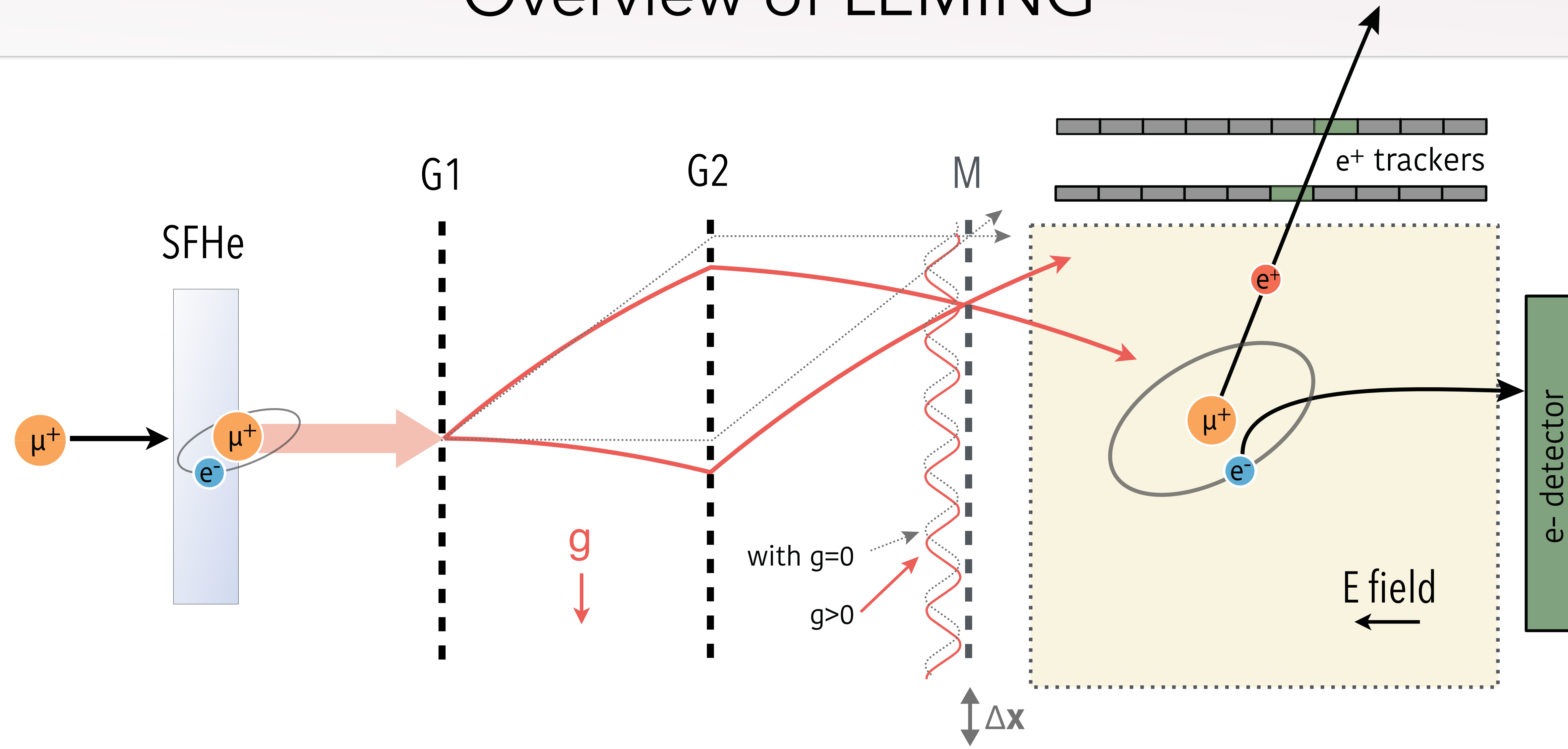

Horizontal cold Mu beam	Interferometer	Detection
Atomic mirror / Microfluidic target	G1, G2 and mask M	e+/e- detectors

Overview of LEMING

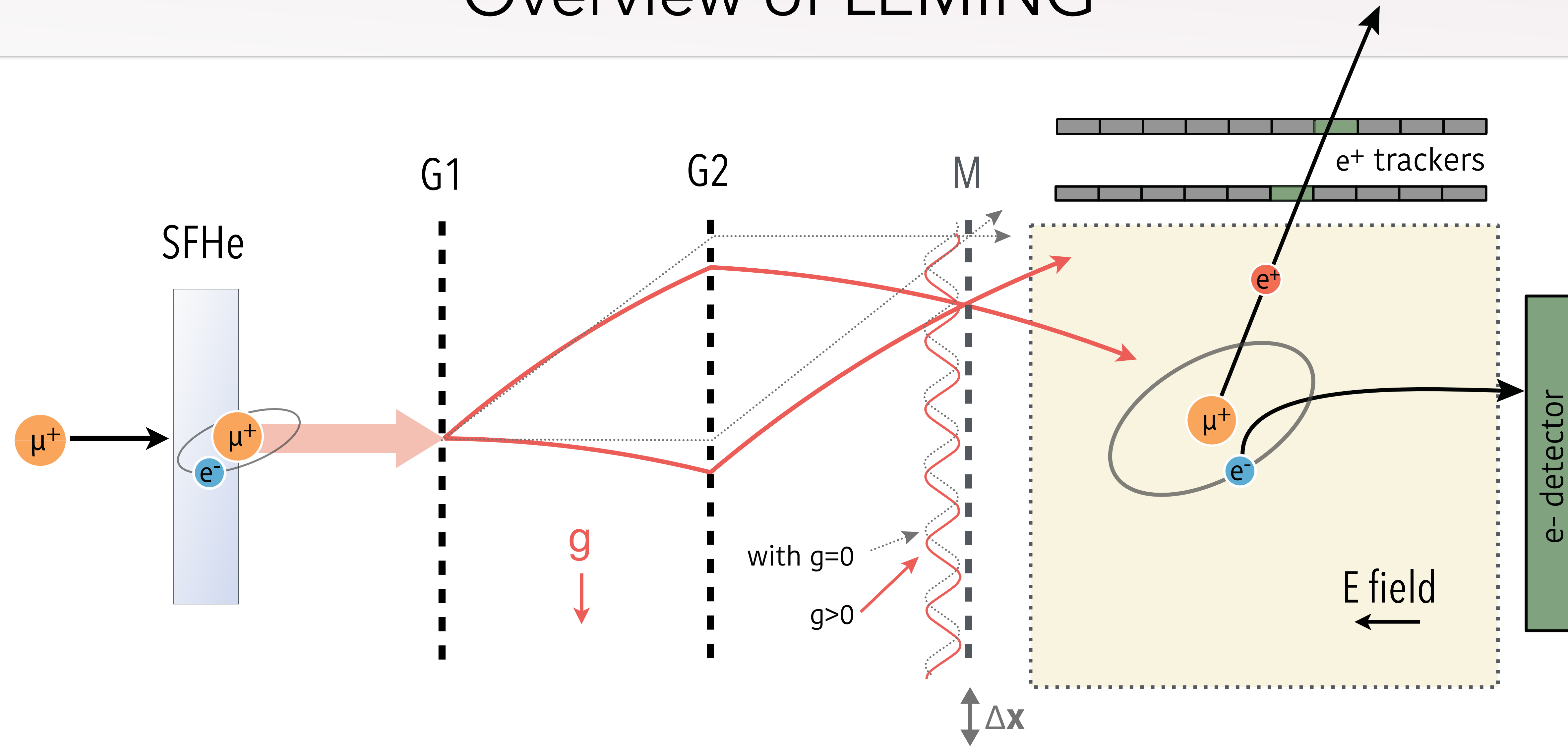

New!

Horizontal cold Mu beam

Atomic mirror / Microfluidic target

Interferometer

G1, G2 and mask M

Detection

e+/e- detectors

Overview of LEMING

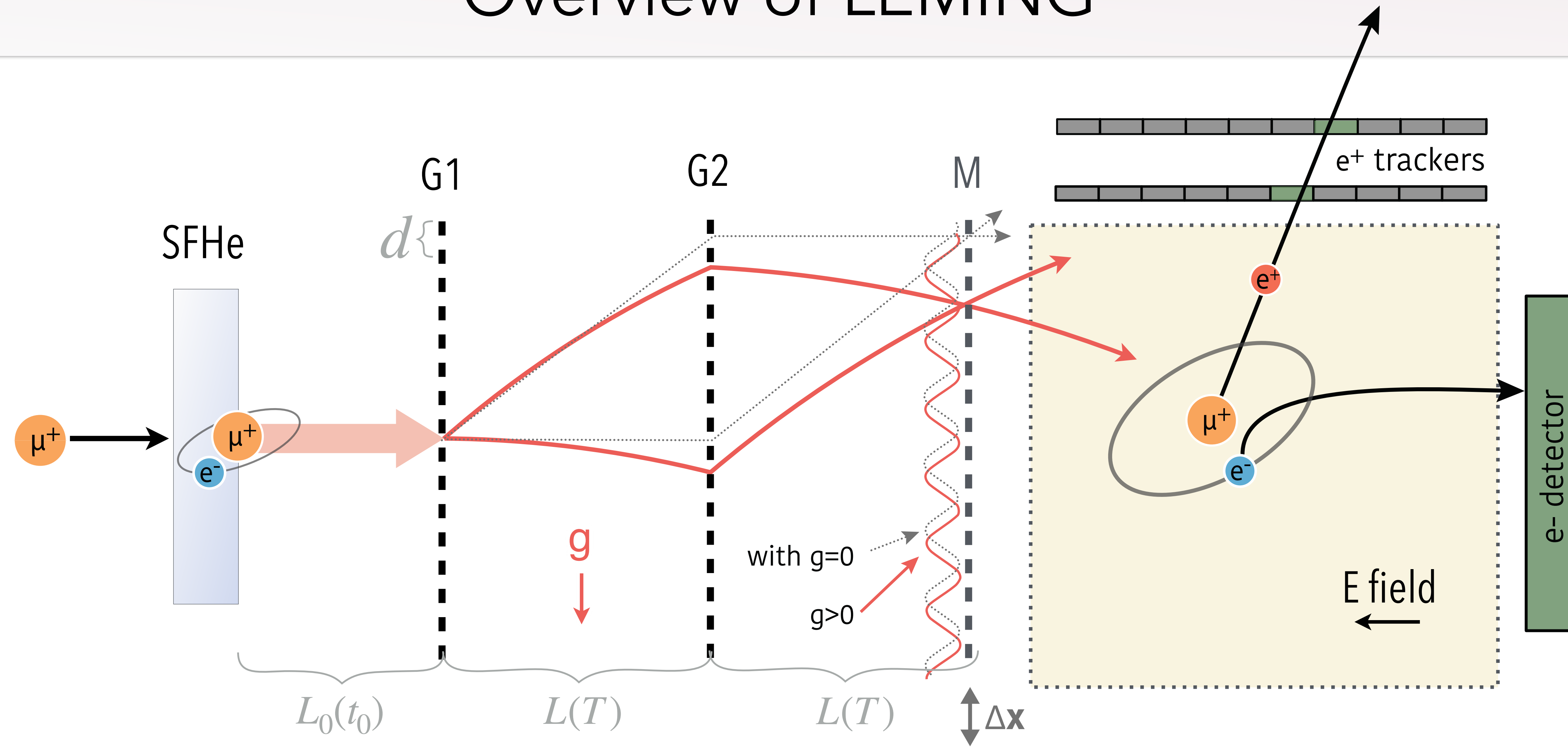

New!

Horizontal cold Mu beam

Atomic mirror / Microfluidic target

Interferometer

G1, G2 and mask M

Detection

e+/e- detectors

Sensitivity $\Delta g \approx \frac{1}{2\pi T^2} \frac{d}{C\sqrt{N_0 \varepsilon \eta^3 e^{-(t_0+2T)/\tau}}}$

$d = 100$ nm
$T \approx 4\ \mu$s
$L \approx 10$ mm

~ 1% sensitivity

At PSI, world's highest intensity cw muons

New cryogenic platform

- Delays and issues, but operates since 2023 summer, compact experimental platform to execute Phase I.
- Large cold plate of ~ 300 mm
- Cooldown time of 22-25 hours
- Base T = 8 mK
- Cooling power:

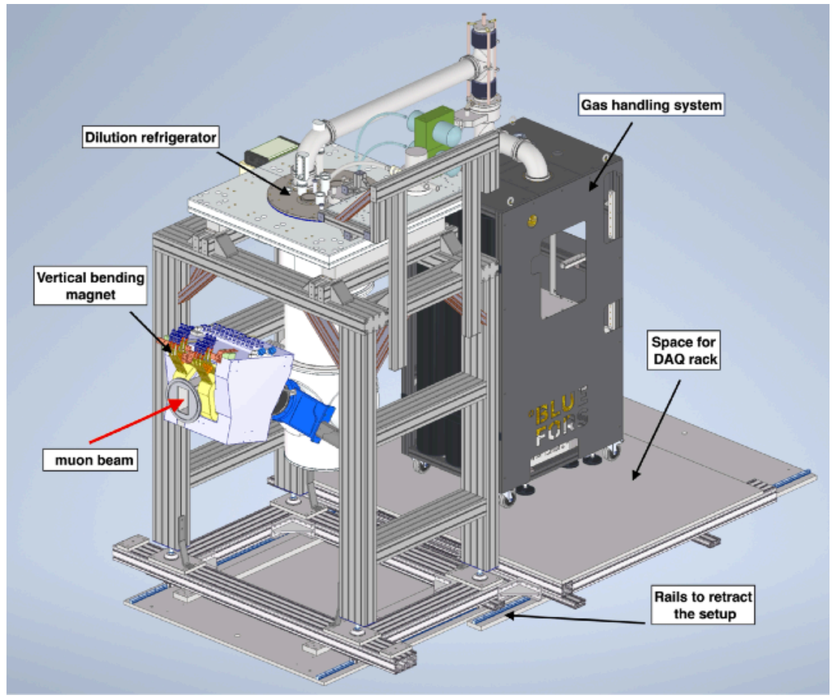

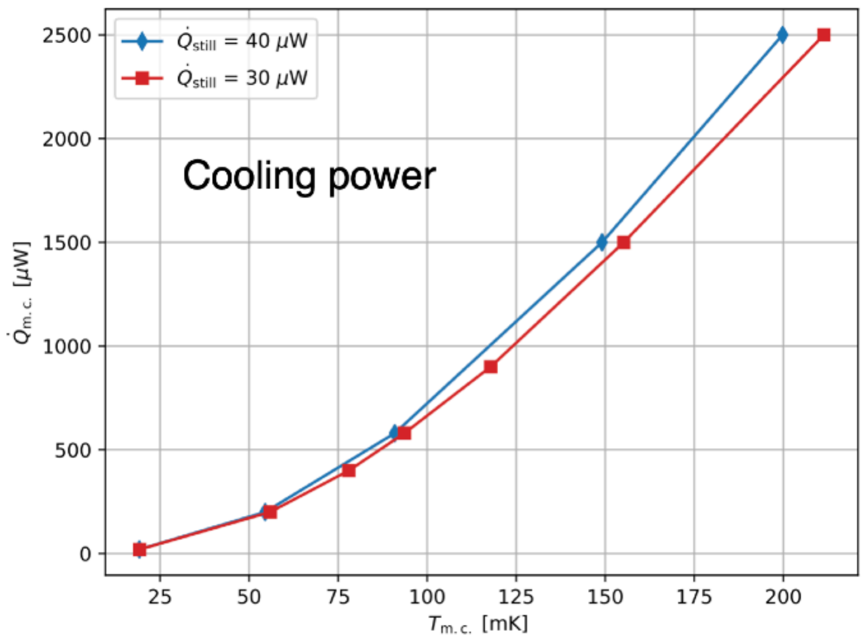

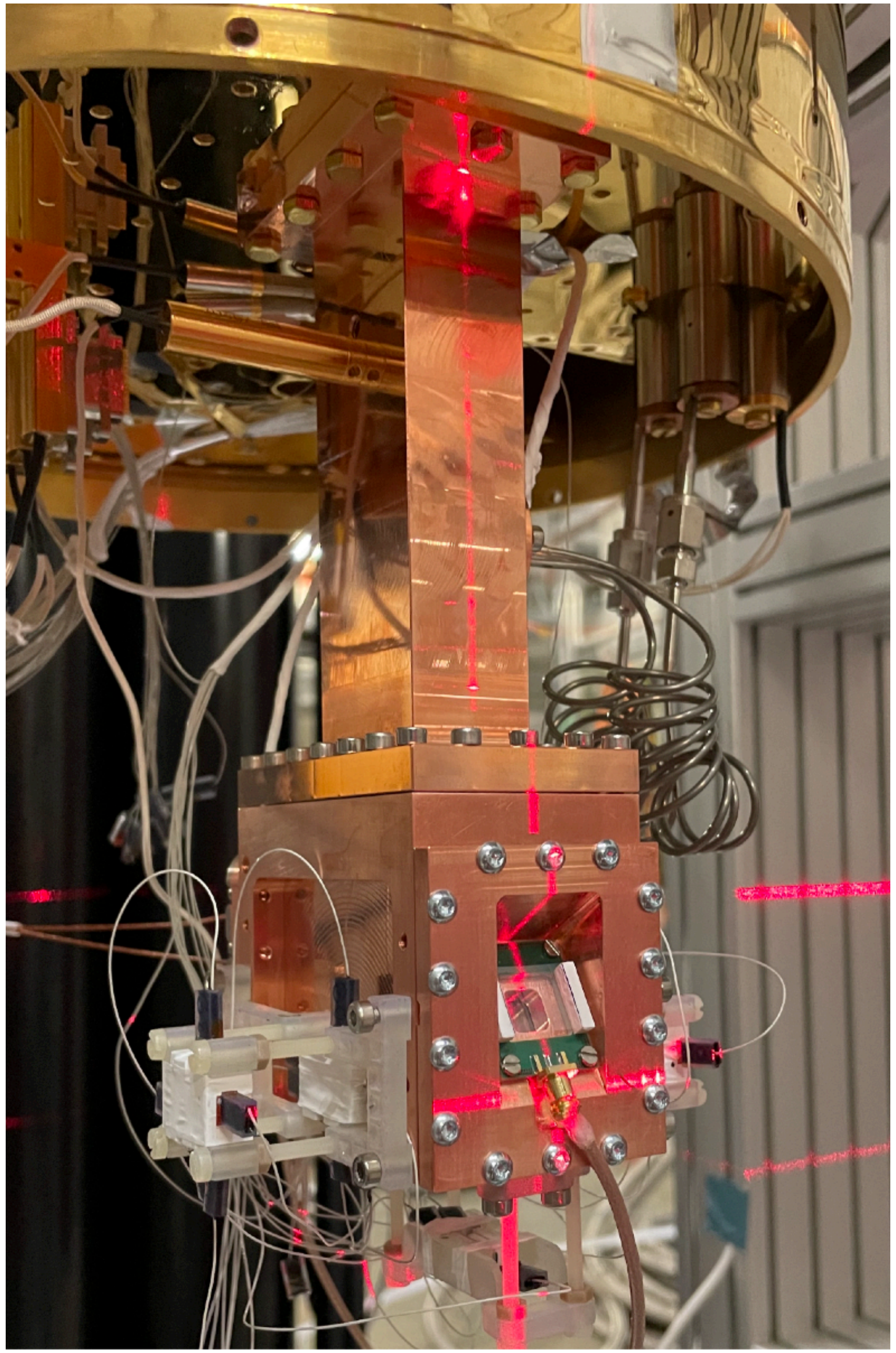

Diffusion time study

- Muons implanted at 11.5-13.0 MeV to different average depth and the diffusion times was studied
- Preliminary result in agreement with the ballistic diffusion model

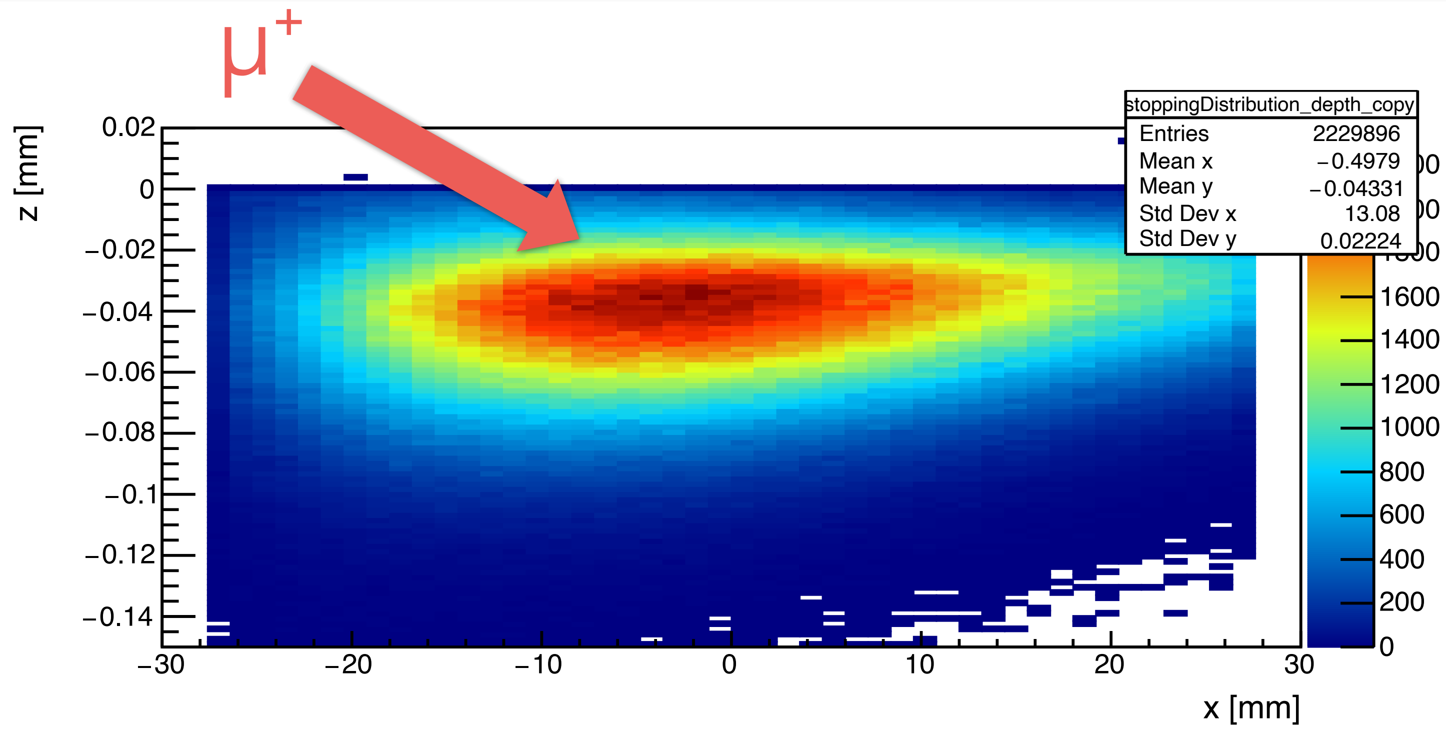

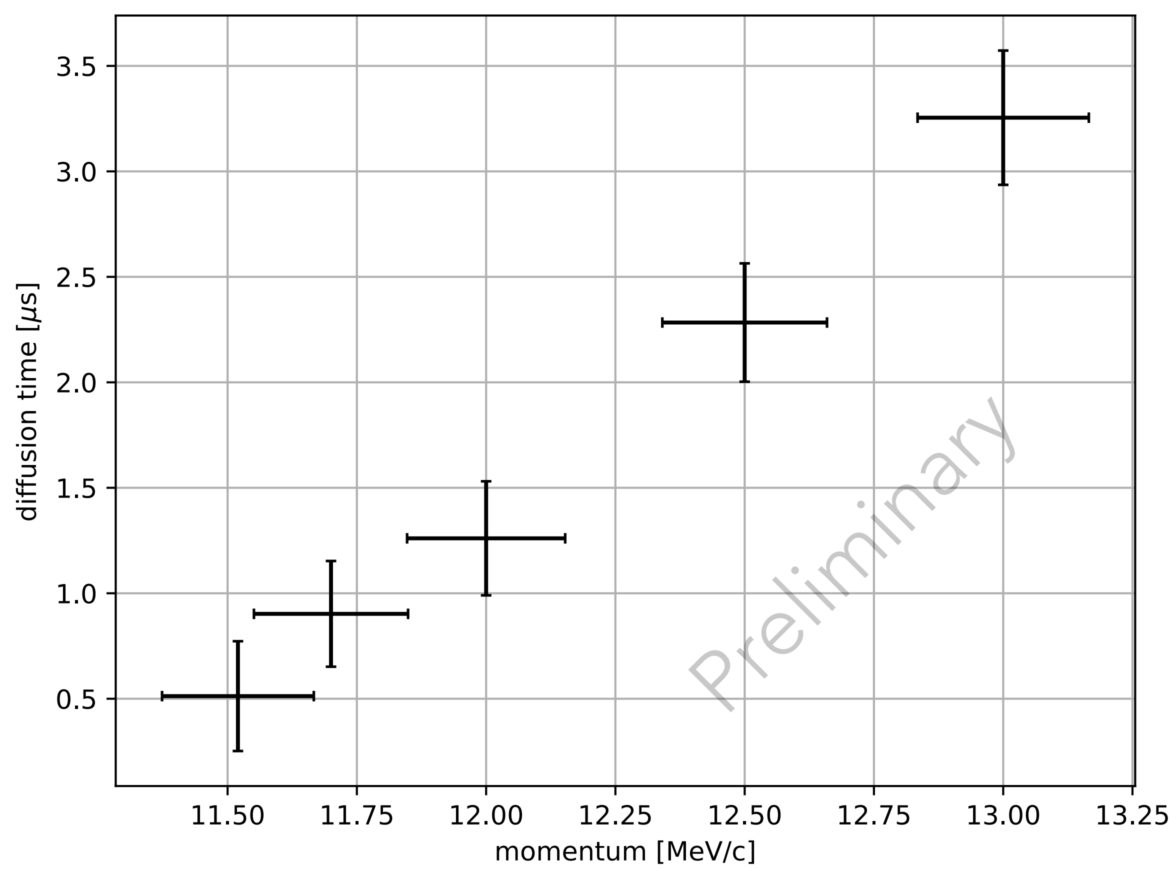

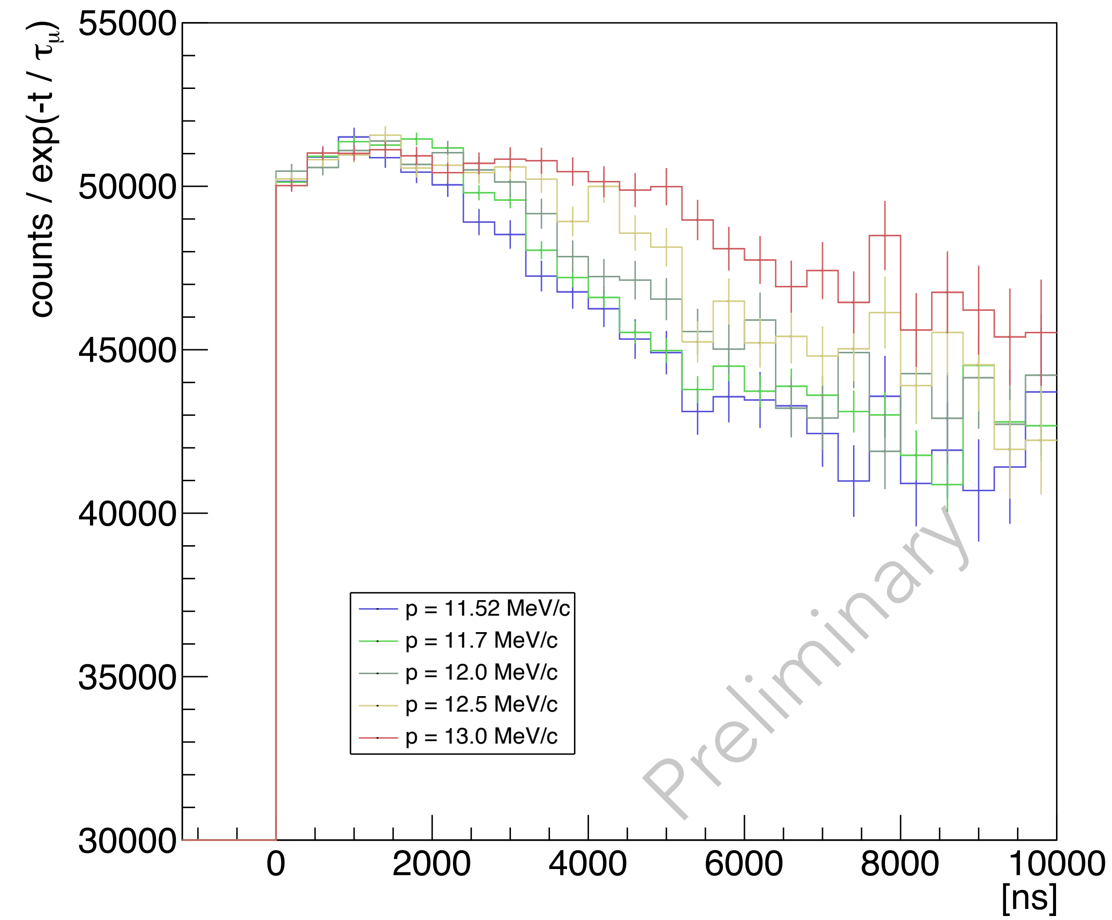

Temperature scan

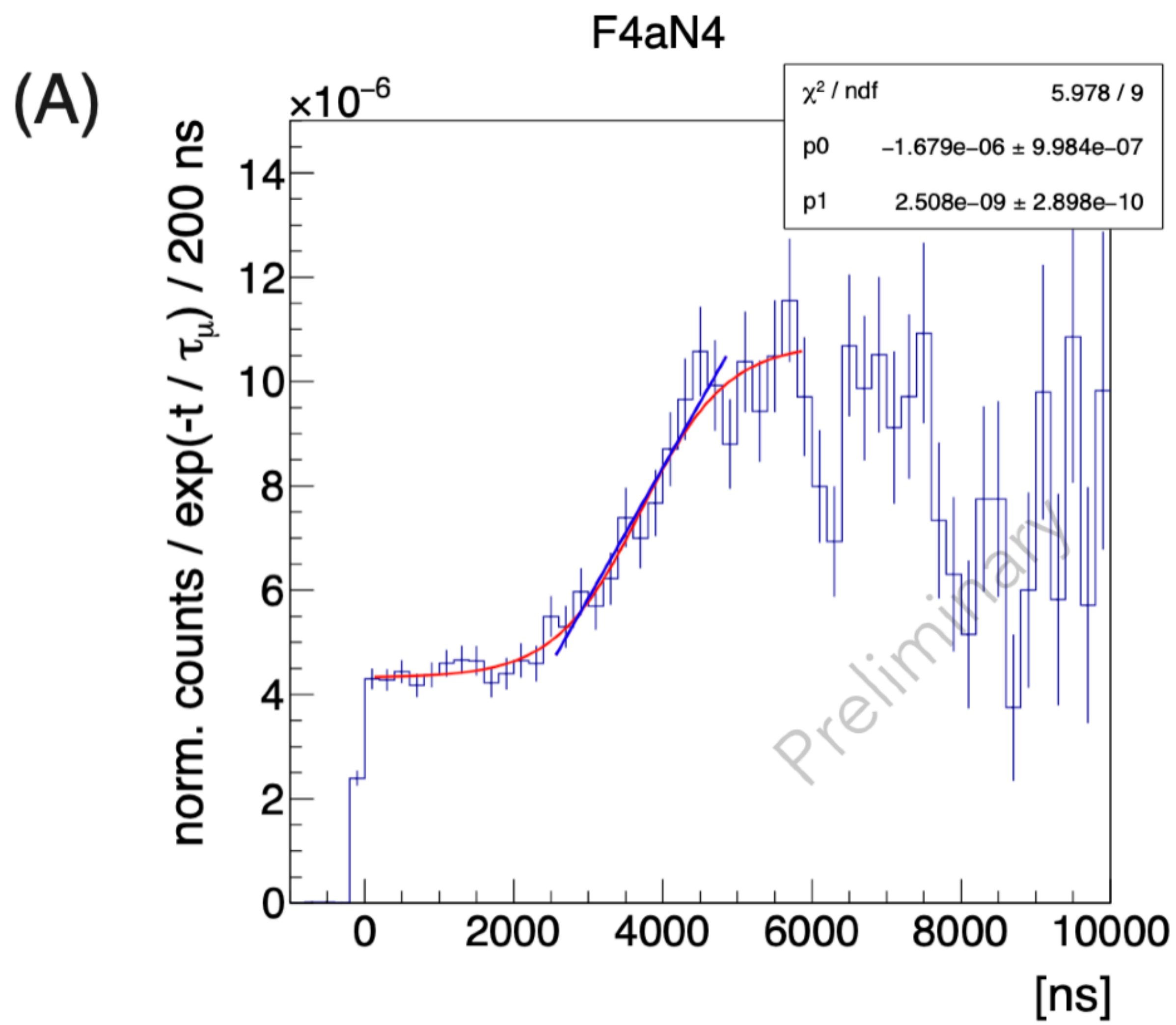

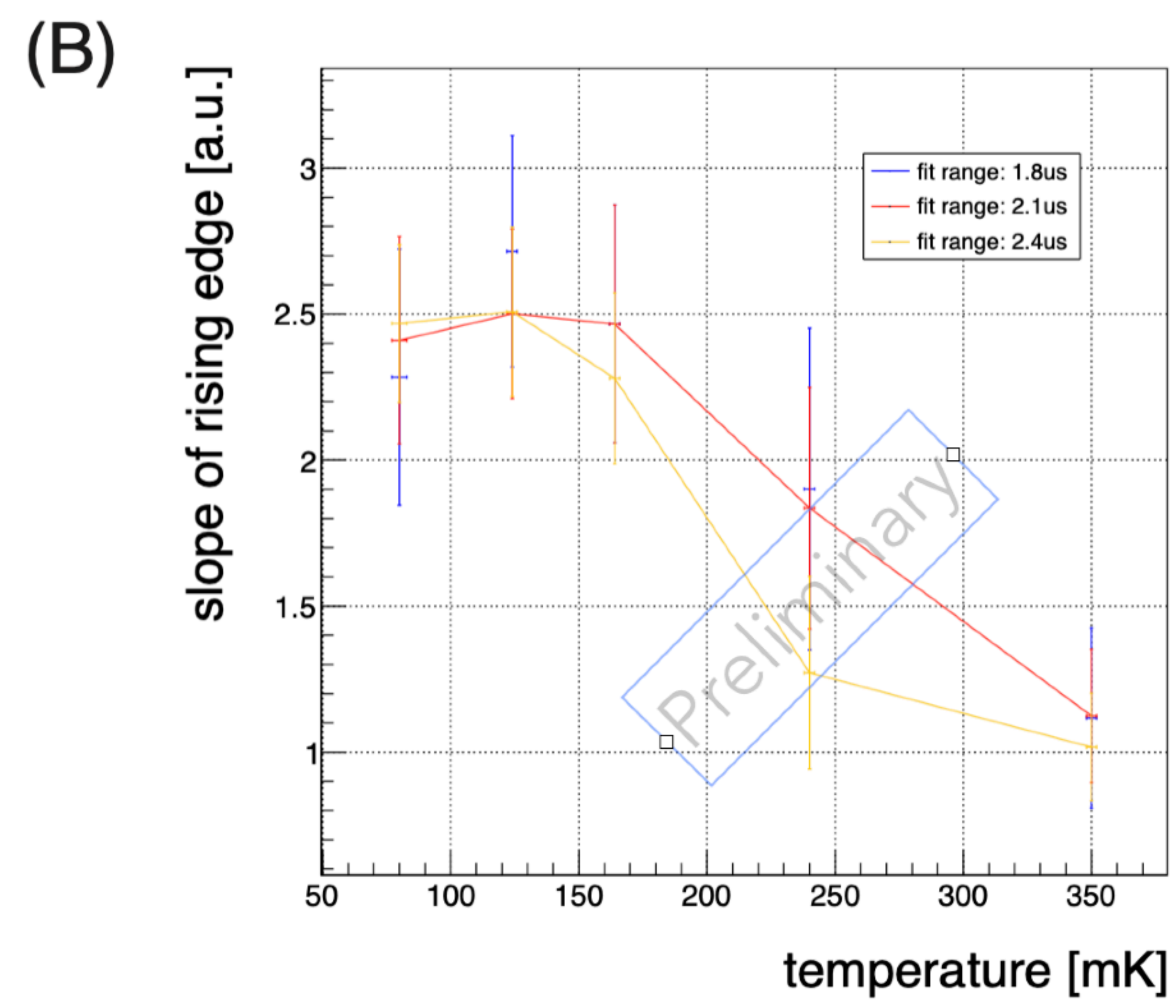

- Adverse scattering effects start above 200 mK
- No obvious advantage at 70 mK vs 120 mK

Setups to develop a horizontal Mu beam

Reflection

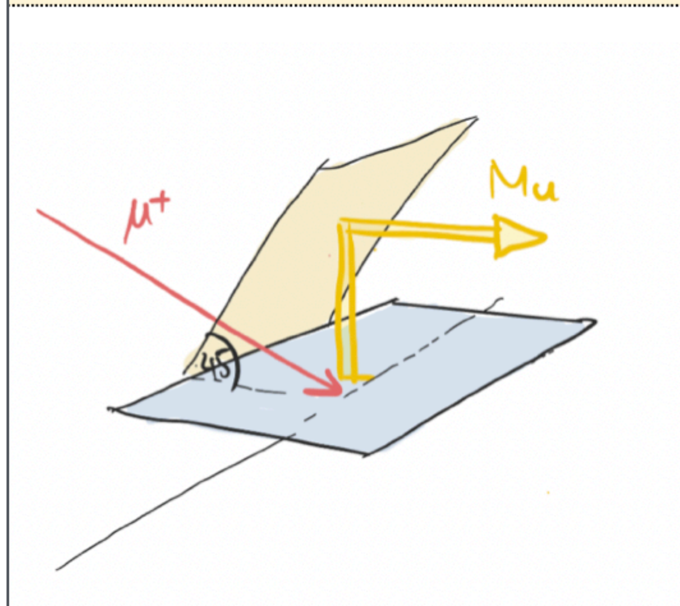

Necessary for the interferometer

Hugely influencing the yield (decay losses)

Microfluidic grating

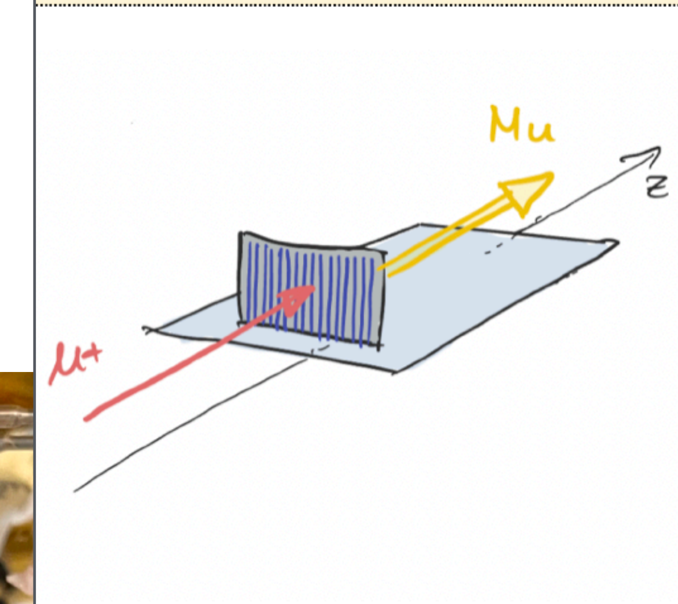

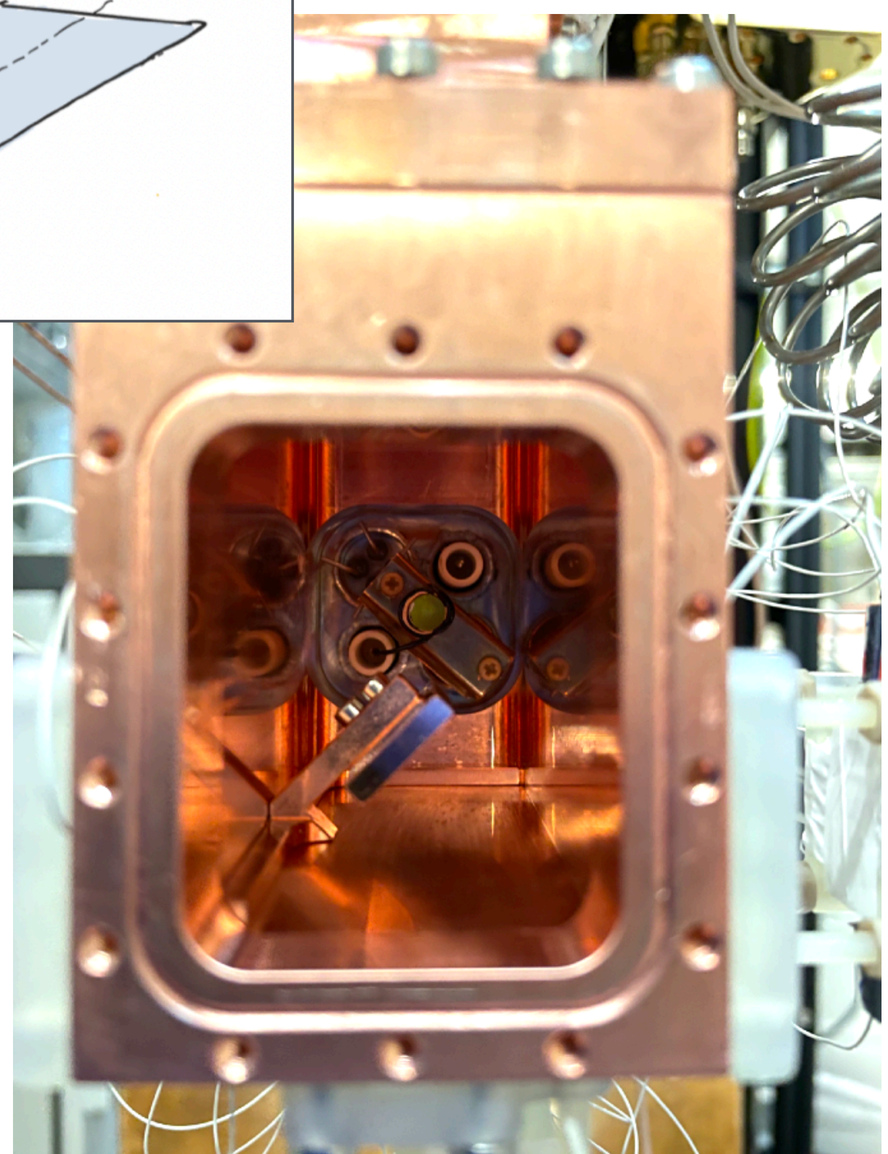

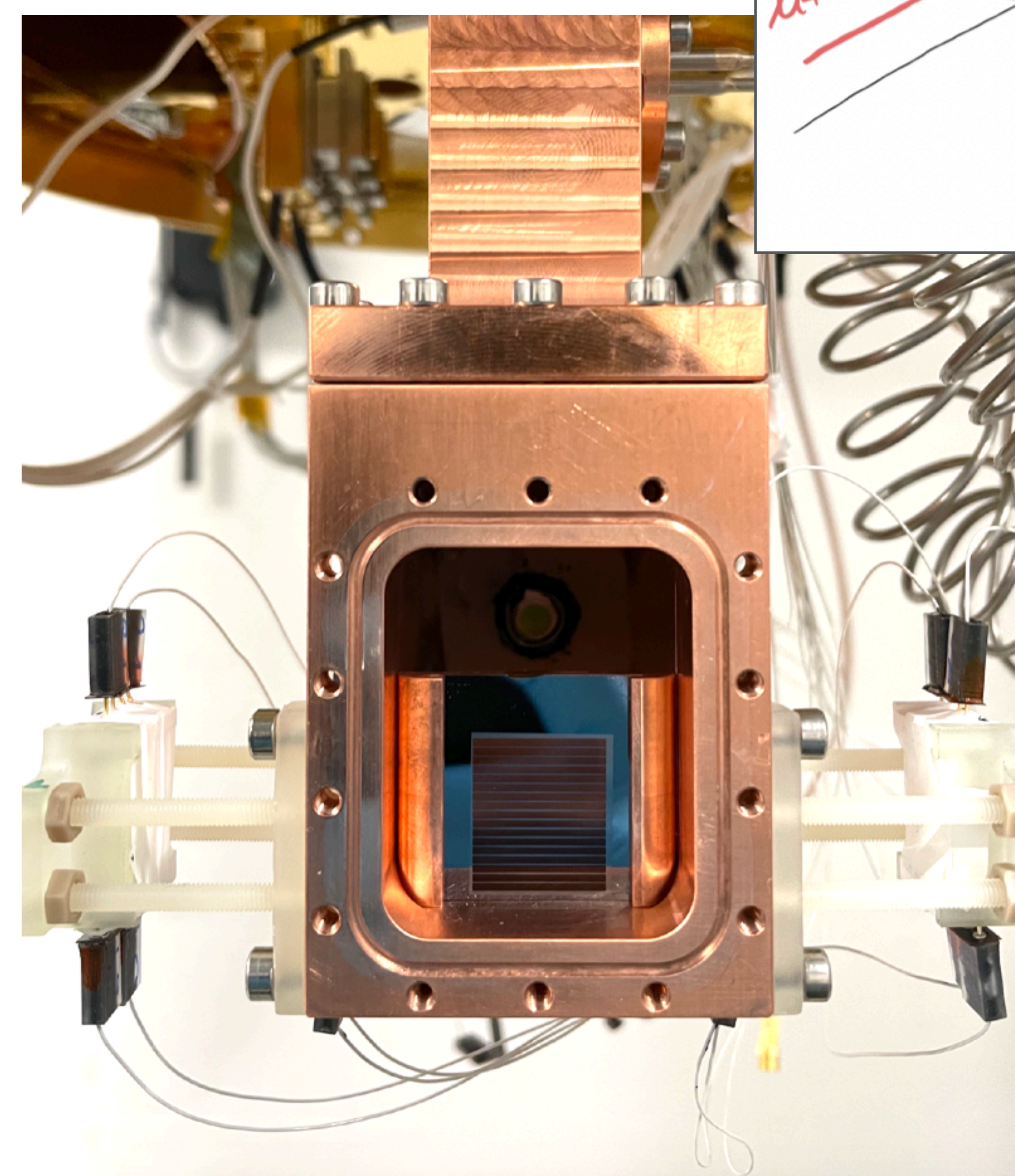

Novel source concept - microfluidic grating

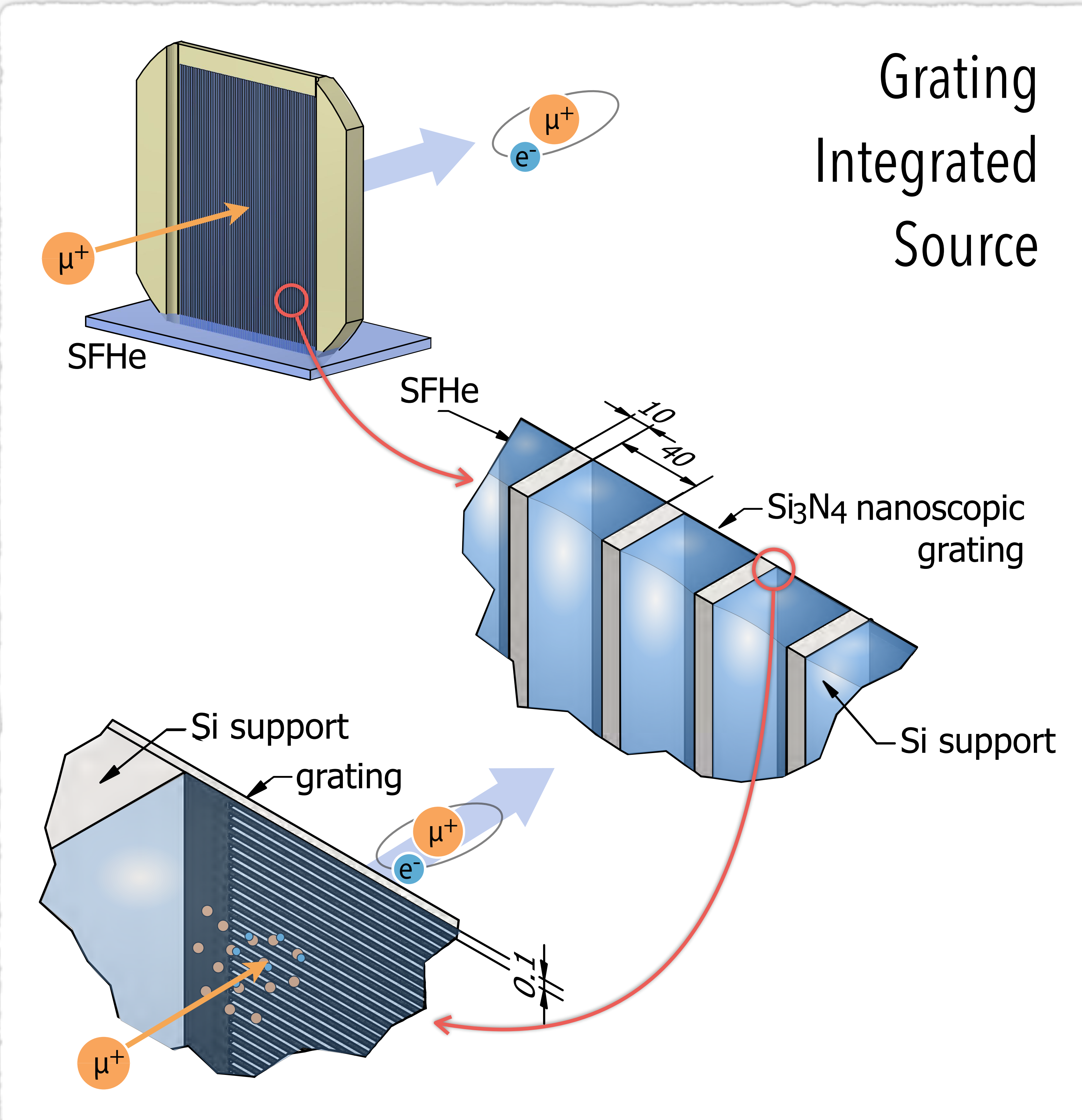

SFHe suspended by the capillary force, between support bars behind the first Si_3N_4 membrane

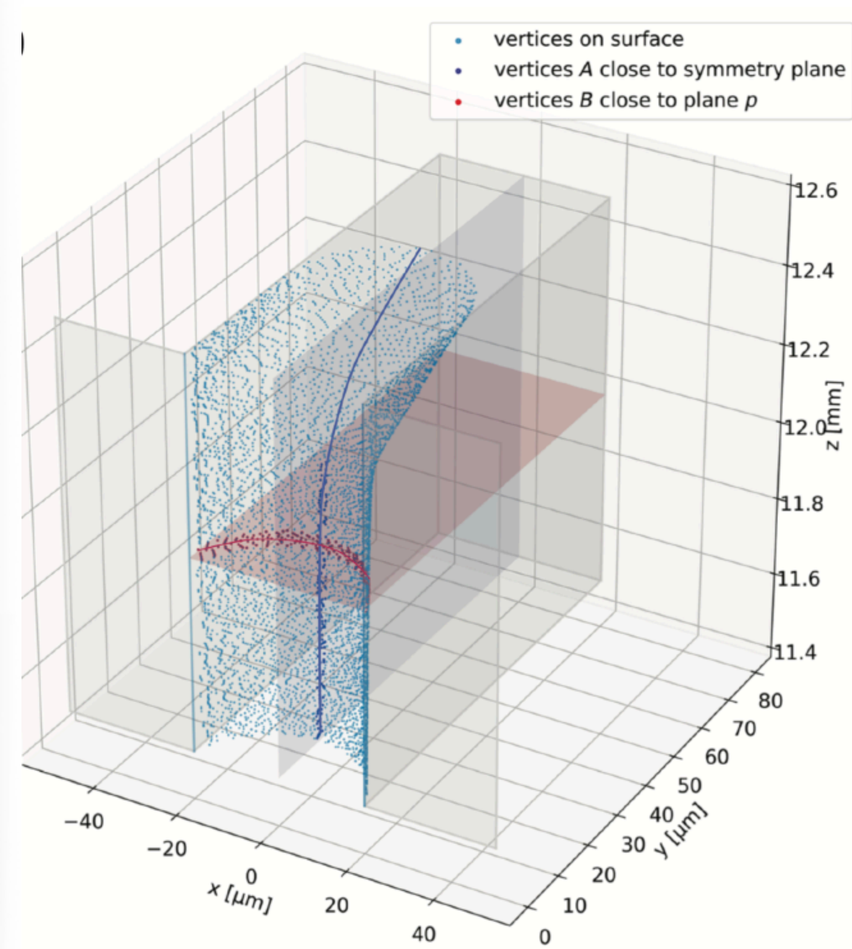

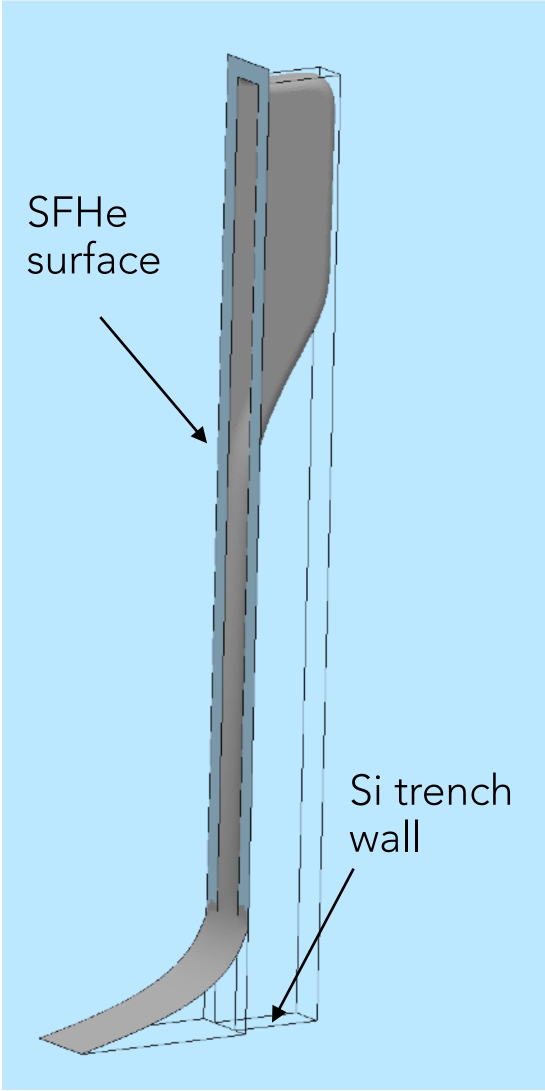

Microfluidic grating prototype

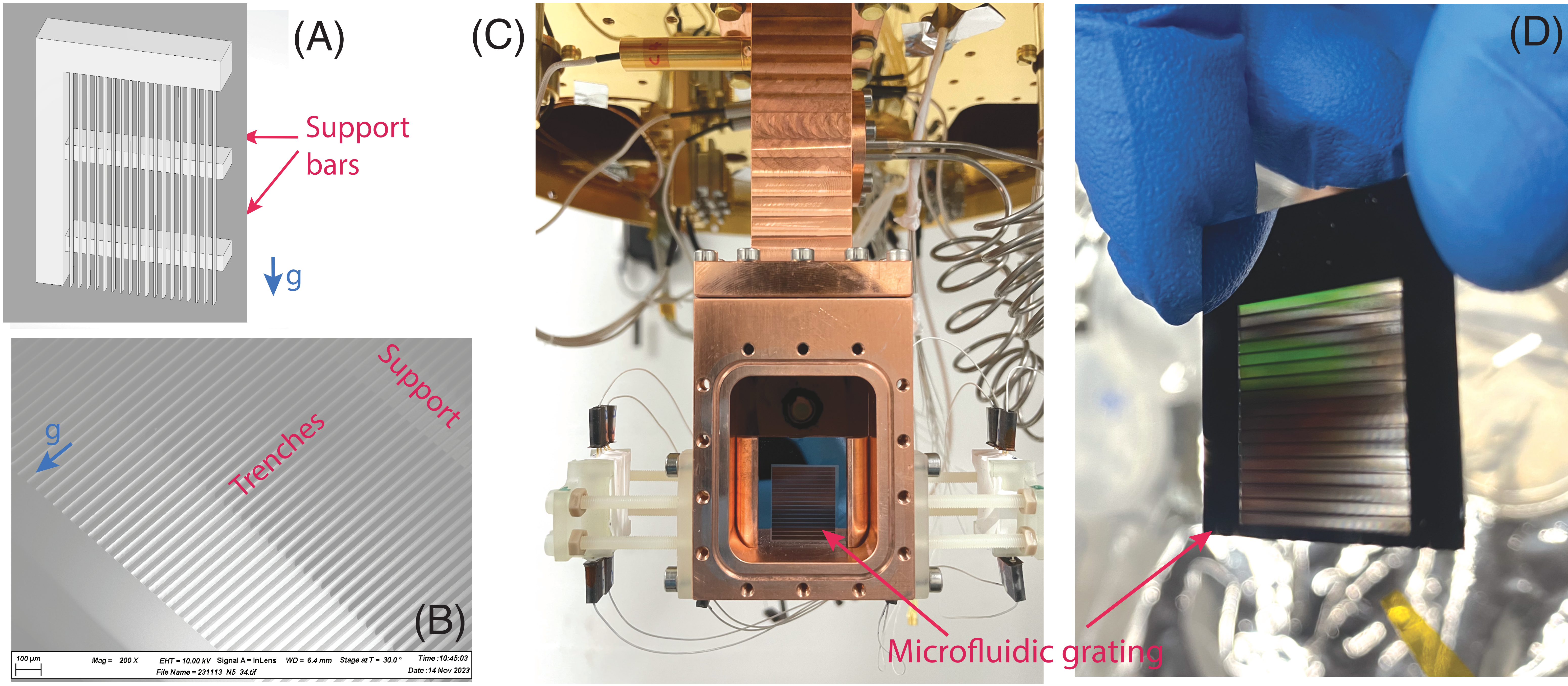

Prototype made by Konstanins Jefimovs, LNQ, PSI

Microfluidic grating in action

Capillary effect (with acetone)

Drying out

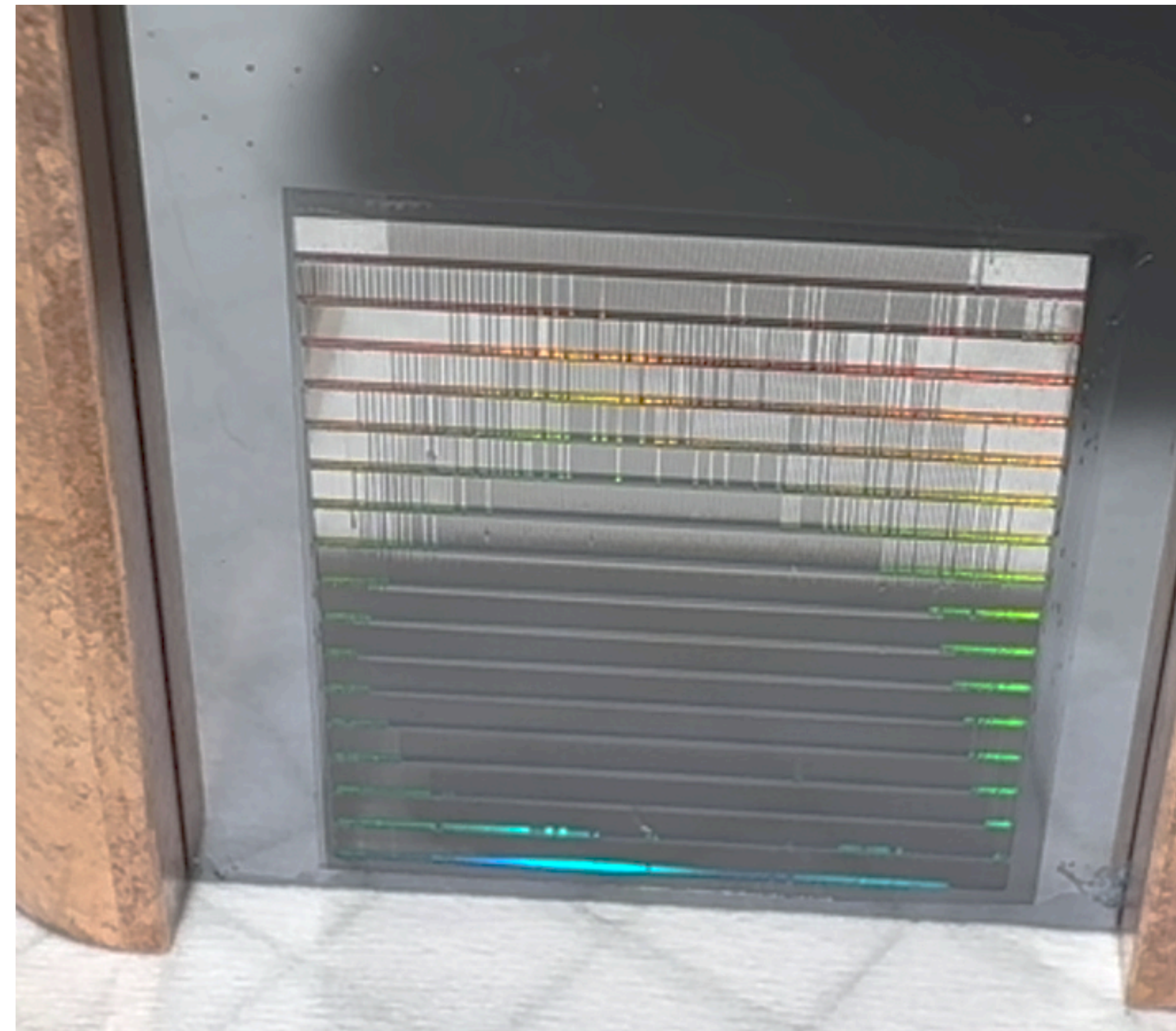

Microfluidic grating in action

Capillary effect (with acetone)

Drying out

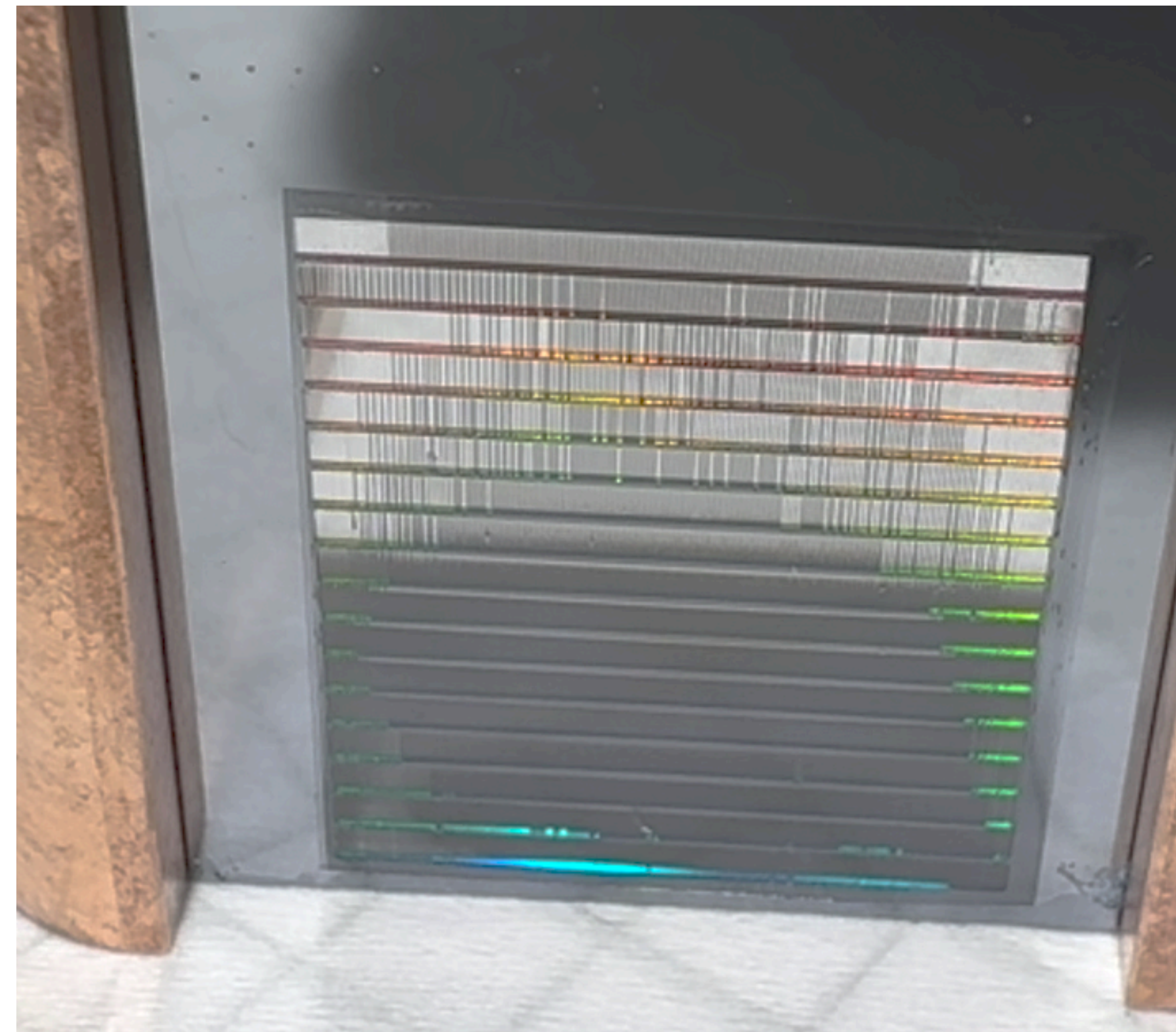

Microfluidic source - preliminary results

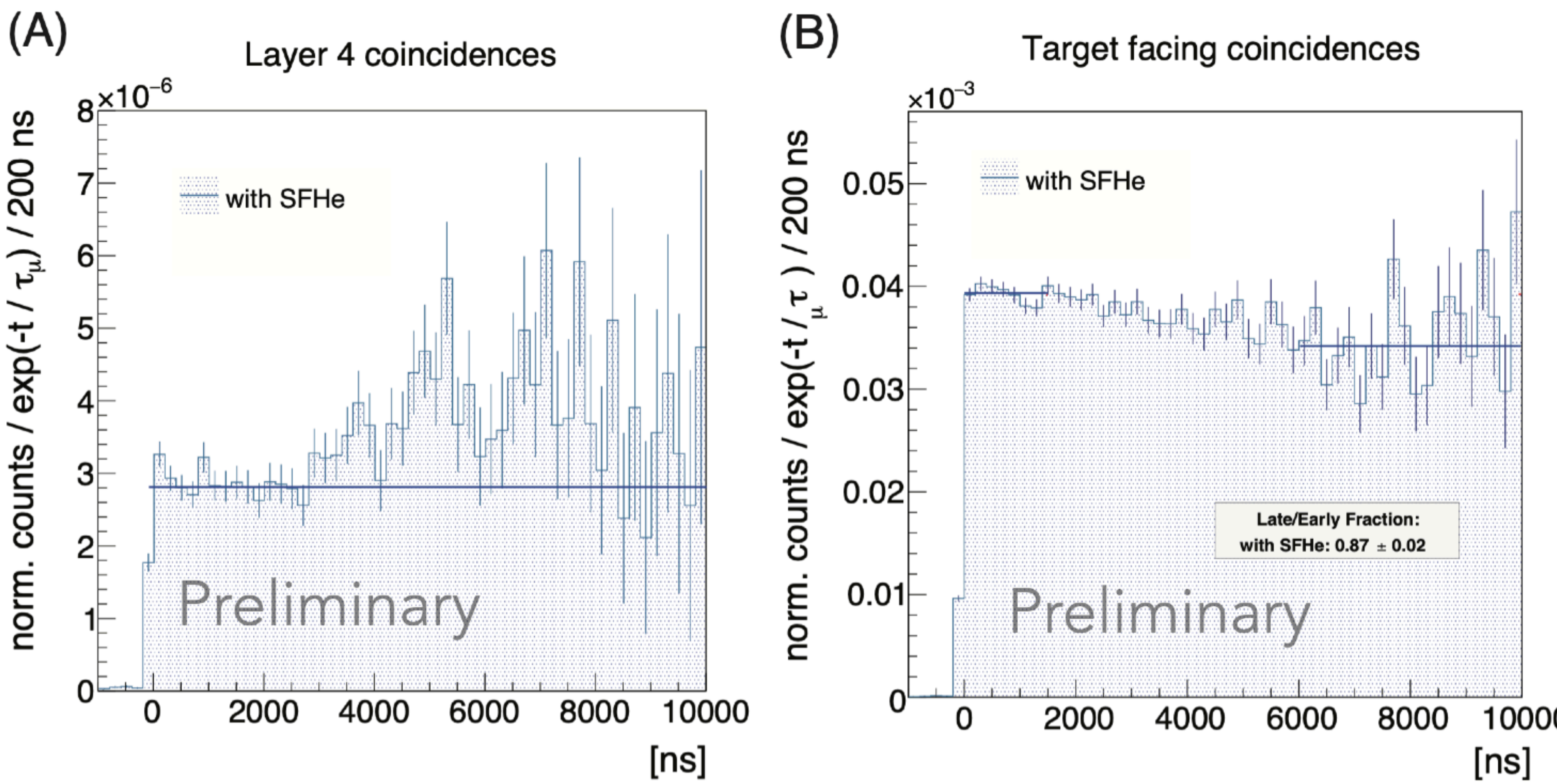

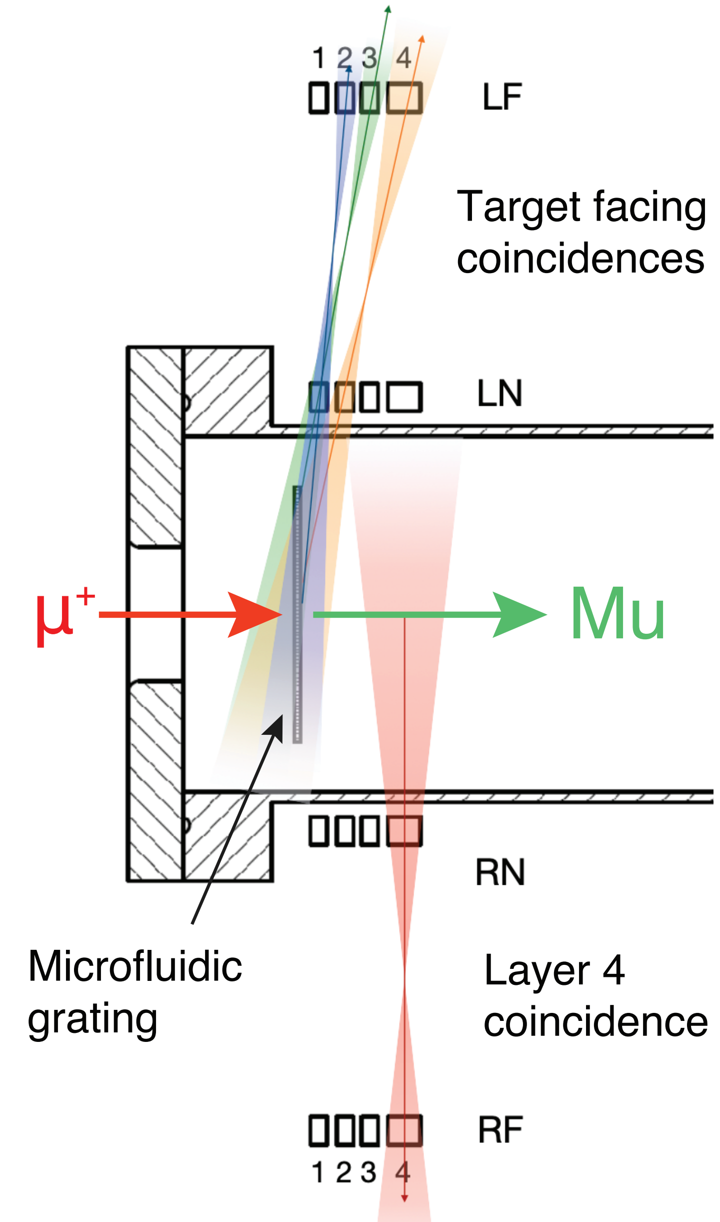

- Clear emission of Mu from the microfluidic target
- Stopped muon to vacuum muonium conversion efficiency seems ca. 1/2 of the free surface emission
- Effected by background further studies are needed

LEMING plans

3 weeks @ piE1 requested for 2024

Assuming success in 2024:

$$\Delta g \approx \frac{1}{2\pi T^2}\frac{d}{C\sqrt{N_0 \epsilon \eta^3 e^{-(t_0+2T)/\tau}}}$$

Grating period
~100 nm

Contrast
$C = A/A_0 \sim 0.3$

Atoms from source
$N_0 > 10^5$/s

Loss factor
$t_0 = 0$ s (!)

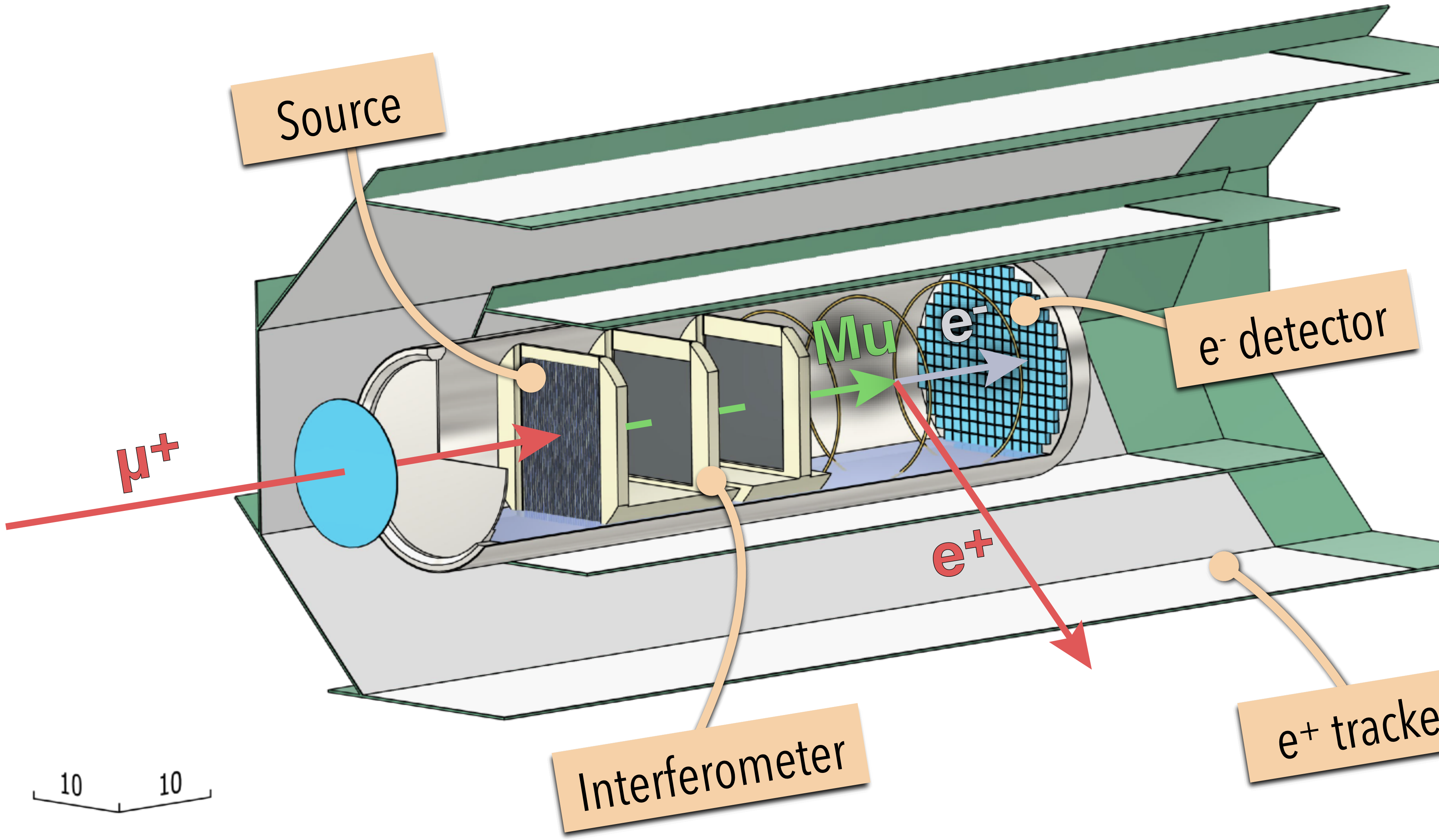

- The test beamtimes are reaching a conclusion
- Experimental layout taking shape, and a full TDR is possible
- Emphasis expected to shift towards the interferometer

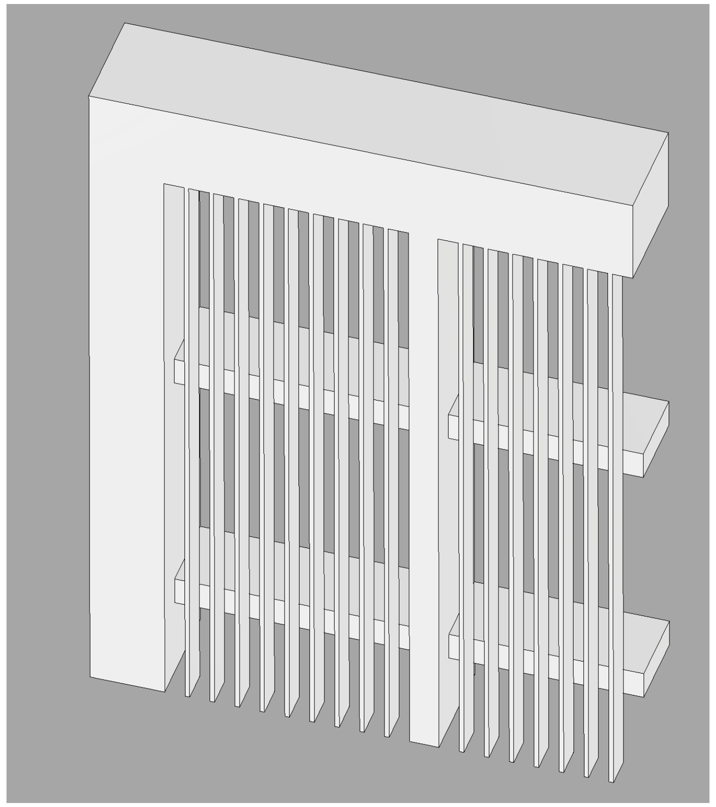

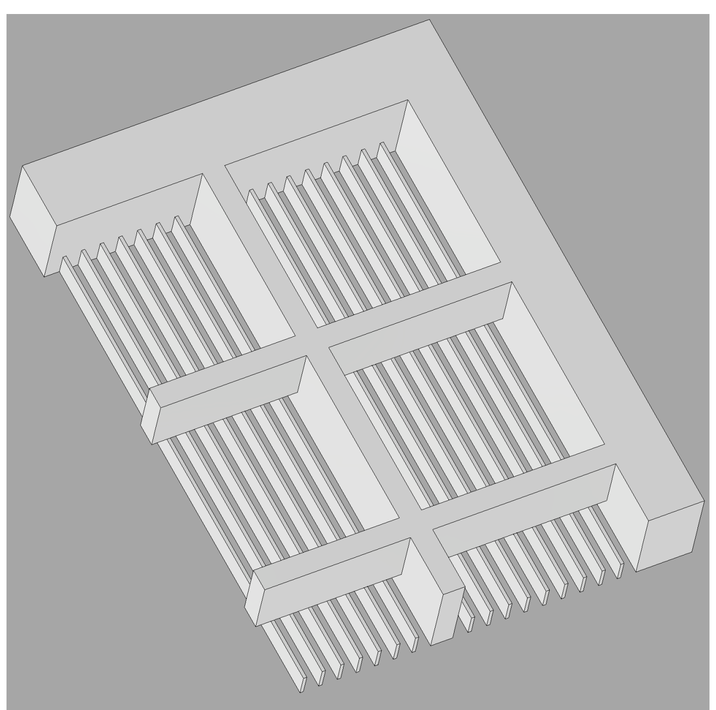

Microfluidic grating

- Study of surface shape and stopping distribution
- Diffusion of Mu in microfluidic target
- Minimizing dead area

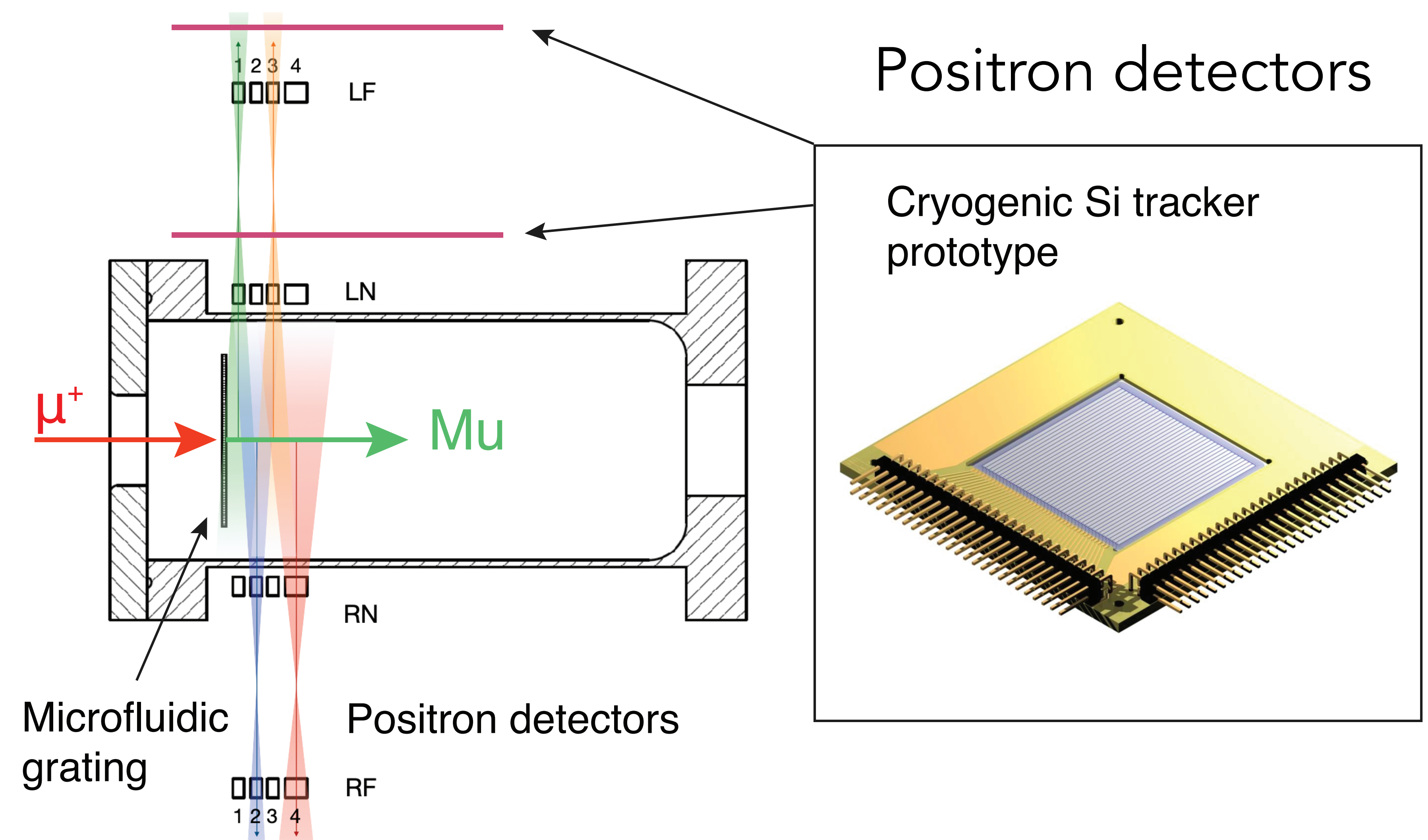

Beamtime 2024: Commissioning atomic e- detectors

- $CsPbBr_3$ shows remarkable scintillation properties at cryogenic temperatures [V. B. Mykhaylyk et al., Nature 10, 8601 (2020)]
- $CsPbBr_3$ has higher light yield than EJ-204 at cryogenic temperatures
- Low voltage onset, 3+ kV

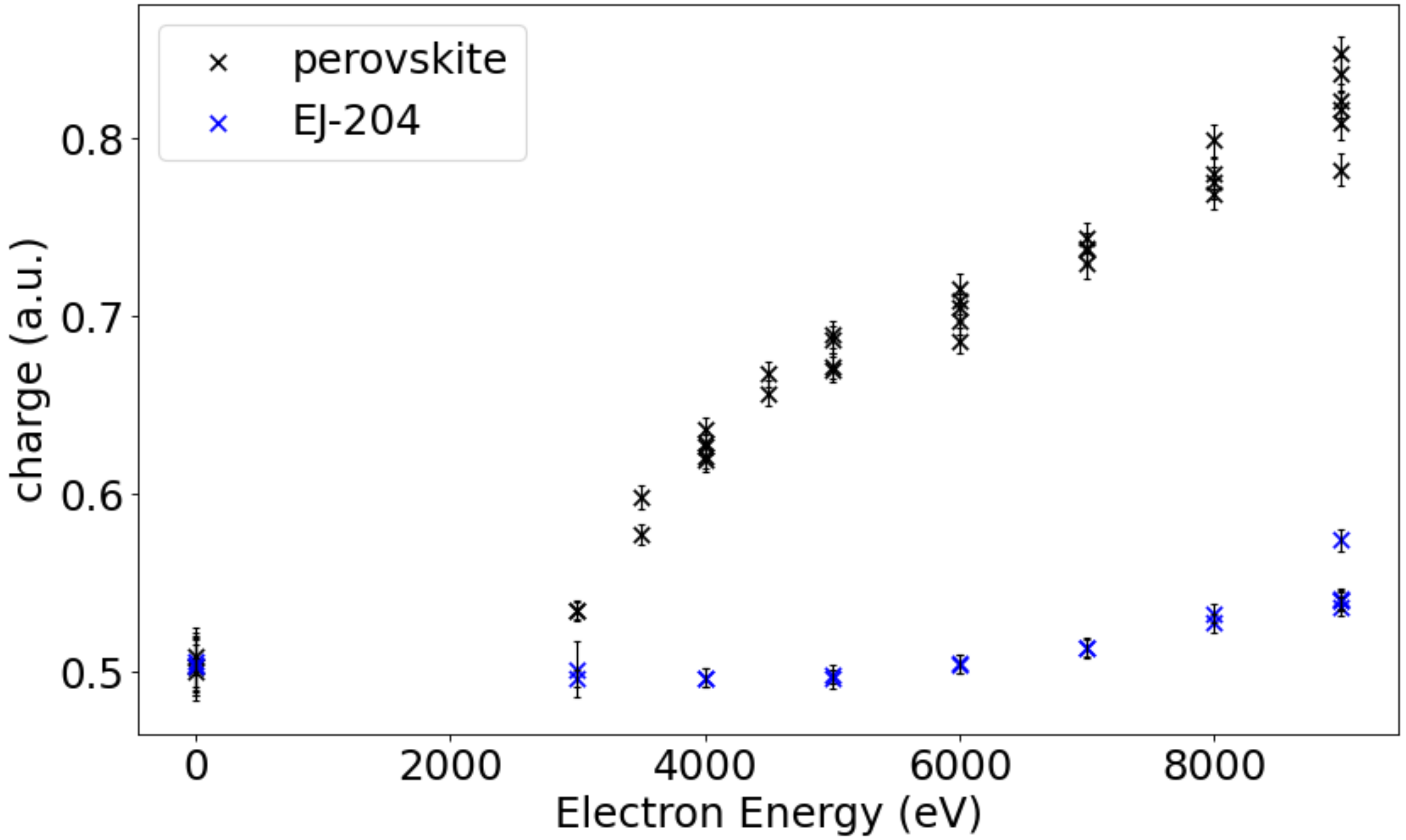

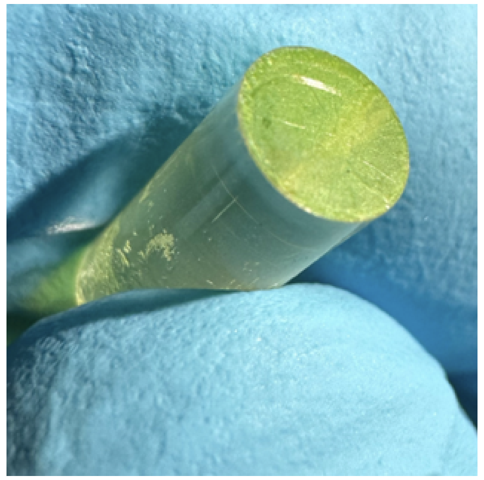

Perovskite Nanocrystals

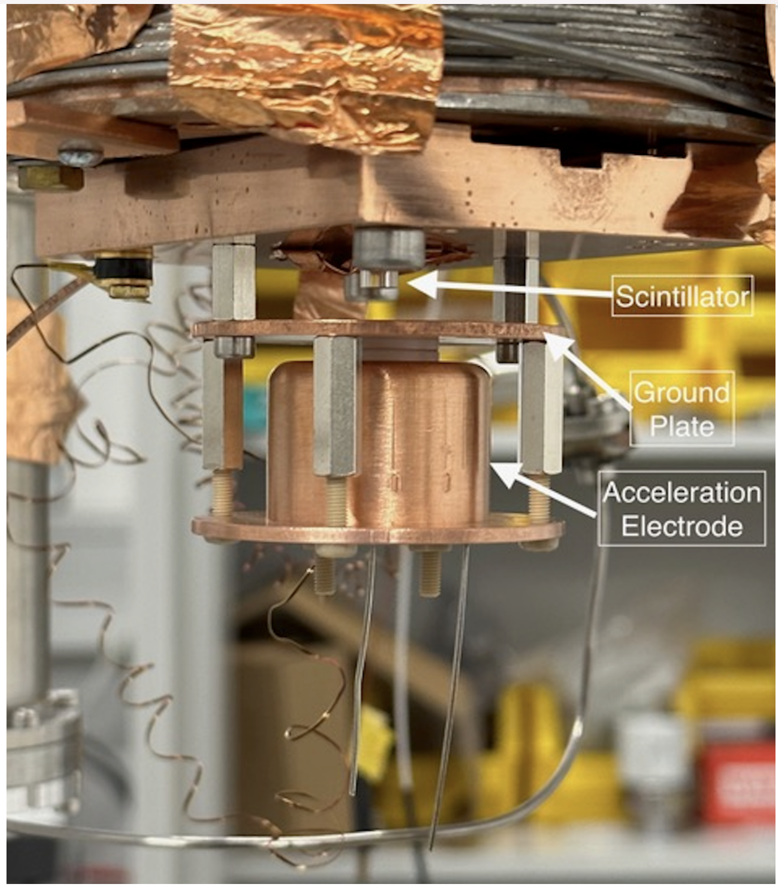

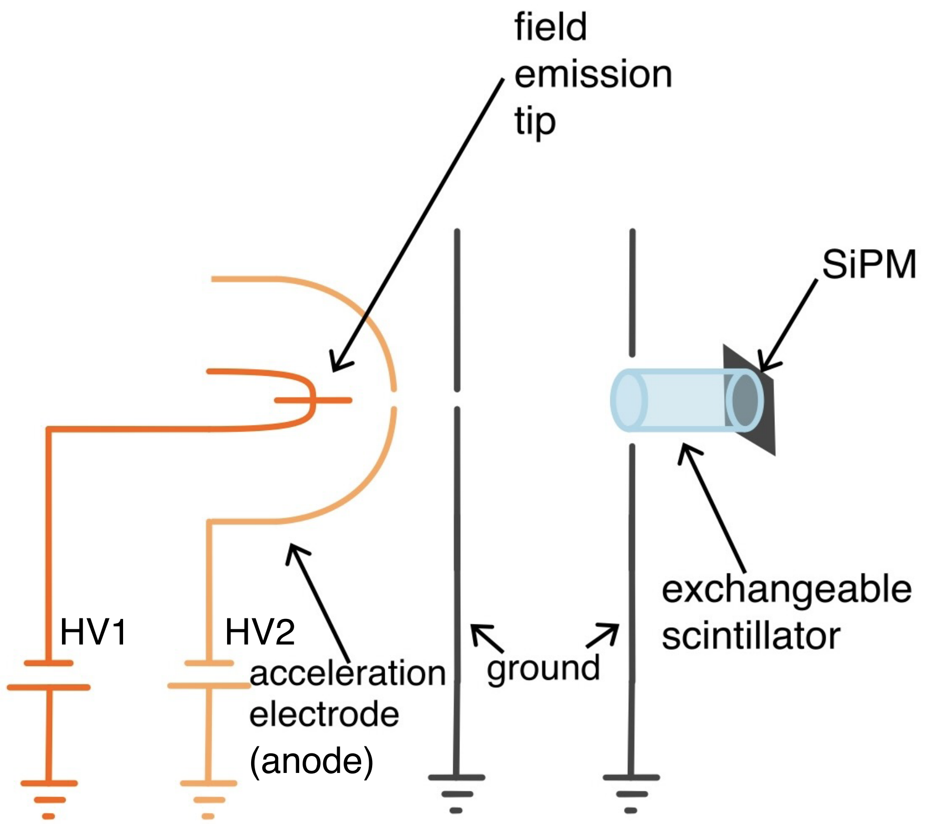

Offline 2024: interferometer progress and plans

Scanning, stabilization, calibration

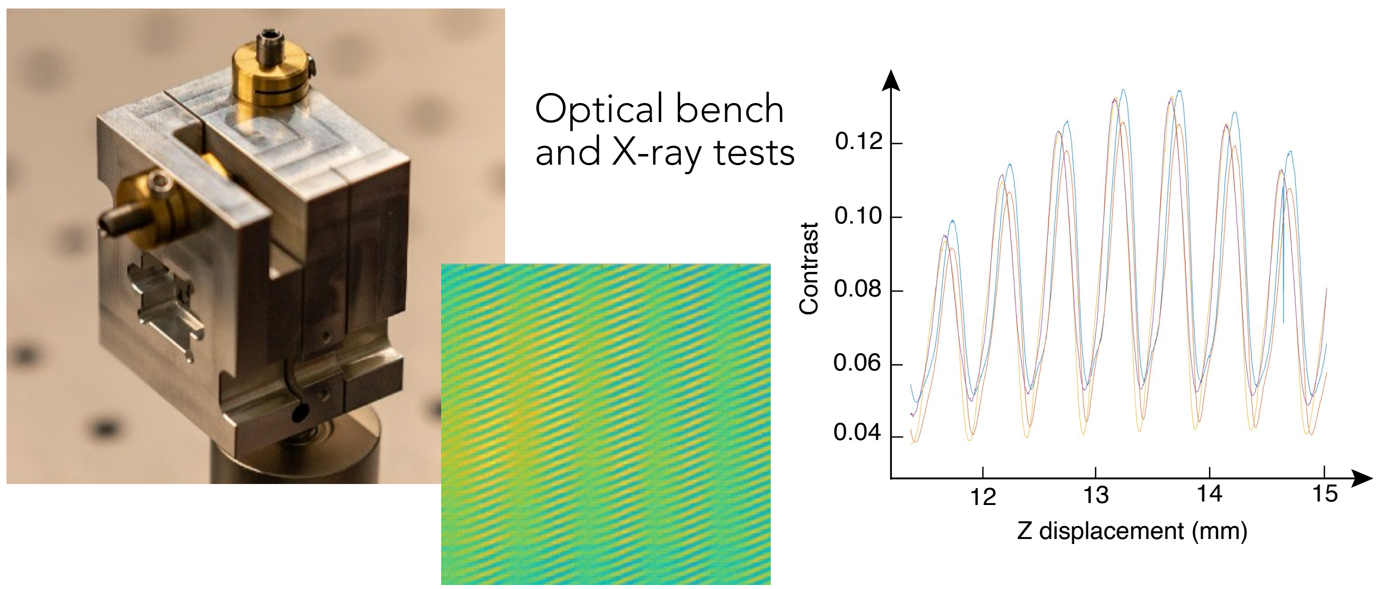

- Monitoring alignment with Fabry-Perot (~10 pm)
- Vertical scanning (~pm) with piezo actuators
- Calibration sources: X-rays and UV laser

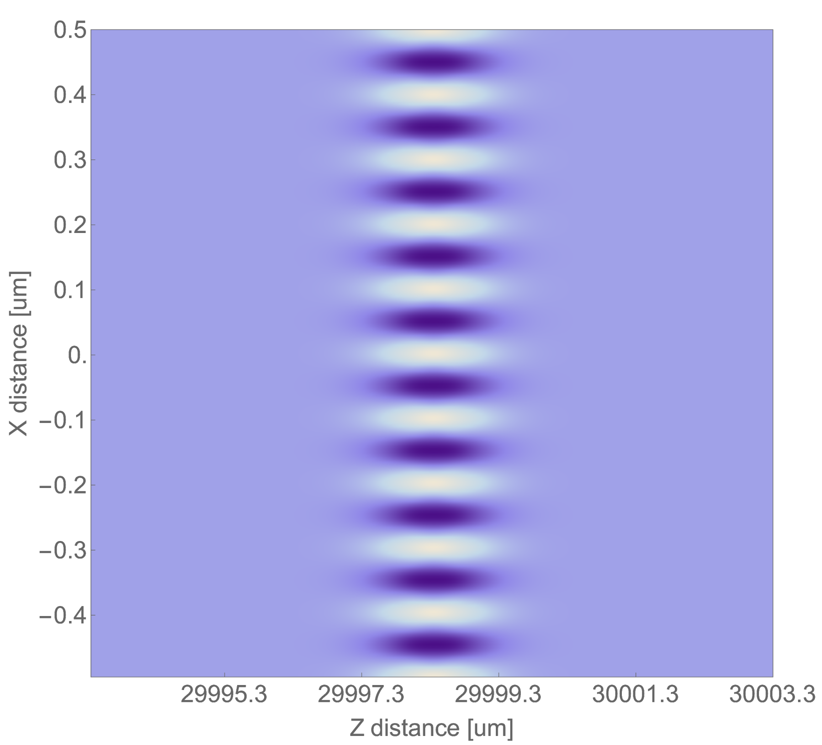

Fabrication

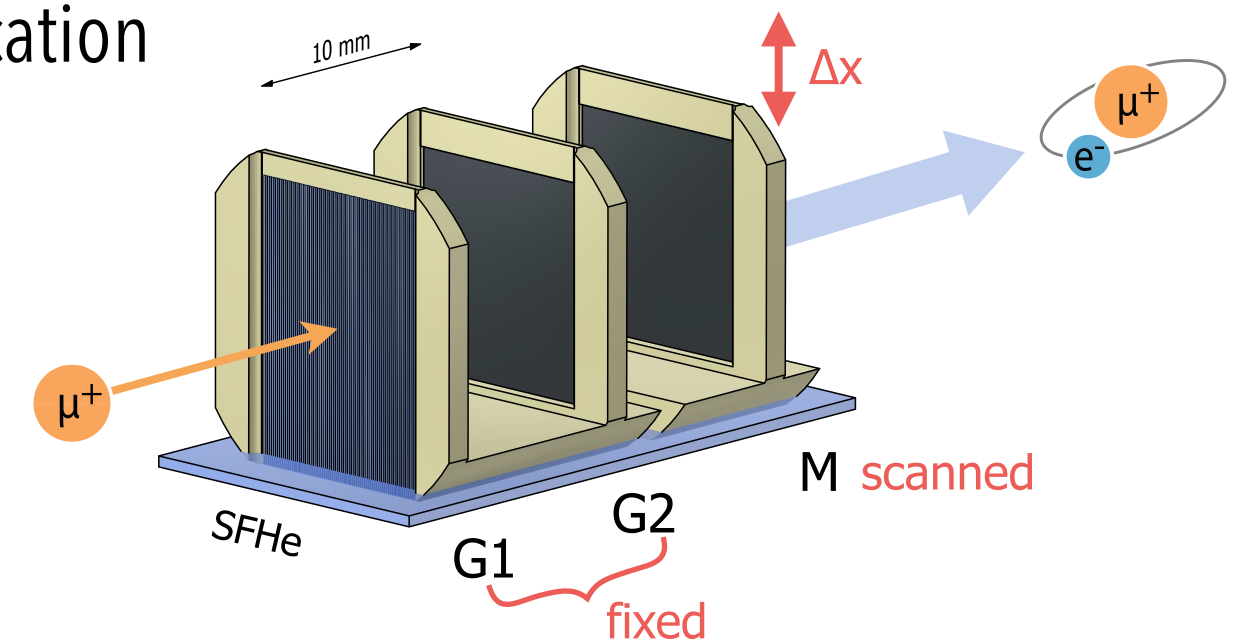

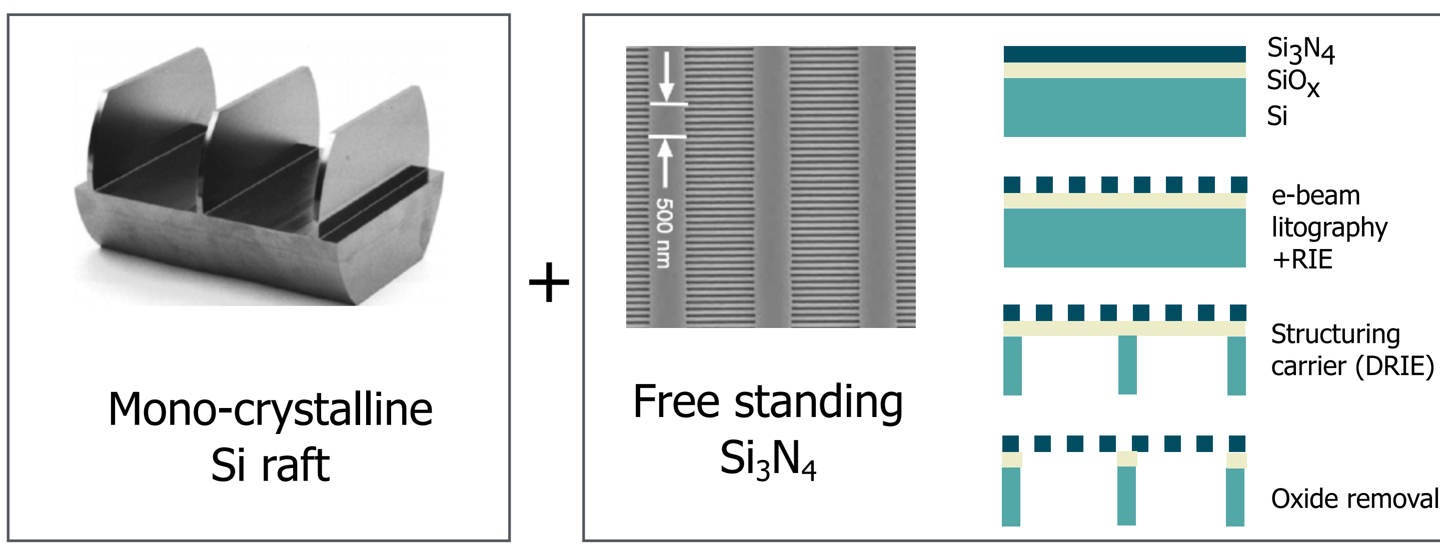

- Fabrication of mono-crystalline Si raft and free standing Si_3N_4 grating separately
- Alignment and **fusion bonding** the parts

Thank you!





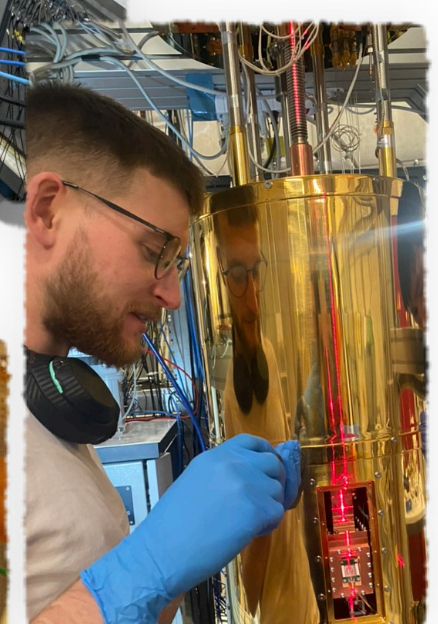

SNSF
Starting
Grant

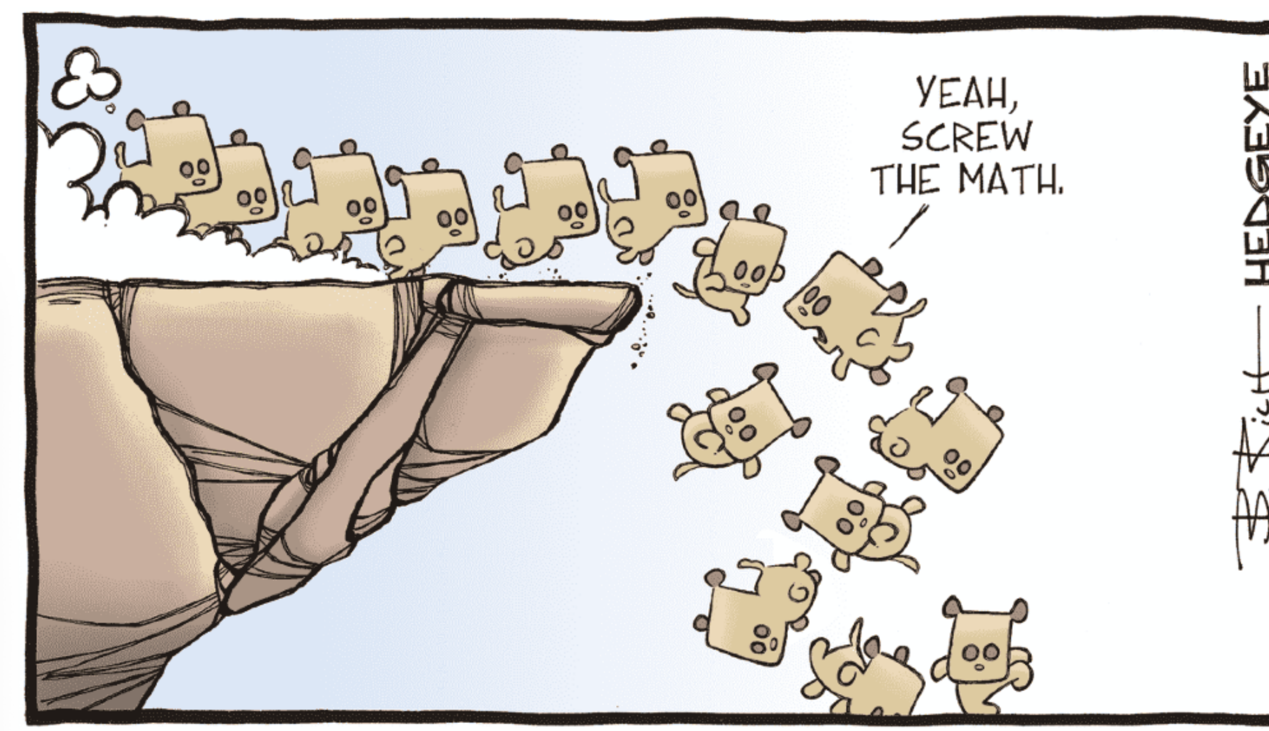

The expected experimental outcome when LEptons in Muonium INteracting with Gravity:

Extra Slides

Impact beyond gravity, spin-offs

Cold Mu atoms

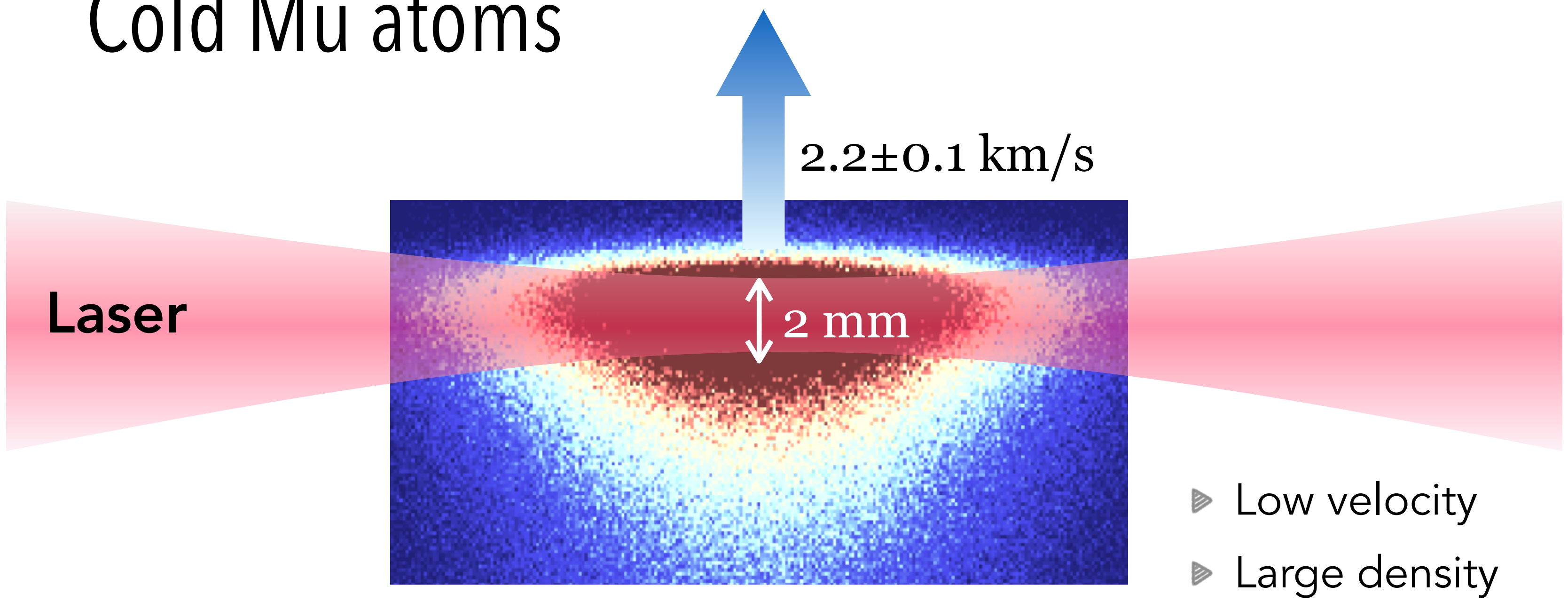

- Low velocity
- Large density phasespace

Cold Mu atoms

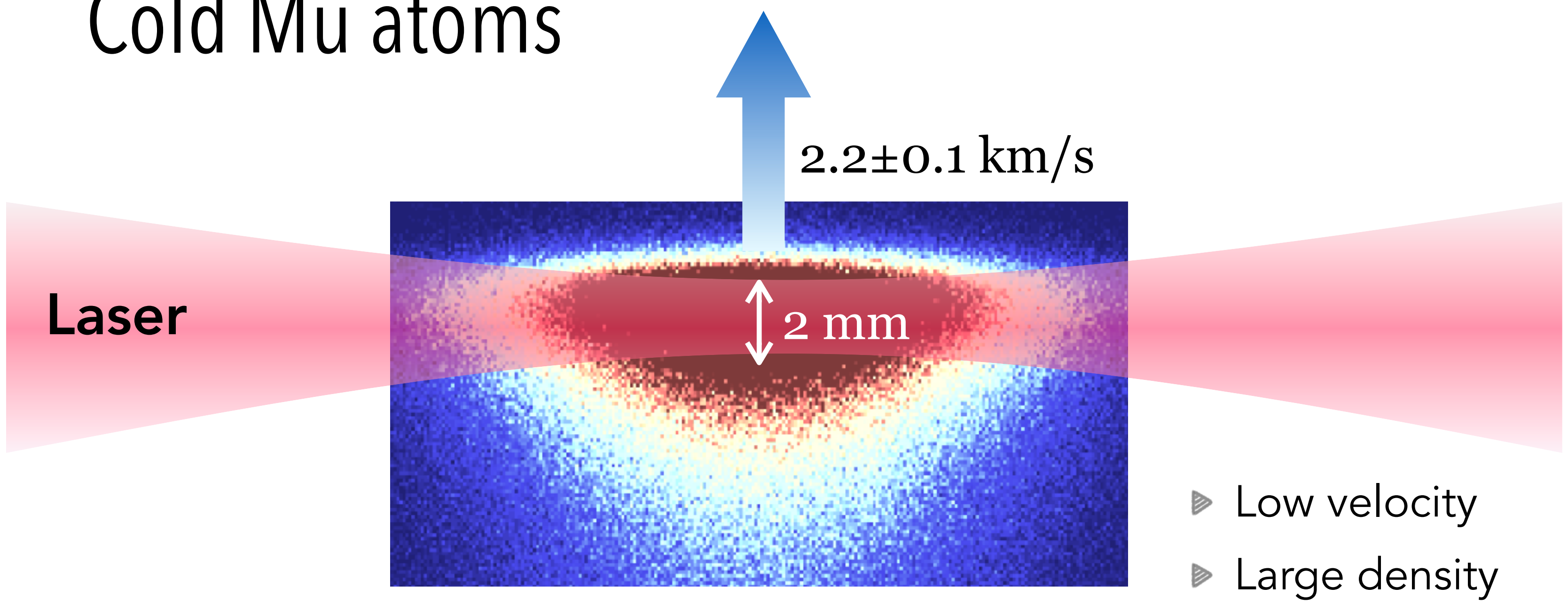

- Low velocity
- Large density phasespace

1S-2S Laser Spectroscopy

Possibility for sub-kHz (~10^{-12}) spectroscopy

- Statistics $\sim \times 10^3$
- Transit-time broadening $\sim 1/3$
- Second order Doppler shift $\sim 1/10$

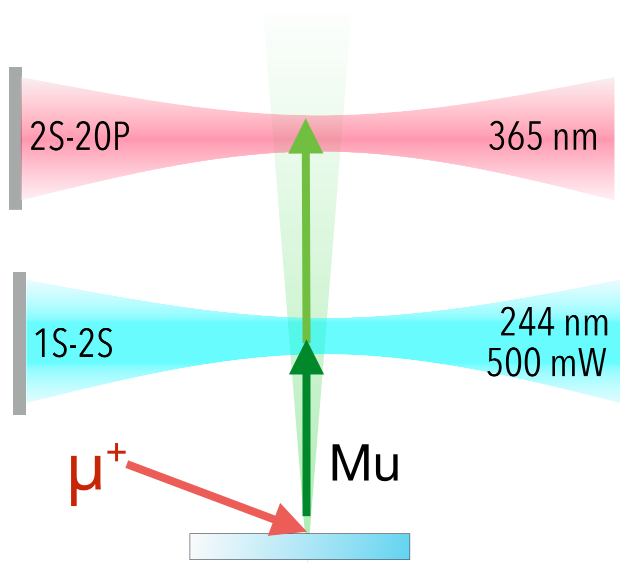

Impact beyond gravity, spin-offs

Cold Mu atoms

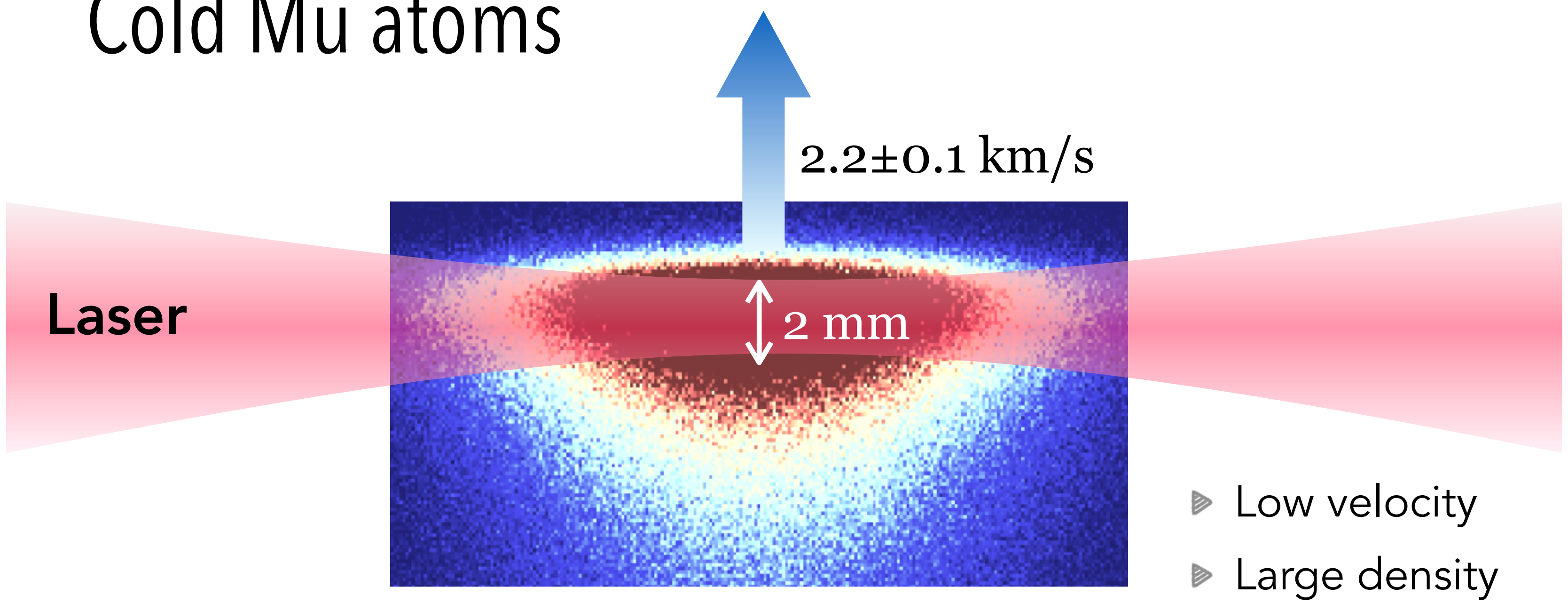

- Low velocity
- Large density phasespace

1S-2S Laser Spectroscopy

Possibility for sub-kHz (~10^{-12}) spectroscopy

- Statistics $\sim \times 10^3$
- Transit-time broadening $\sim 1/3$
- Second order Doppler shift $\sim 1/10$

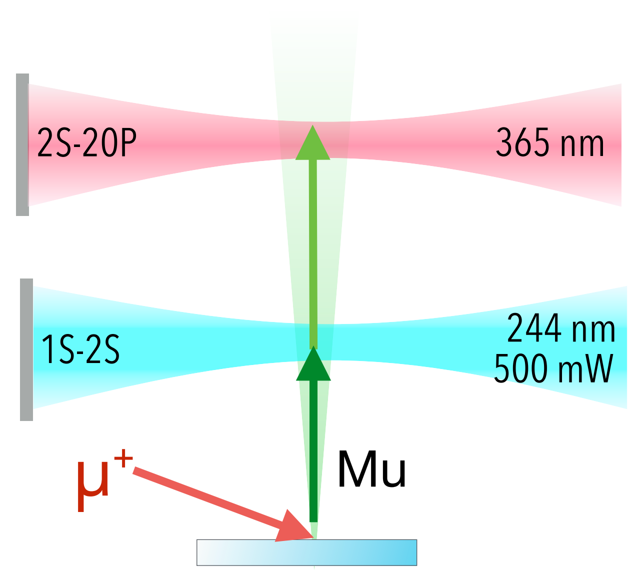

High brightness muon beam

Muon colliders

Sustainable, precision HEP

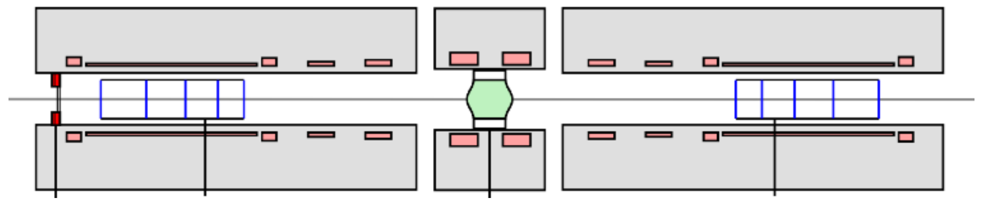

Alternative to ionization cooling (MICE), *Nature* **578** (53-57) 2020

Solid state physics, muon EDM

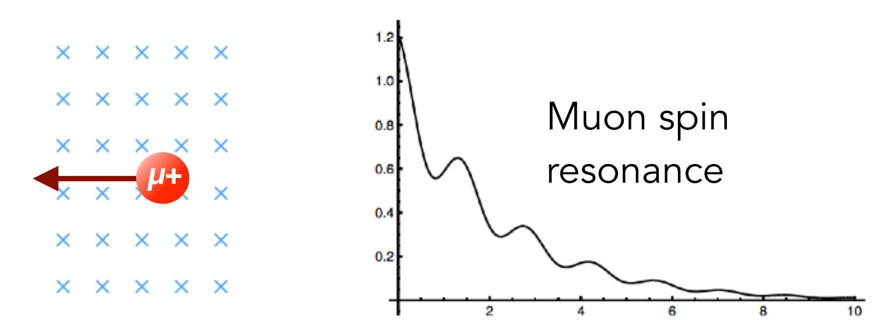

Cryogenic detection techniques (WP2)

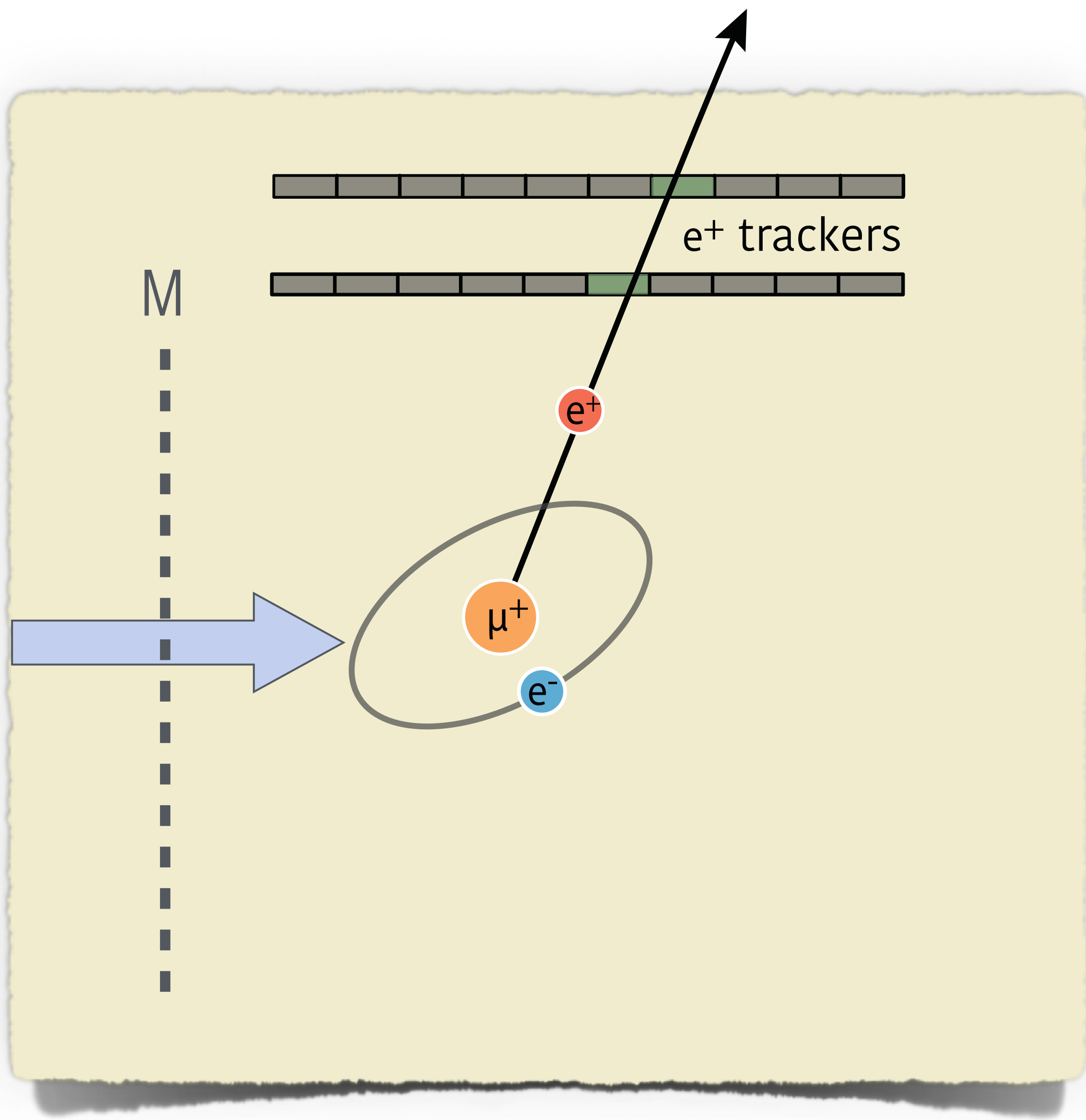

Positron tracker

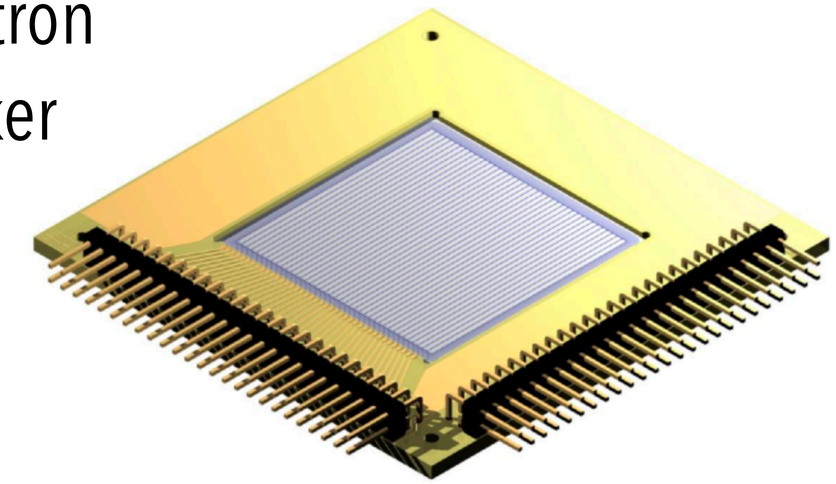

- 1 K temperature, limited cooling power
- low noise, decoupled preamplifiers

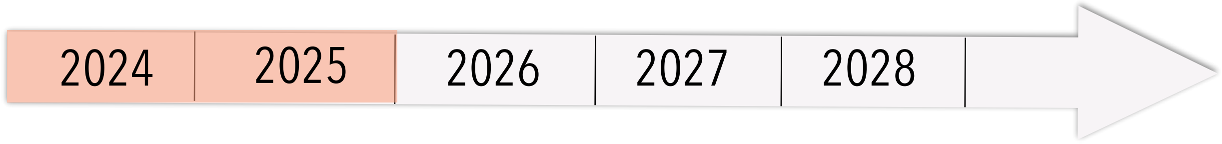

J. Zhang *et al* 2022 *JINST* **17** P06024

Cryogenic detection techniques (WP2)

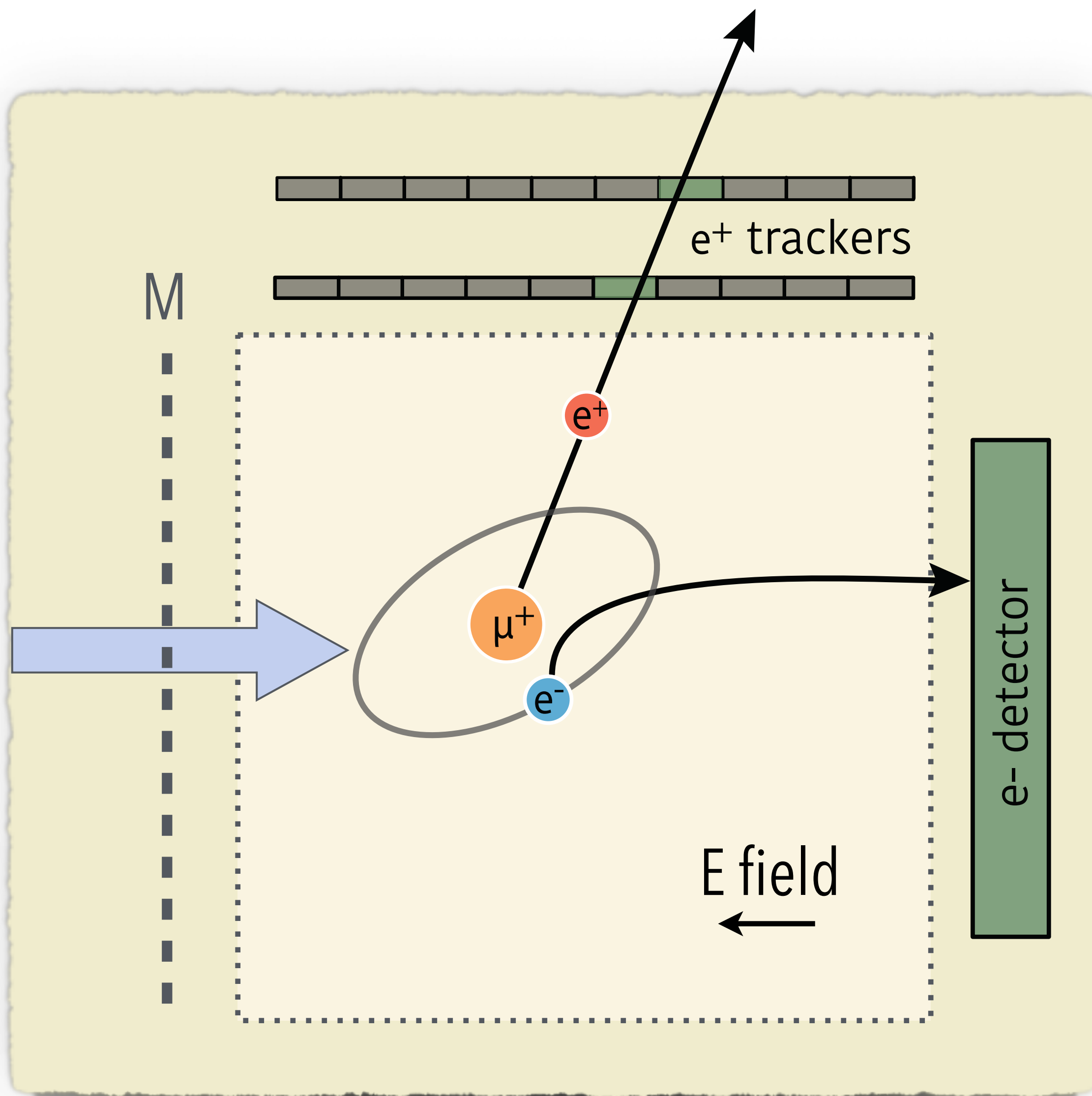

2024 | 2025 | 2026 | 2027 | 2028

Positron tracker

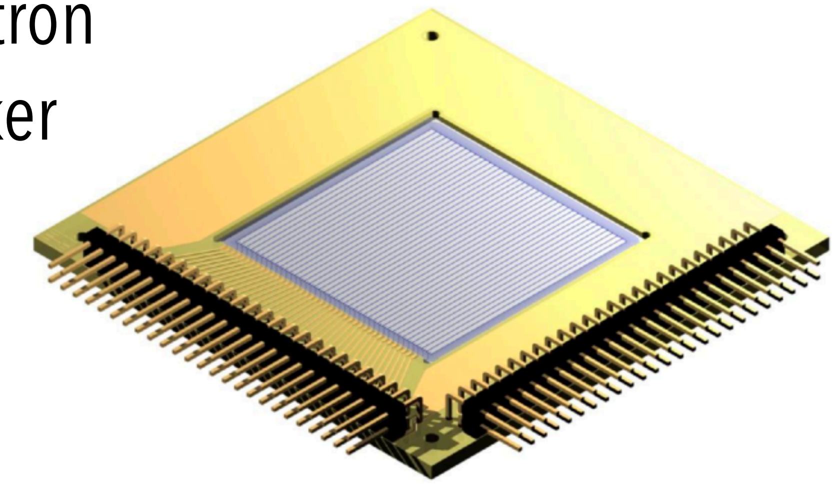

- 1 K temperature, limited cooling power
- low noise, decoupled preamplifiers

Electron counter

- low threshold (~keV)
- 0.1 K "wet" environment with SFHe film

Perovskite Nanocrystals

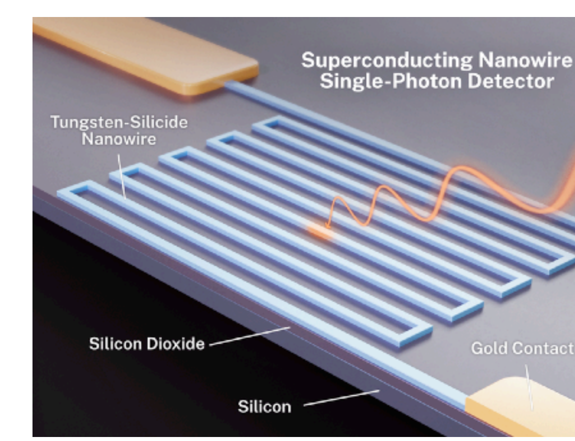

Superconductive nanowires

J. Zhang *et al* 2022 *JINST* **17** P06024

Emission vs background

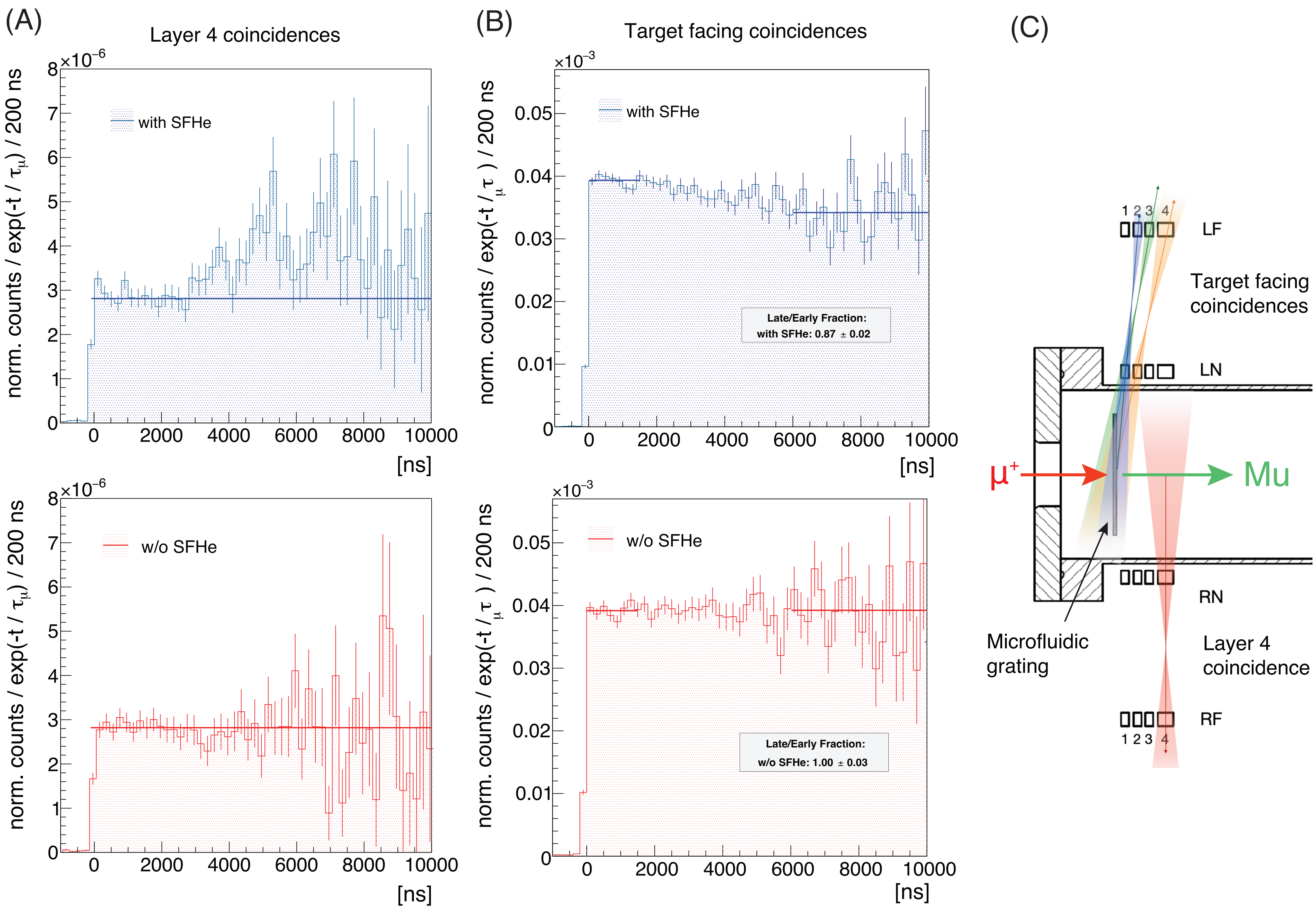

Projected sensitivity with high intensity muon beams

Optimizing the length

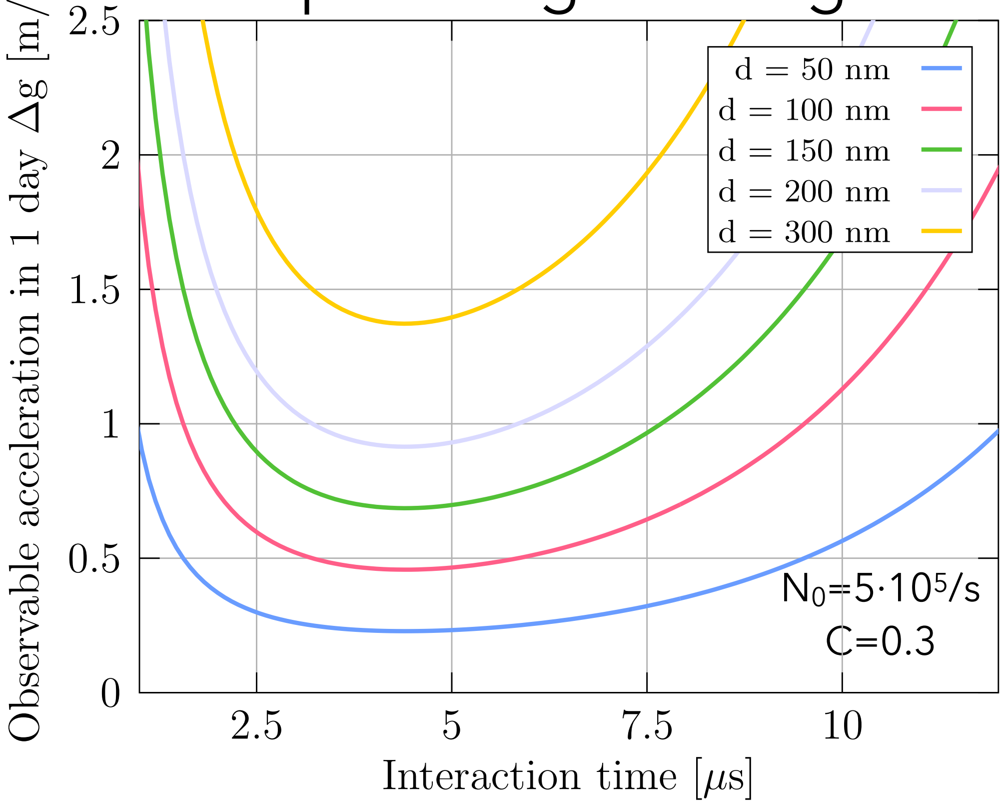

With λ_{Mu} = 1.6 nm (SFHe beam) L_0=3 mm, L=10 mm, d=100 nm, C=0.3 ($L_T = d^2/\lambda$ = 6 μm), η=0.3, ε=0.7

Determining sign of g: less than a day with Mu source of $N_0 > 5\cdot10^5$/s, C > 0.3

SFHe source @PSI:
10^5/s -10^6/s depending on muon beam scenarios

- $I(p) \sim p^{3.5}$
- Δp/p (FWHM) ~ 0.03 -0.1
- ΔE/E ~ 0.06 – 0.2

Sensitivity over time

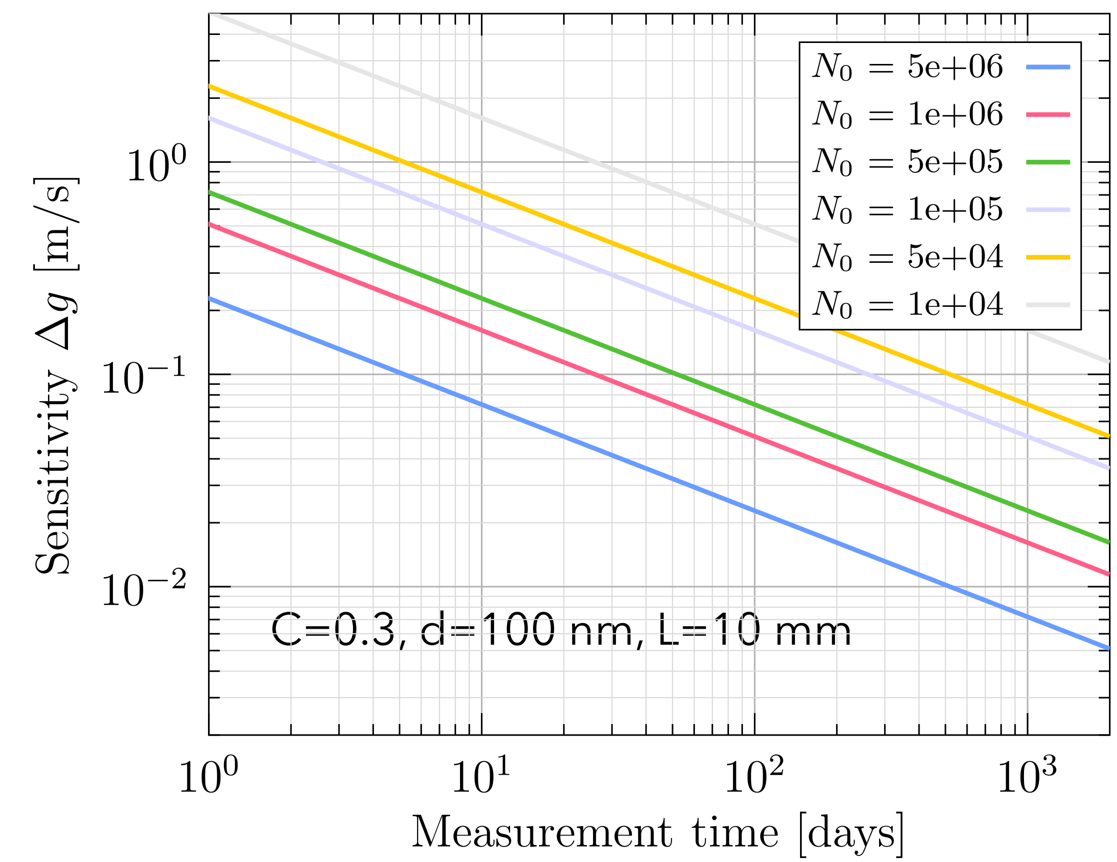

Beam	p [MeV/c]	Yield [μ^+/s]	1σ [mm]	Yield in d = 10 mm	**Aerogel,** back implantation **23 MeV/c (3%)**	**SFHe source,** front implantation **12.5 MeV/c (10%)**
piE5	**28**	**5×10^8**	**8.5**	**9.8×10^7**	**1.5×10^6**	**0.6×10^6 ***
HiMB-3	28	1×10^{10}	30	1.75×10^8	2.6×10^6	1.1×10^6 *

Amenability of the atomic beam for interferometry

- Model: using mutual intensity functions from statistical optics
- Calculations assume a Gaussian Schell-model beam

w_0 ~ beam width (aperture)
ℓ_0 ~ transverse coherence length

ℓ_0 relates to the angular spread ($\boldsymbol{\alpha}$) of the atoms (via the Cittert-Zernike theorem) as:

$$\ell_0 \approx \frac{\lambda}{\alpha} \approx \frac{1.6\ \mathrm{nm}}{50/2200} = 70\ \mathrm{nm}$$

$\boldsymbol{\alpha}$ ~ 22 mrad, and ℓ_0 ~ 70 nm - close to the grating pitch size

- Contrast = 0.3
- Given there is enough high quality Mu atoms, might be feasible!

model based on: McMorran et al., PRA 78 (2008)

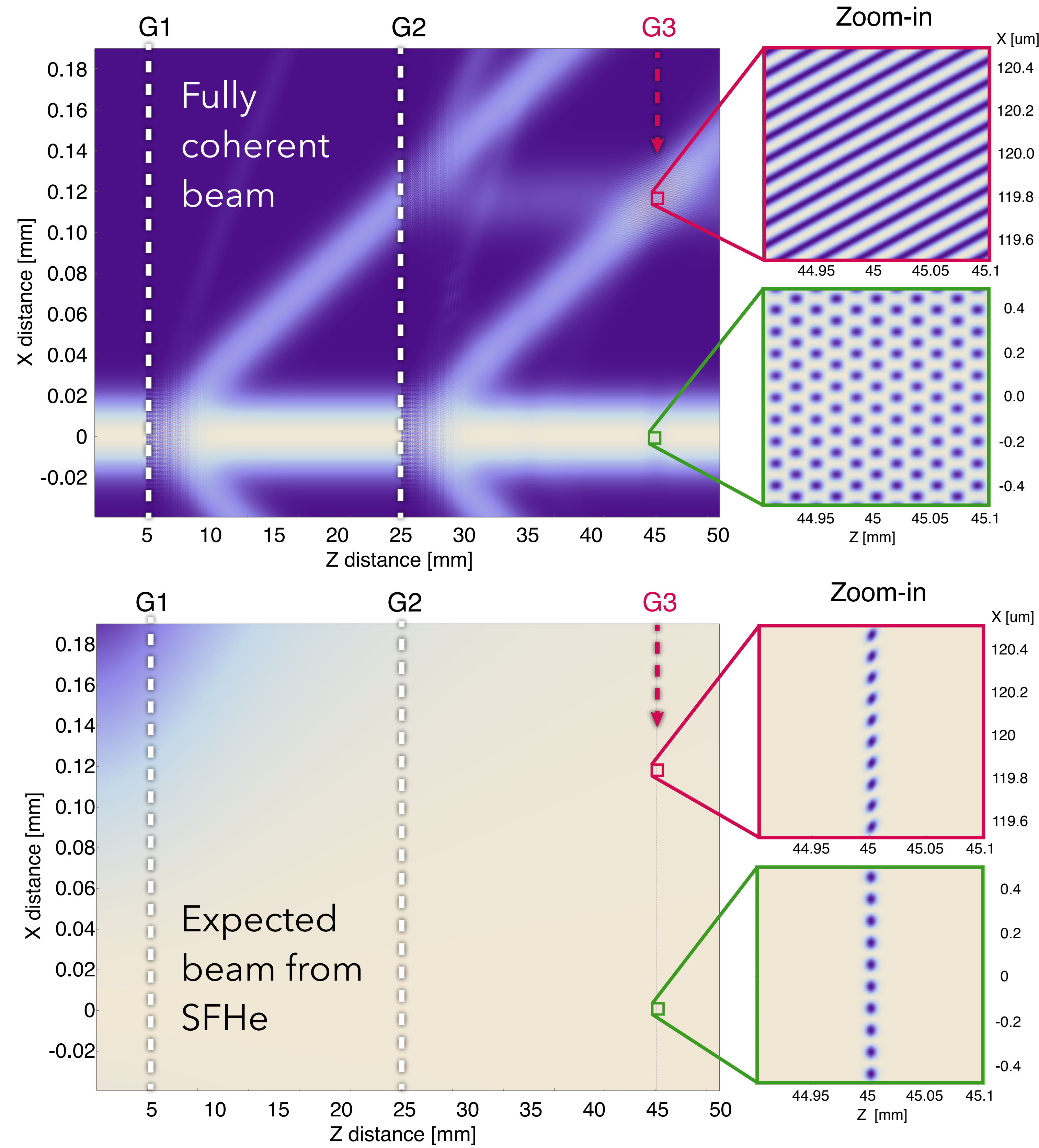

Precision physics motivation: Mu spectroscopy

Present	Exp. acc.	H(1S-2S)+μp	Muonium HFS
	4×10^{-9}	6×10^{-13}	2×10^{-8}

1s-2s - V. Meyer et al., PRL 84(6) (2000)
HFS - W. Liu et al 82, 711 (1999)

$$E(1s-2s) \simeq \frac{3}{4} R_\infty \left(1 - \frac{m_e}{m_\mu}\right) + \mathrm{QED}(\alpha, \mathrm{m_e} \ldots)$$

Precision physics motivation: Mu spectroscopy

	Exp. acc.	H(1S-2S)+μp	Muonium HFS
Present	4×10^{-9}	6×10^{-13}	2×10^{-8}

1s-2s - V. Meyer et al., PRL 84(6) (2000)
HFS - W. Liu et al 82, 711 (1999)

$$E(1s-2s) \simeq \frac{3}{4} R_\infty \left(1 - \frac{m_e}{m_\mu}\right) + \mathrm{QED}(\alpha, \mathrm{m_e} \ldots)$$

	Exp. acc.	
Future	4×10^{-12}	$\frac{m_\mu}{m_e}$ with 1×10^{-9} rel. acc.

Precision physics motivation: Mu spectroscopy

Present

	Exp. acc.	H(1S-2S)+μp	Muonium HFS
Present	4×10^{-9}	6×10^{-13}	2×10^{-8}

1s-2s - V. Meyer et al., PRL 84(6) (2000)
HFS - W. Liu et al 82, 711 (1999)

$$E(1s-2s) \simeq \frac{3}{4} R_\infty \left(1 - \frac{m_e}{m_\mu}\right) + \mathrm{QED}(\alpha, \mathrm{m_e} \ldots)$$

Future

Exp. acc. 4×10^{-12}

$\frac{m_\mu}{m_e}$ with 1×10^{-9} rel. acc.

Application in muon g-2 experiments

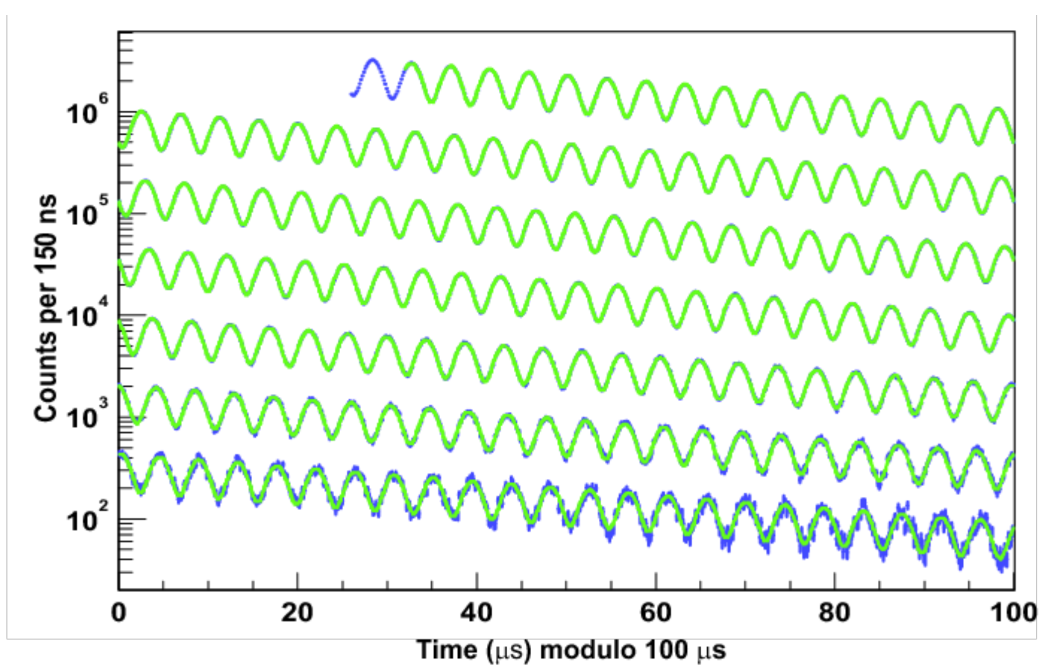

Muonium HFS (22 ppb) or **future Mu-Mass 1 ppb**

From storage ring [~200 ppb]

$$\frac{g-2}{2} = \frac{m_\mu}{e}\frac{\omega_a}{B} = \frac{\mu_p}{\mu_e}\frac{m_\mu}{m_e}\frac{g_e}{2}\frac{\omega_a}{\omega_p}$$

Hydrogen maser [3 ppb]

Electron g-2 + QED [0.26 ppt]

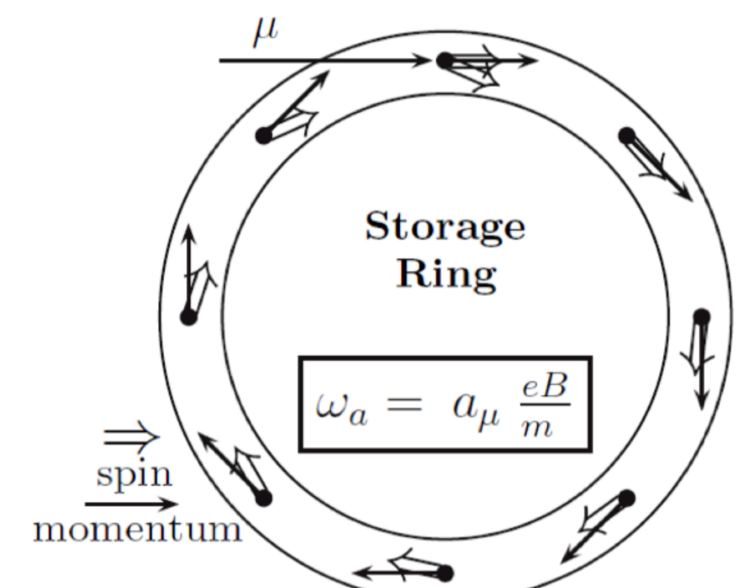

Spectroscopy

- We are producing about the **same amount** of cold Mu than the best room temperature sources, in a small, directed beam
- Small spotsize would offer high **ionization efficiencies**, as a viable way to produce low energy muons, especially for pulsed sources
- The large yield of slow atoms mean that 1s-2s spectroscopy can benefit a lot - **small spotsize**, slow atoms

Spectroscopy

Statistical uncertainty
At least 100-fold improvement in intensity compared to present MuMass M beam, > 1 OM improvement

Transit-time broadening $\Delta\nu \approx 0.4 \cdot \frac{v}{w}$ w is the waist size

Factor of 2-3 reduction due to reduced velocity, same factor increase of excitation efficiency.

Second order Doppler shift $\Delta\nu_{d2} \approx -\nu_0 \frac{v^2}{2c^2}$ $\nu_0 \approx 2.46 \times 10^{15}\,\mathrm{Hz}$

A well known velocity distribution can allow for correction with appropriate lineshape modelling, uncertainty driven by the uncertainty in velocity:

$$\sigma_{\nu_{d2}} \approx \left|\frac{\partial \nu_{d2}}{\partial v}\right| \sigma_v \approx -\nu_0 \frac{v \cdot \sigma_v}{c^2}$$

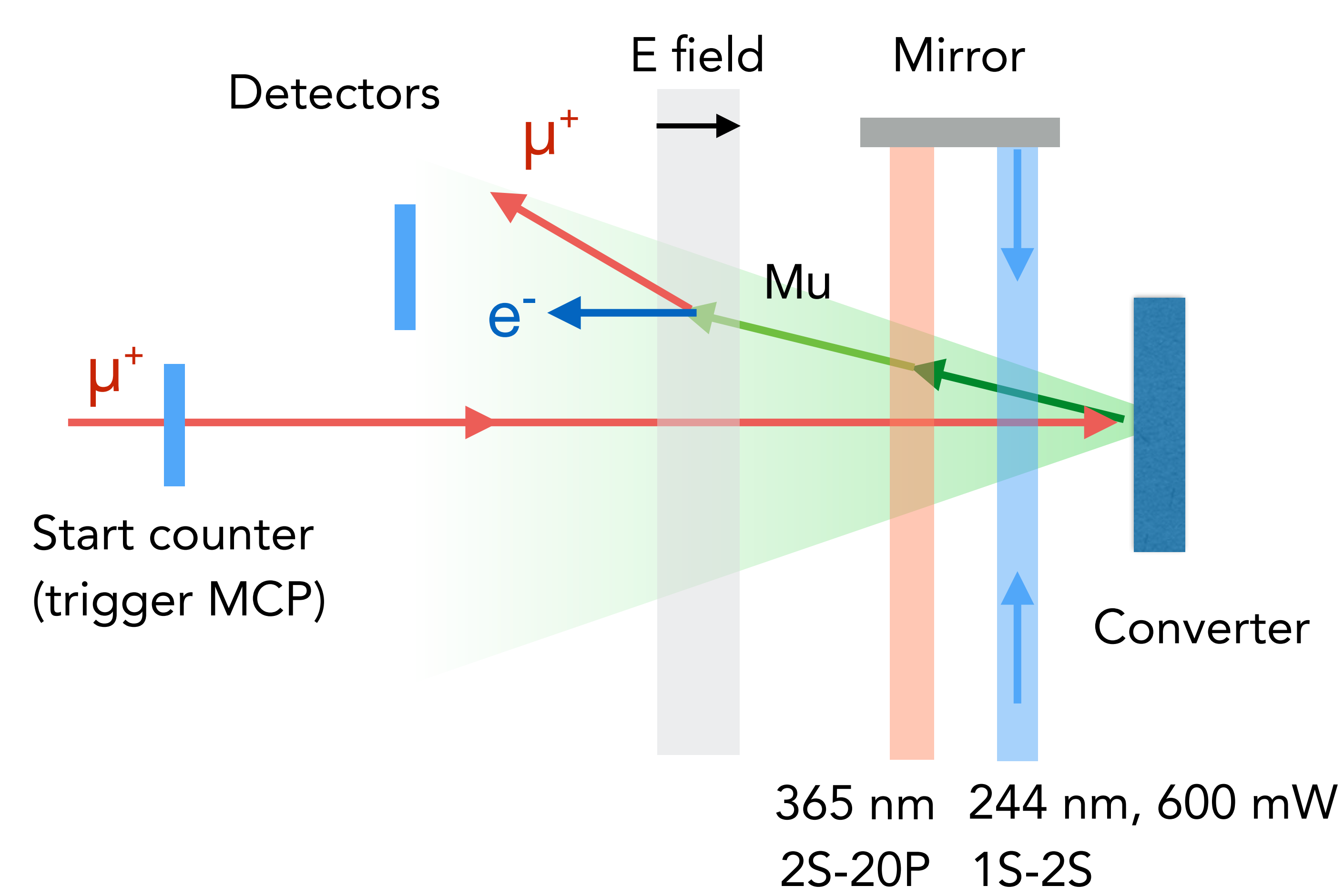

Beamtime request

- 3 weeks at piE1

- **3-4 days*:** Setting up the beamline, beam alignment with beam scanners, and cryostat cooldown. (* 3 days if the setup is already prepared the zone, 4 days with moving included)
- **2 days:** Alignment and momentum tuning (ranging) in the dry V1 Si target, background measurement, detector calibrations.
- **2 days:** Ranging in SFHe filled microfluidic setup, commissioning of the Si positron trackers and the V1 atomic electron detector.
- **3 days:** Dedicated measurement of emitted Mu atoms from the microfluidic target using the positron trackers, and preferably atomic electron detector.
- **2 days:** Warmup, disassembly, mounting the V2 setup and cooldown.
- **3 days:** Measurement of Mu emission from V2 Si target and V2 atomic electron detector.
- **2 days:** Warmup, disassembly, mounting V3 setup and cooldown.
- **3 days:** Measurement of Mu emission from V3 Si target and V3 atomic electron detector.

Tests of the weak equivalence principle

Foundation of GR. Many formulations since Galilei:

Usually describing that he outcome of any local experiment conducted in gravitational field (local g acceleration) must be the same than in an accelerating lab, where a=g.

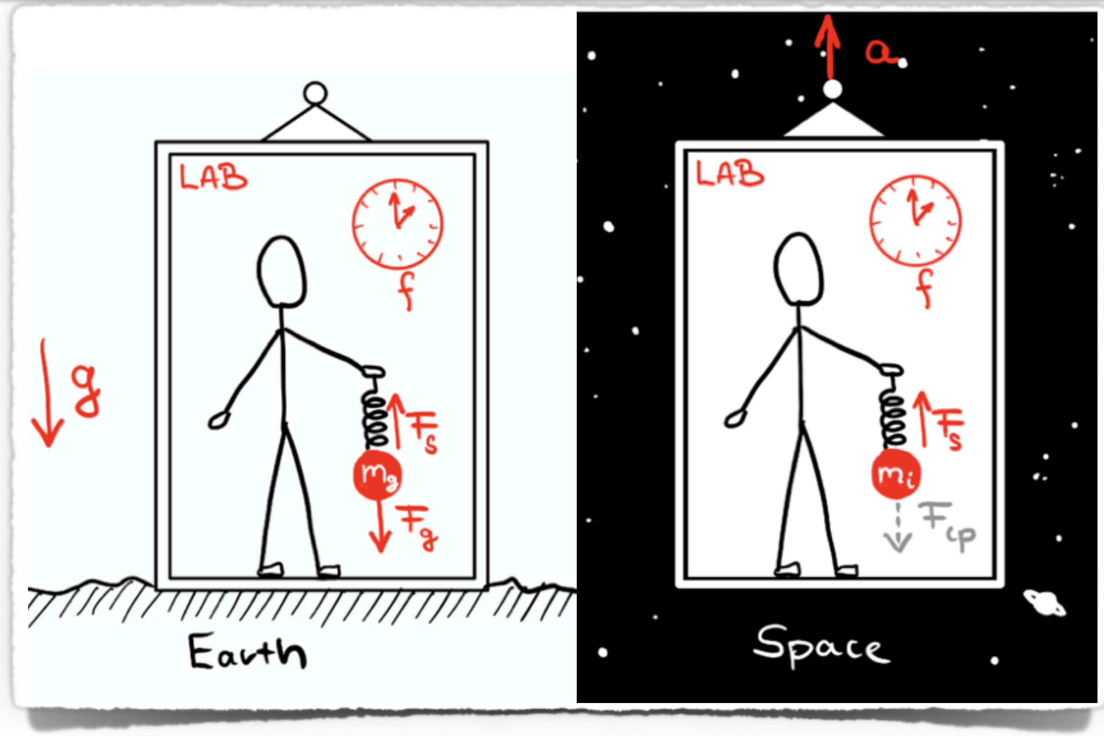

Various experimental consequences:

- Universality of free fall, $\eta(1,2) = 2\frac{|g_1 - g_2|}{|g_1 + g_2|}$
- Local Lorentz invariance
- Local position invariance:
  - universality of clocks,
  - lack of variation of fundamental constants

- Needs to be tested in different experiments sensitive to one of the above!

Torsion pendula

Original setup of Eötvös (1910, Hungary)

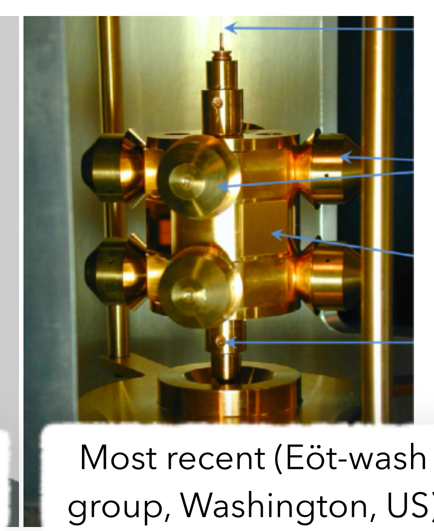

Most recent (Eöt-wash group, Washington, US)

$\eta(\mathrm{Be,Ti}) = [0.3 \pm 1.8] \times 10^{-13}$

S.Schlamminger et al, Phys Rev Lett 100 (2008) 041101

Satellite experiments

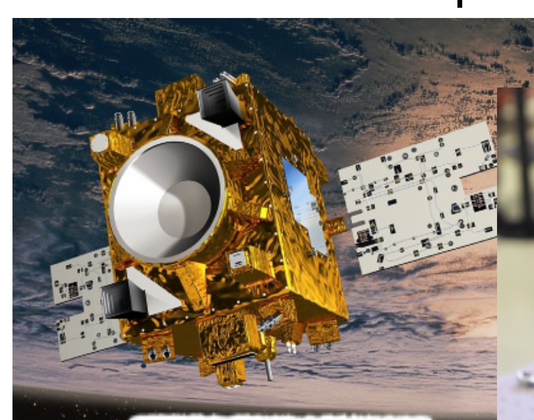

MICROSCOPE experiment

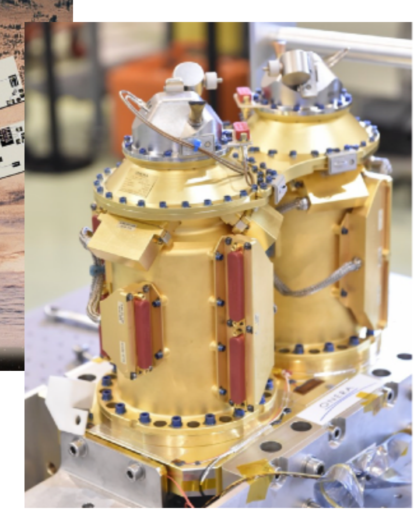

$\eta(\mathrm{Ti,Pt}) = [1 \pm 9(\mathrm{stat}) \pm 9(\mathrm{syst})] \times 10^{-15}$

https://doi.org/10.1103/PhysRevLett.119.231101

Tests on the largest and smallest scales

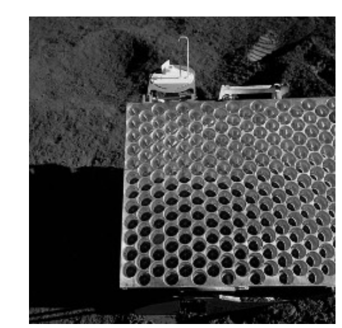

Lunar Laser Ranging Experiment

Atom interferometry

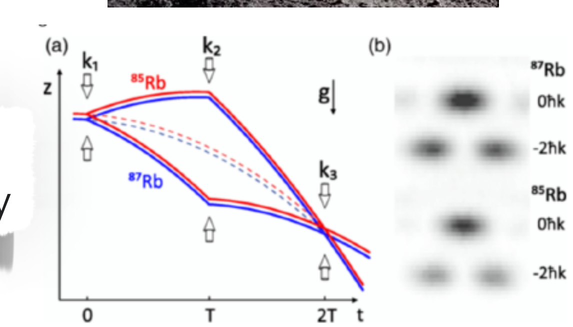

$\eta(^{85}\mathrm{Rb},^{87}\mathrm{Rb}) = [1.6 \pm 1.8(\mathrm{stat}) \pm 3.4(\mathrm{syst})] \times 10^{-12}$

https://doi.org/10.1103/PhysRevLett.125.191101

Feasibility studies 2019-22

M production in low temperature SFHe

- MuSR measurements
- >70% muon to muonium conversion

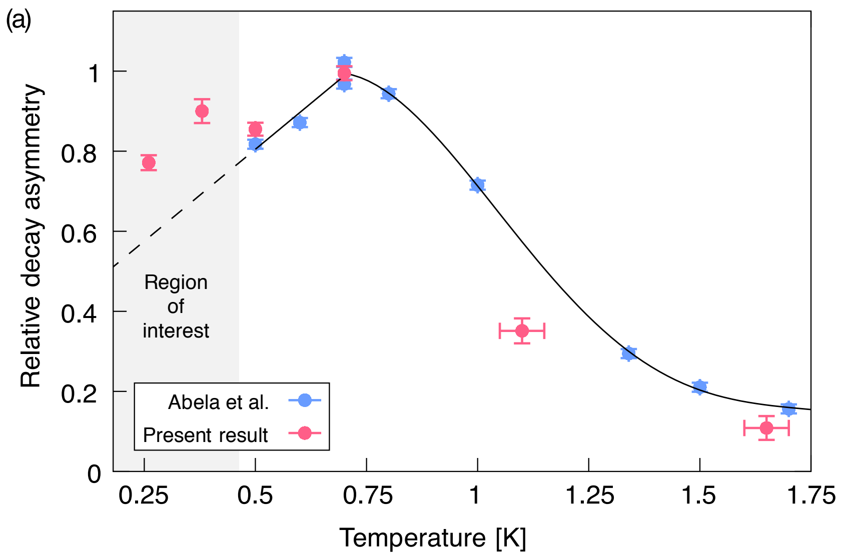

Indication of M atoms reflecting on SFHe films, 0.5 K

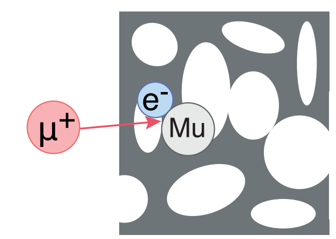

- M dephasing/ sticking to aerogel

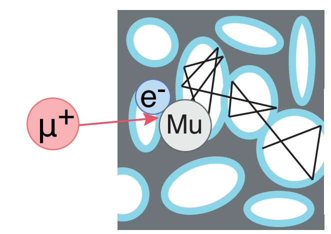

- M precessing in SFHe coated aerogel pores

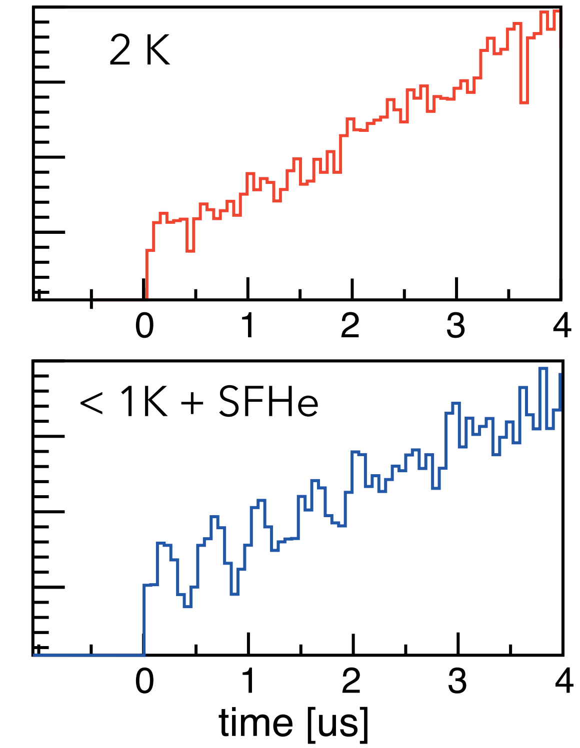

Cryogenic detector developments

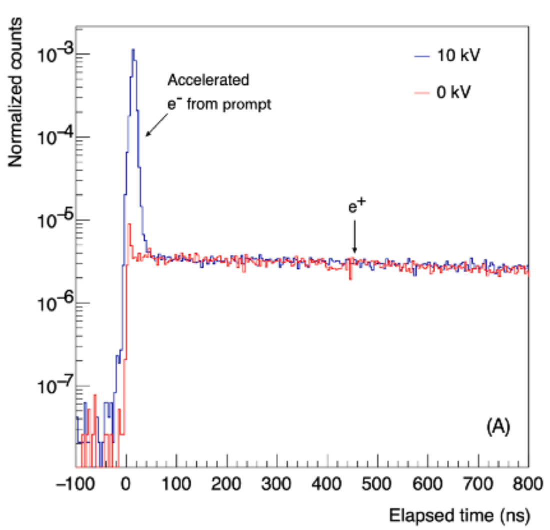

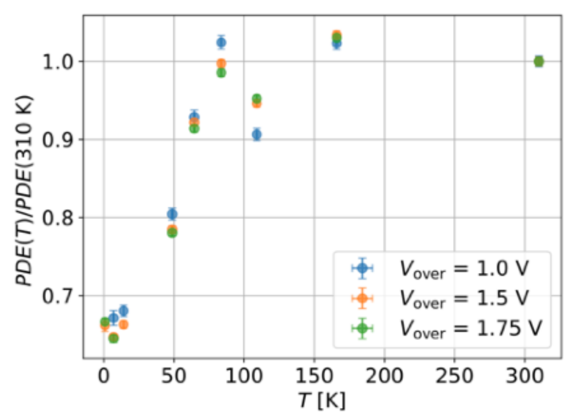

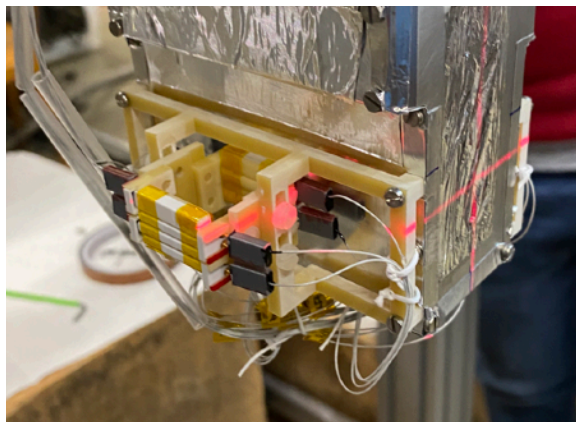

- SiPM-based scintillator detectors reliably operate at min. temp: T<0.2 K

Study of M scattering in He gas

- Tracking of M atoms in room temperature chambers
- Realization that T < 0.3 K is needed - dilution refrigerator

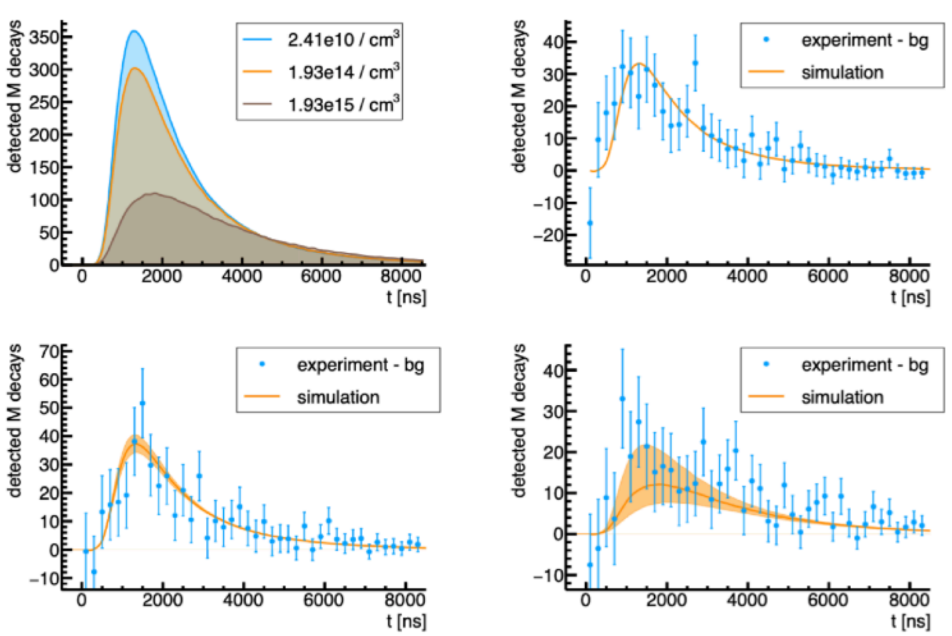

Theory: Mu from superfluid helium

Creation and diffusion in SFHe

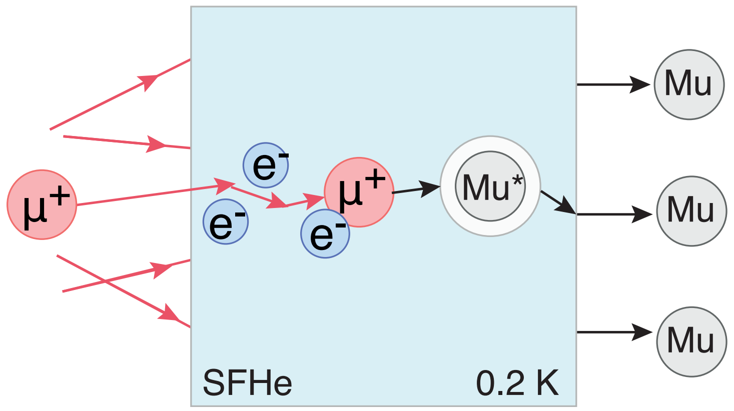

- Effective mass from VdW core repulsion for all H isotopes ~ 2.5 M_{He}
- This makes M a relatively small impurity: might avoid hydrodynamic losses (vortex creation)
- Thermalization below the roton gap (v≈50 m/s)

- At 0.2 K phonon density is small:

$$n_{ph} = 2 \times 10^{19} T^3 \mathrm{cm}^{-3} \approx 10^{16}/\mathrm{cm}^3$$

- Small phonon density makes scattering unlikely in μs times:

$$\frac{1}{\tau_c} \approx 4.8 \times 10^7 T^7 \approx 5/s$$

Taqqu, Physics Procedia 17 (2011) 216–223,
Kirch & Khaw: Int. J. of Mod. Phys. 30, (2014)
Soter & Knecht, SciPost Physics Proceedings 031 (2021).

Theory: Mu from superfluid helium

Creation and diffusion in SFHe

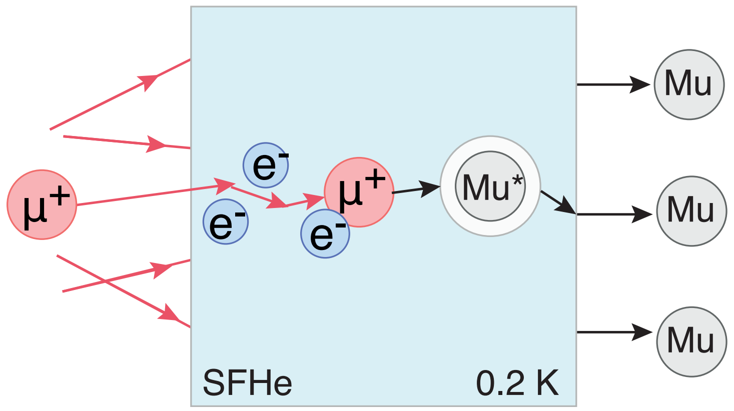

- Effective mass from VdW core repulsion for all H isotopes ~ 2.5 M_{He}
- This makes M a relatively small impurity: might avoid hydrodynamic losses (vortex creation)
- Thermalization below the roton gap (v≈50 m/s)

- At 0.2 K phonon density is small:

$$n_{ph} = 2 \times 10^{19} T^3 \text{cm}^{-3} \approx 10^{16}/\text{cm}^3$$

- Small phonon density makes scattering unlikely in μs times:

$$\frac{1}{\tau_c} \approx 4.8 \times 10^7 T^7 \approx 5/s$$

Taqqu, Physics Procedia 17 (2011) 216–223,
Kirch & Khaw: Int. J. of Mod. Phys. 30, (2014)
Soter & Knecht, SciPost Physics Proceedings 031 (2021).

Surface ejection

- M and H, D, T chemical potentials:
- E/k_B~ 270 K and 37 K, 14 K , 7 K

M. Saarela and E. Krotscheck, JLTP 90, 415 (1993)

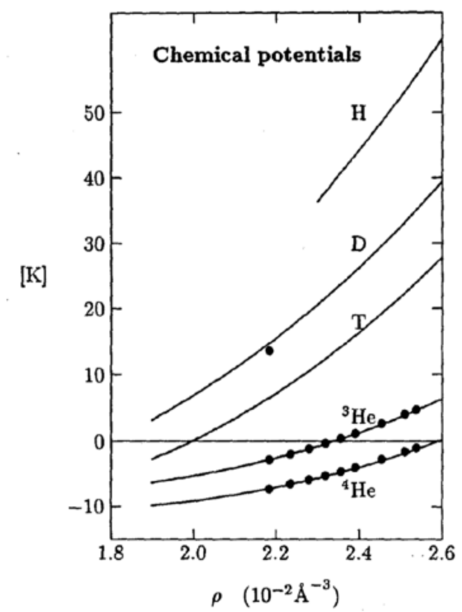

- M atoms are ejected from bulk SFHe with E = 23 meV, v = 6300 m/s

- Low thermal energy spread (+/- 100 m/s)
- Narrow angular distribution (~30 mrad)

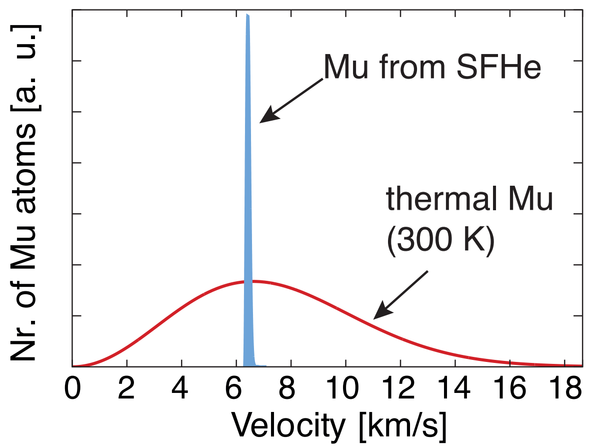

Theory: Mu from superfluid helium

Creation and diffusion in SFHe

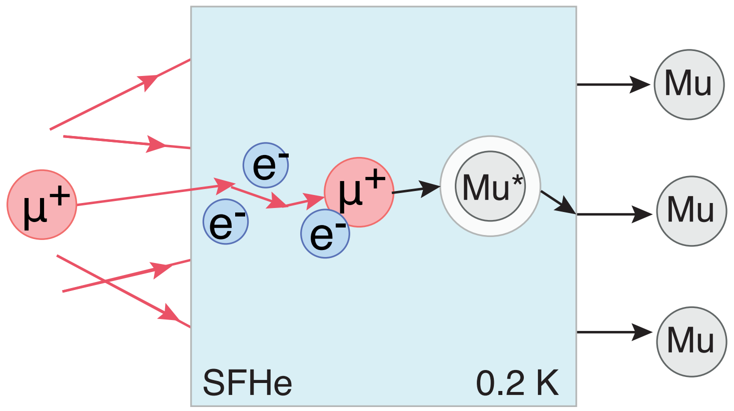

- Effective mass from VdW core repulsion for all H isotopes ~ 2.5 M_{He}
- This makes M a relatively small impurity: might avoid hydrodynamic losses (vortex creation)
- Thermalization below the roton gap (v≈50 m/s)

- At 0.2 K phonon density is small:

$$n_{ph} = 2 \times 10^{19} T^3 \mathrm{cm}^{-3} \approx 10^{16}/\mathrm{cm}^3$$

- Small phonon density makes scattering unlikely in μs times:

$$\frac{1}{\tau_c} \approx 4.8 \times 10^7 T^7 \approx 5/s$$

Taqqu, Physics Procedia 17 (2011) 216–223,
Kirch & Khaw: Int. J. of Mod. Phys. 30, (2014)
Soter & Knecht, SciPost Physics Proceedings 031 (2021).

Surface ejection

- M and H, D, T chemical potentials:
- E/k_B~ 270 K and 37 K, 14 K , 7 K

M. Saarela and E. Krotscheck, JLTP 90, 415 (1993)

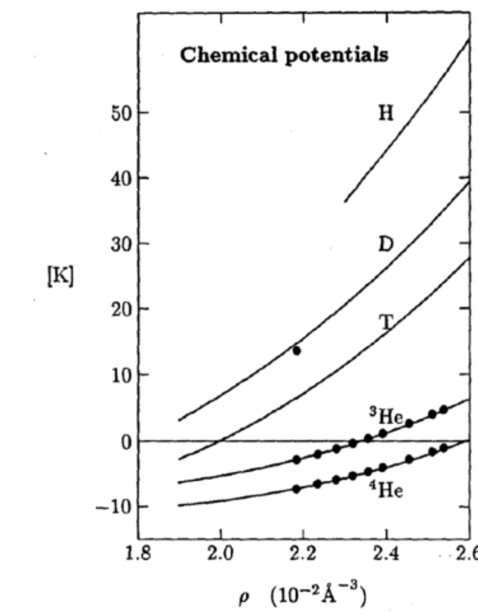

- M atoms are ejected from bulk SFHe with E = 23 meV, v = 6300 m/s

- Low thermal energy spread (+/- 100 m/s)
- Narrow angular distribution (~30 mrad)

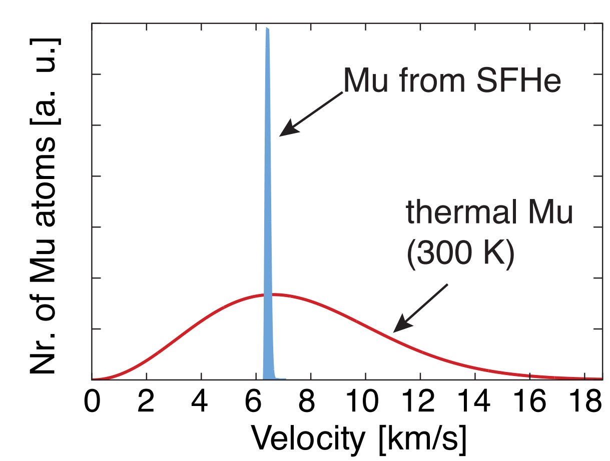

Reflection

- Reflection of a SFHe coated polished surfaces
- whispering gallery modes?

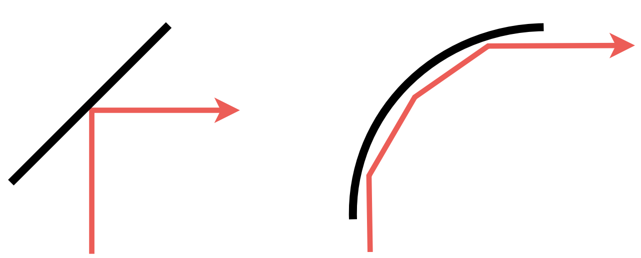

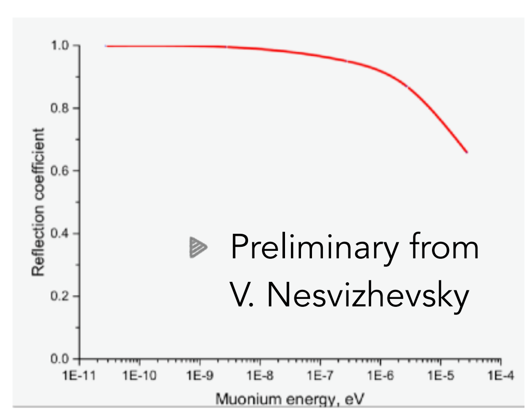

- Preliminary from V. Nesvizhevsky

Optical test bench

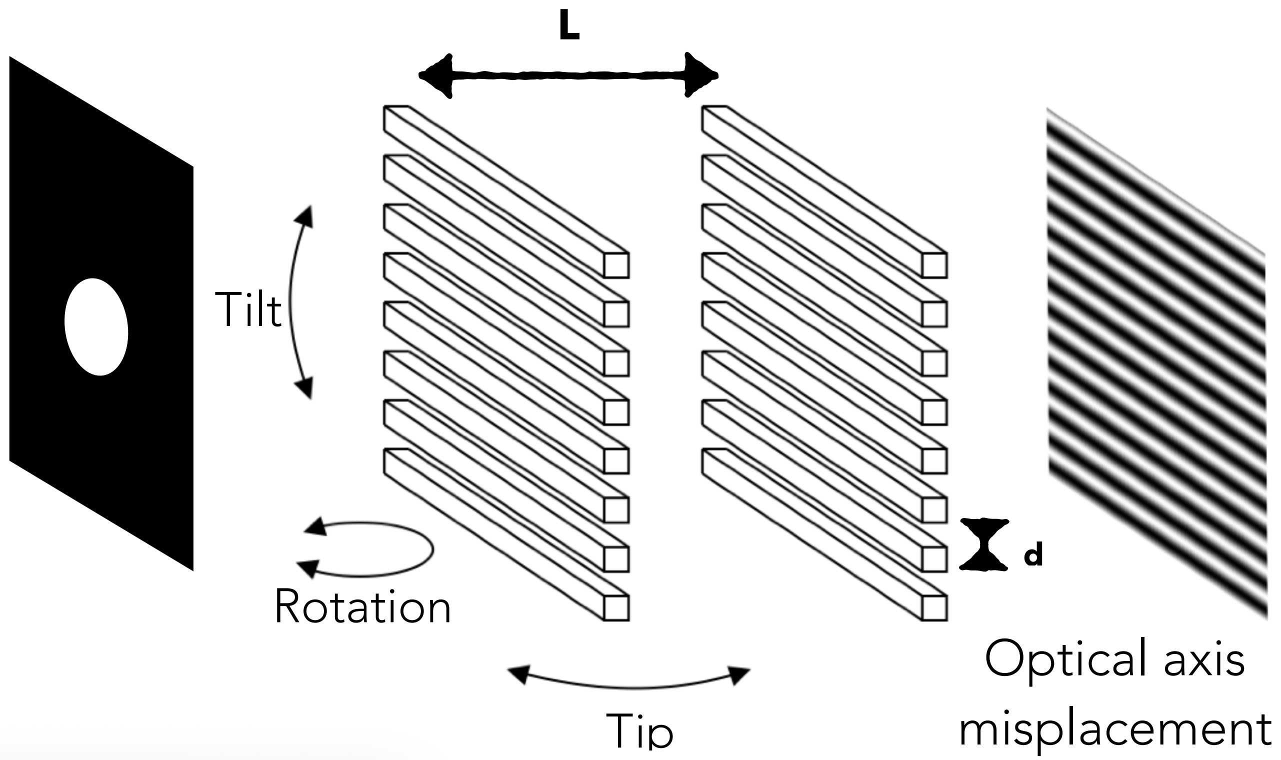

Developing a vertical stage with low vibrations.
Piezo movement without cantilevers.

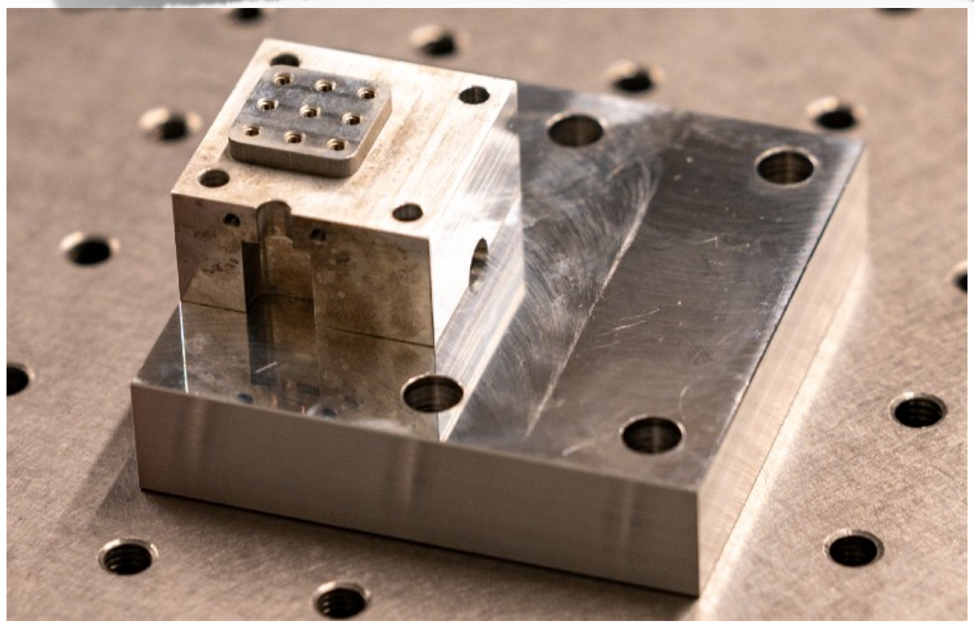

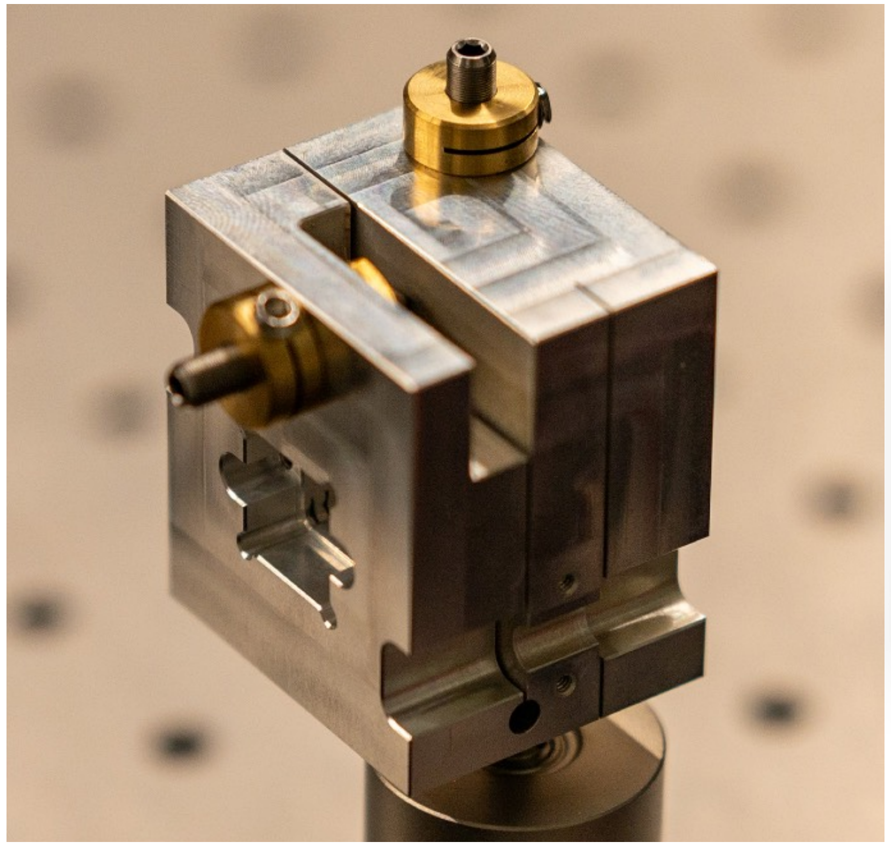

New model removing degrees of freedom in our setup via precision mechanics. Wire EDM and 5 axis milling allows us to commission precision pieces

Optical test bench results I.

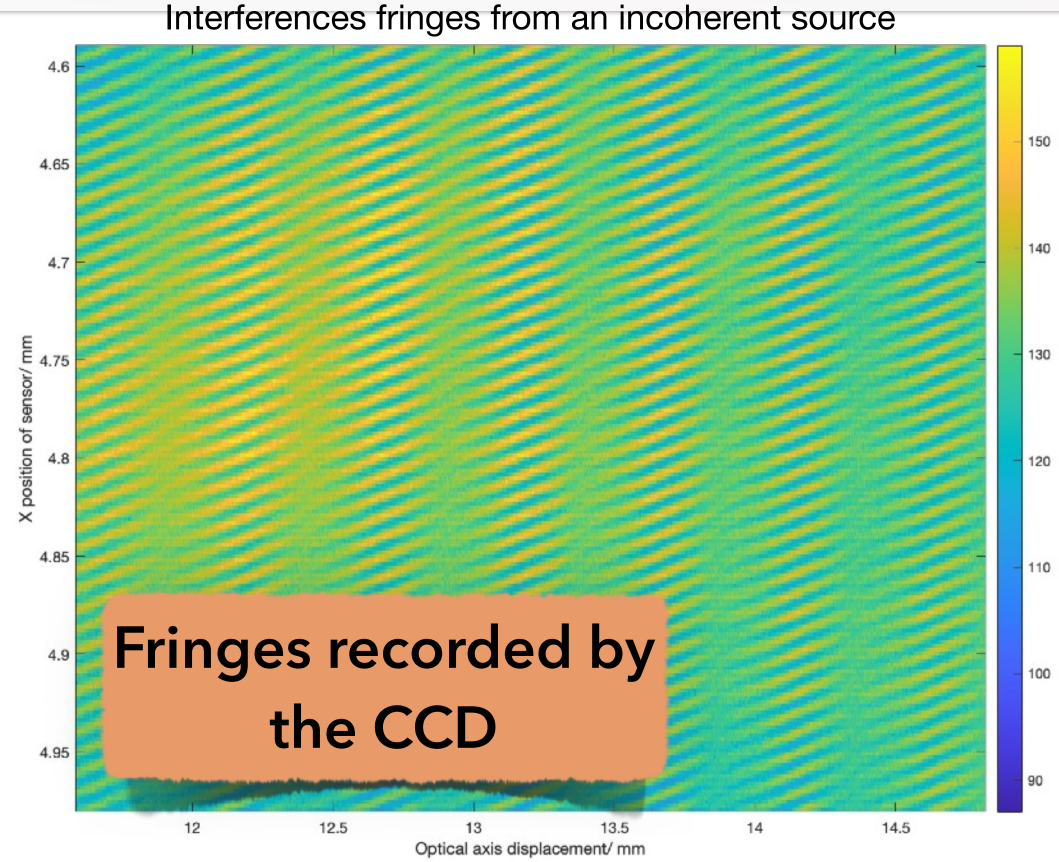

Fringes recorded by the CCD

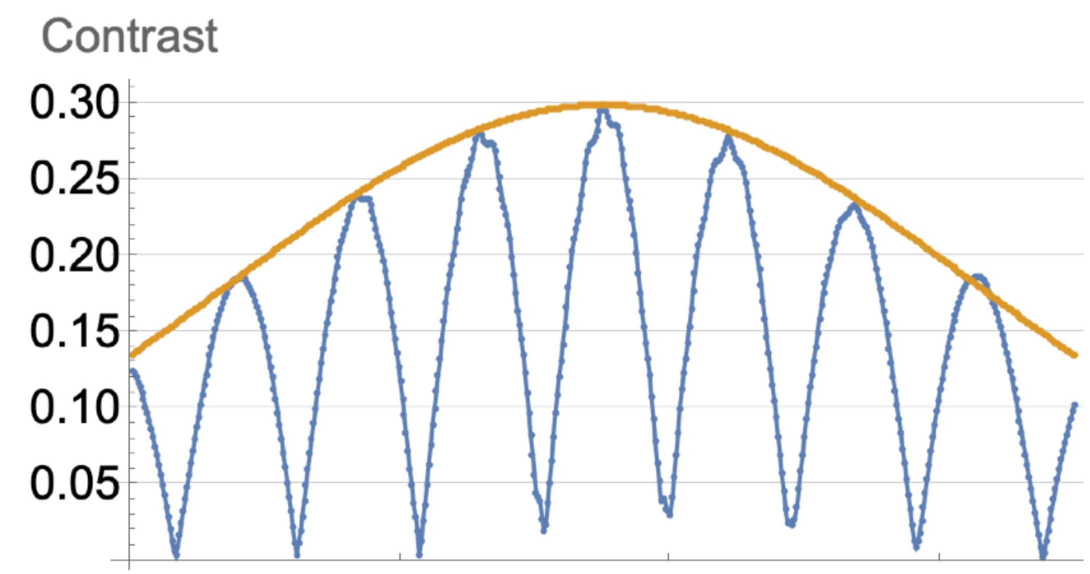

Simulated results

A simulation using a Gaussian-Schell model beam, of the experimental setup

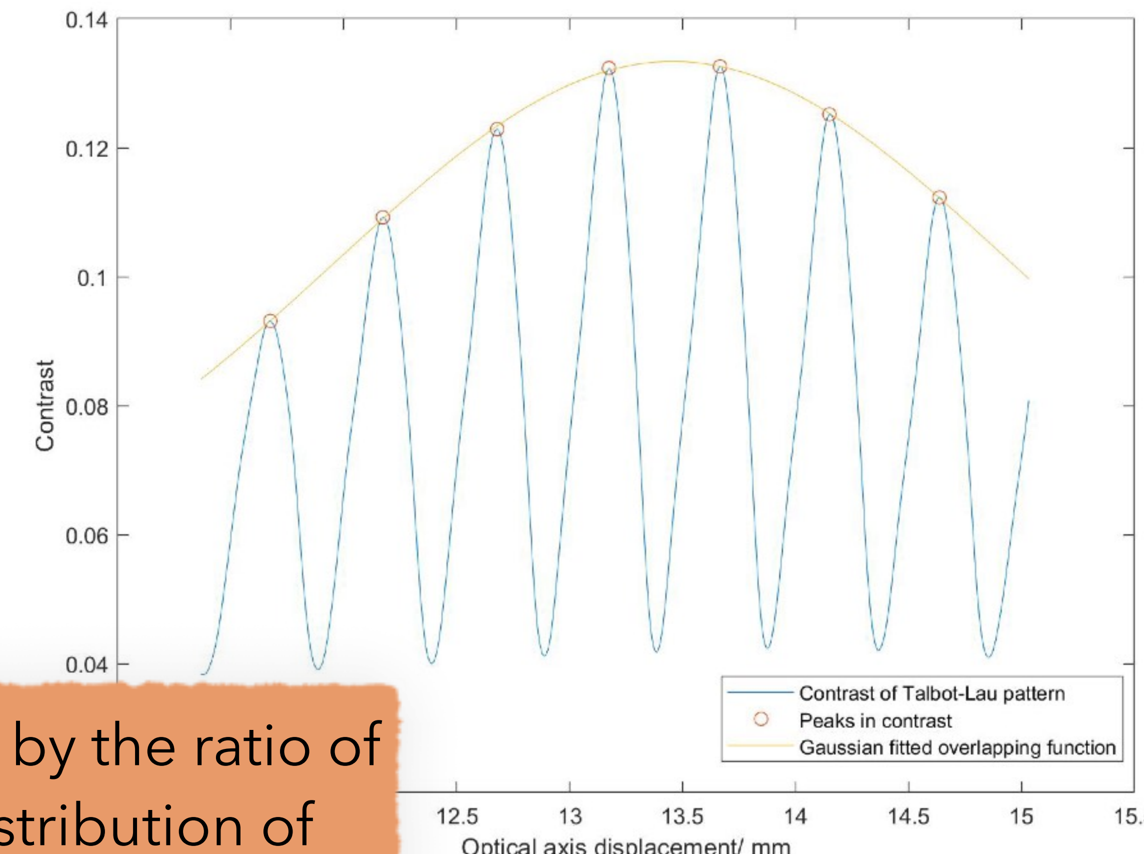

Experimental results

from our to visible light interferometer with 10um gratings, 635nm incoherent light

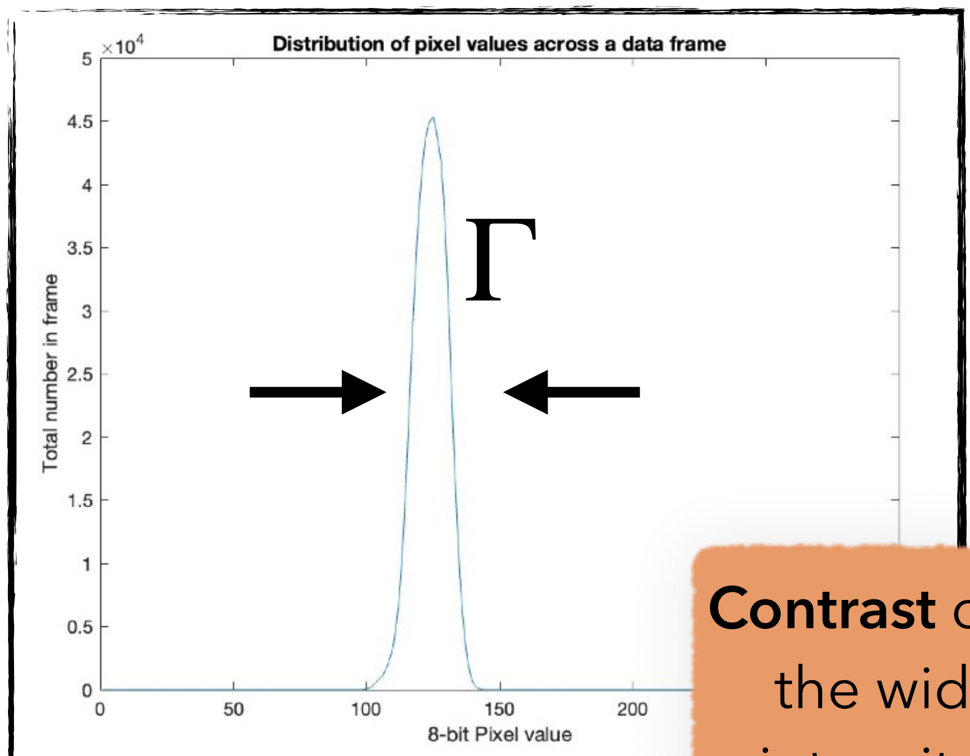

$$\ell = \frac{D\lambda}{d}$$

Contrast determined by the ratio of the width of the distribution of intensity versus the mean value.

Optical bench results II.

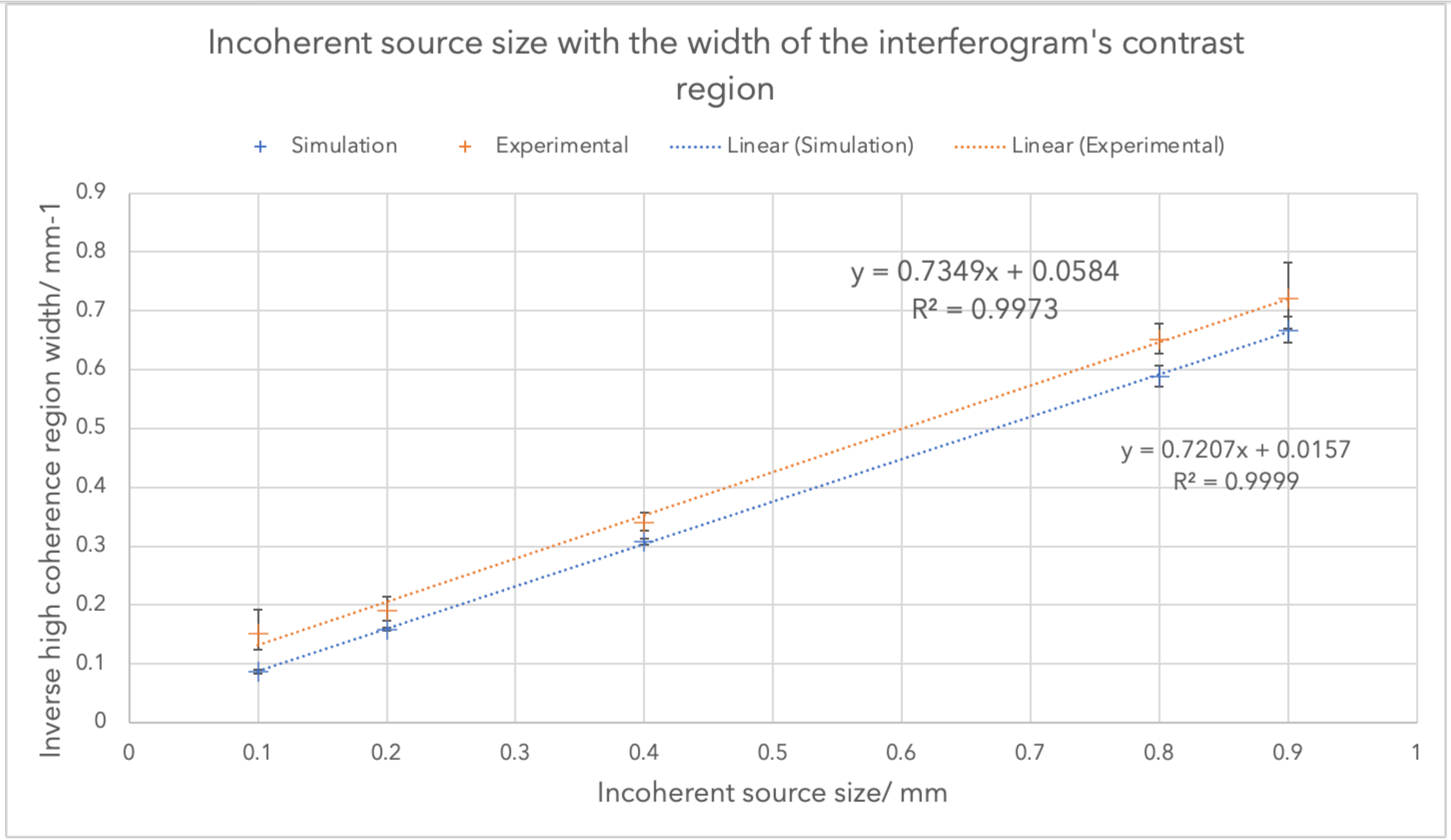

Scaling of the high-contrast region: The width of the region in which the interferometer fringes can be observed scales inversely with the size of an incoherent source. The gradient of this scaling is dependent on both the wavelength and distance of the source from the interferometer.

Measuring misalignment: The data frames can be split into n x n regions. The splitting between the maxima indicates a quadrant being misplaced. This can be used to calculate the tip and tilt of the camera.

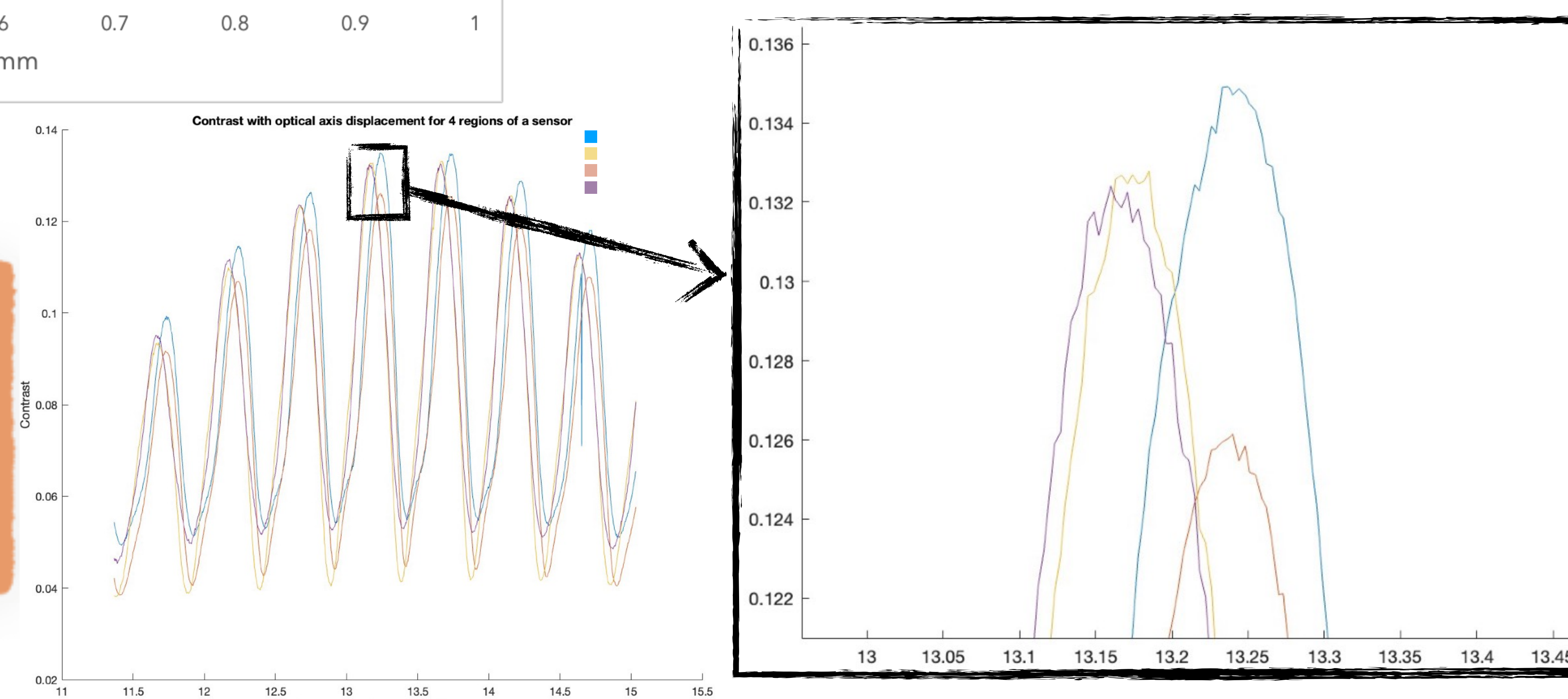

Visible and X-ray bench tests

Shielded box with interlock

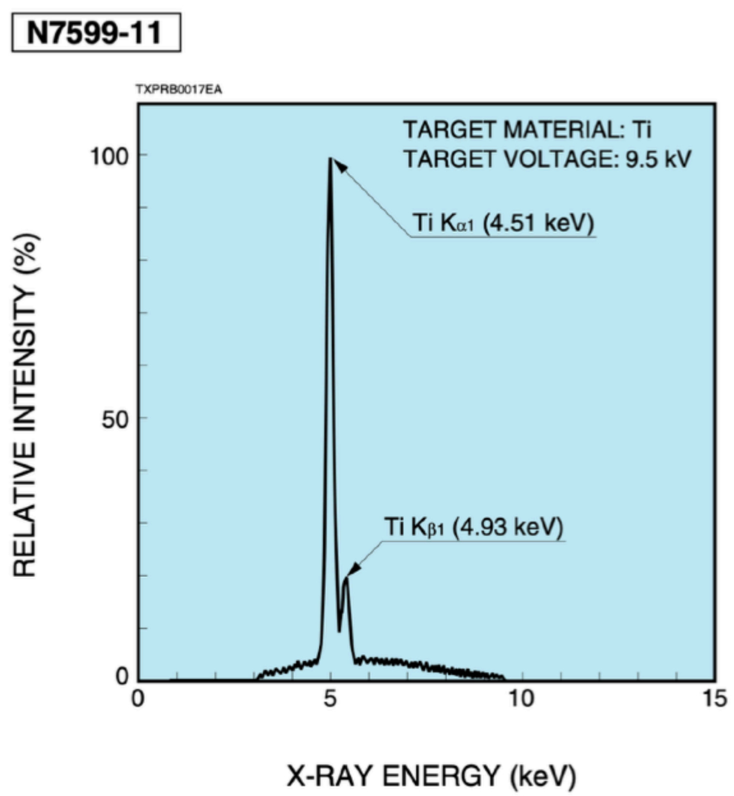

Source

1. Name of device: N7599-11
2. Manufacturer: Hamamatsu
3. Tube Voltage (maximum): 10keV
4. Operational tube voltage: 4.5-9.5keV
5. Tube current: 0.2 mA
6. Radiation angle: 71 deg

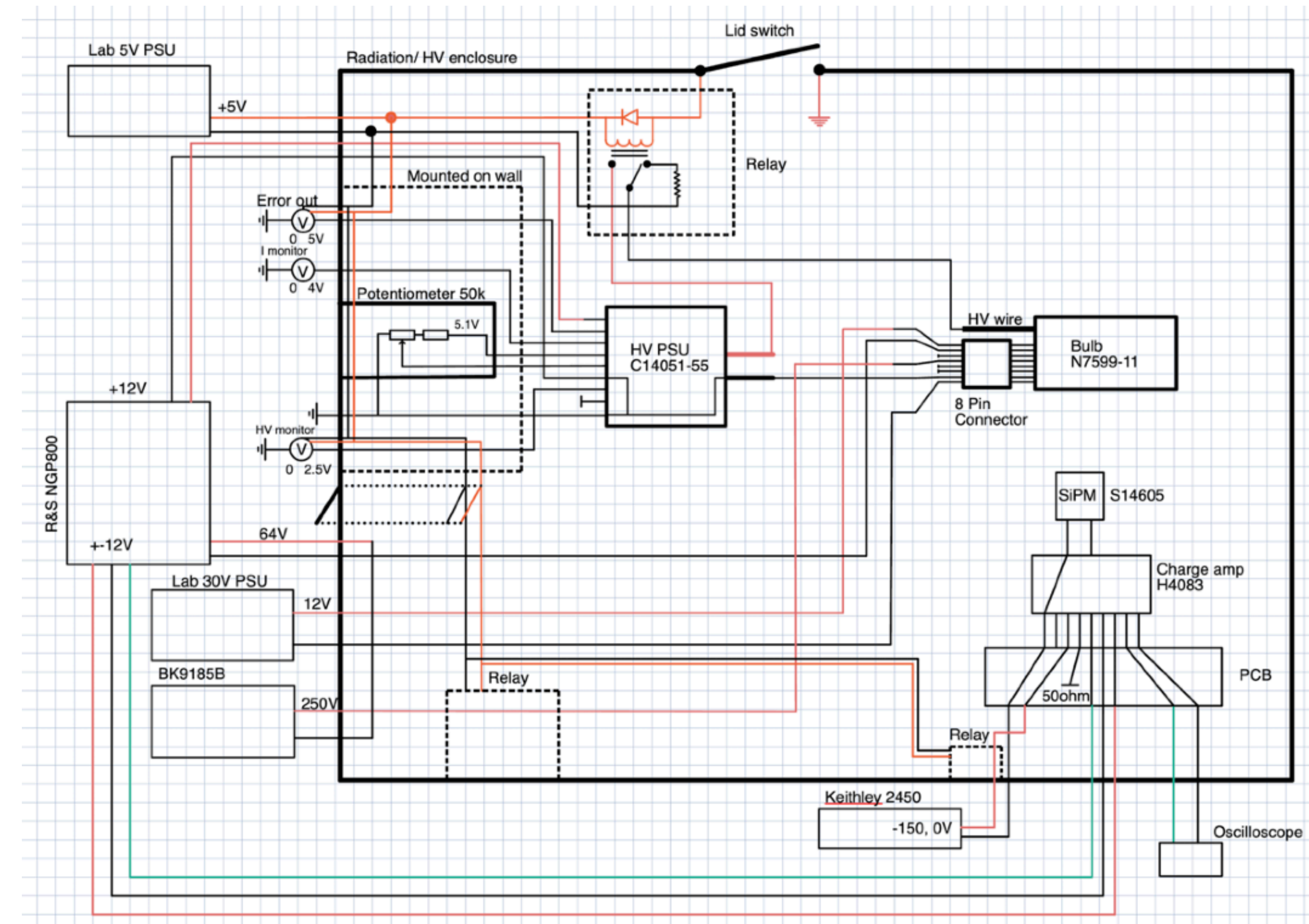

Detector

S14605 - Si PIN photodiode

Test of the scanning method

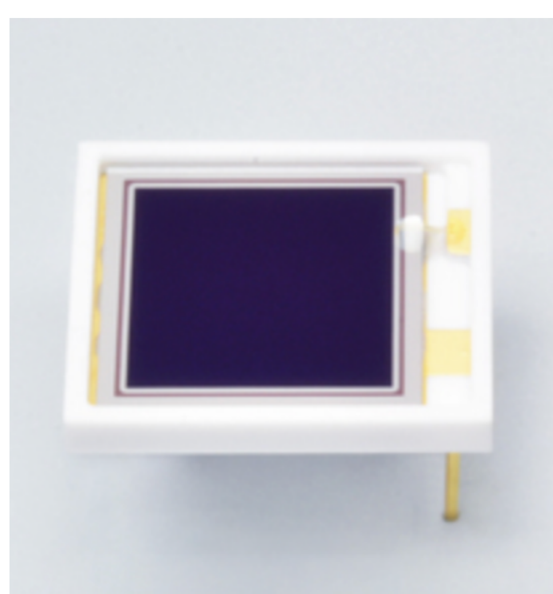

Shielding for L9873 (9.5keV, but 7W rather than our 2W)

Shielding material	Thickness/ mm
SUS304 Stainless	0.22
Aluminium	1.3
PVC	2.2
Acrylic	21.7

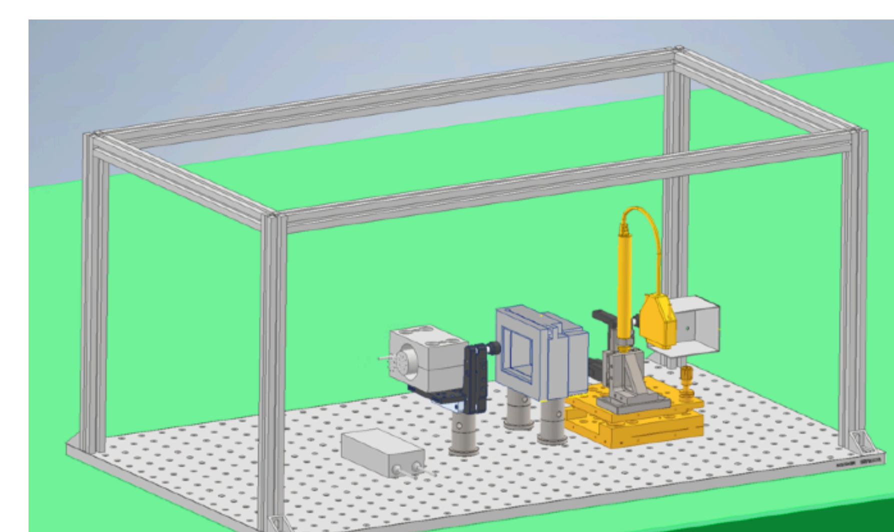

- Single electrons detected with high efficiency down to 15 keV
- Sensitive even between the wires

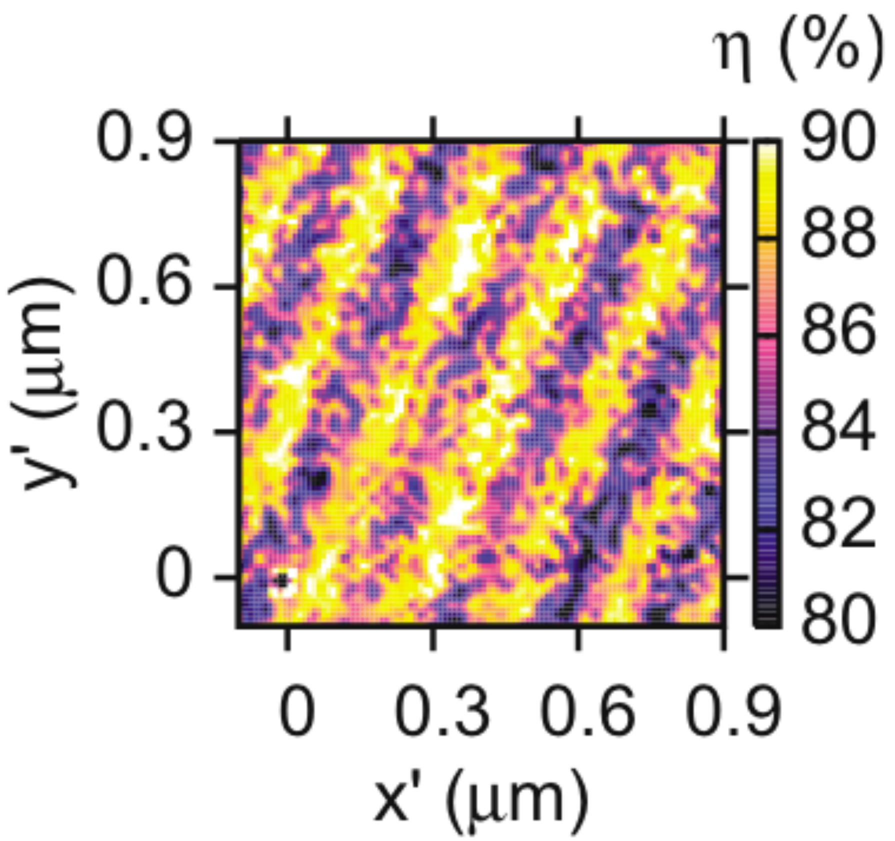

Detection efficiency of SCNW for single electrons (30 keV) from [M. Rosticher *et al.*, Appl. Phys. Lett. **97,** 18 (2010)]

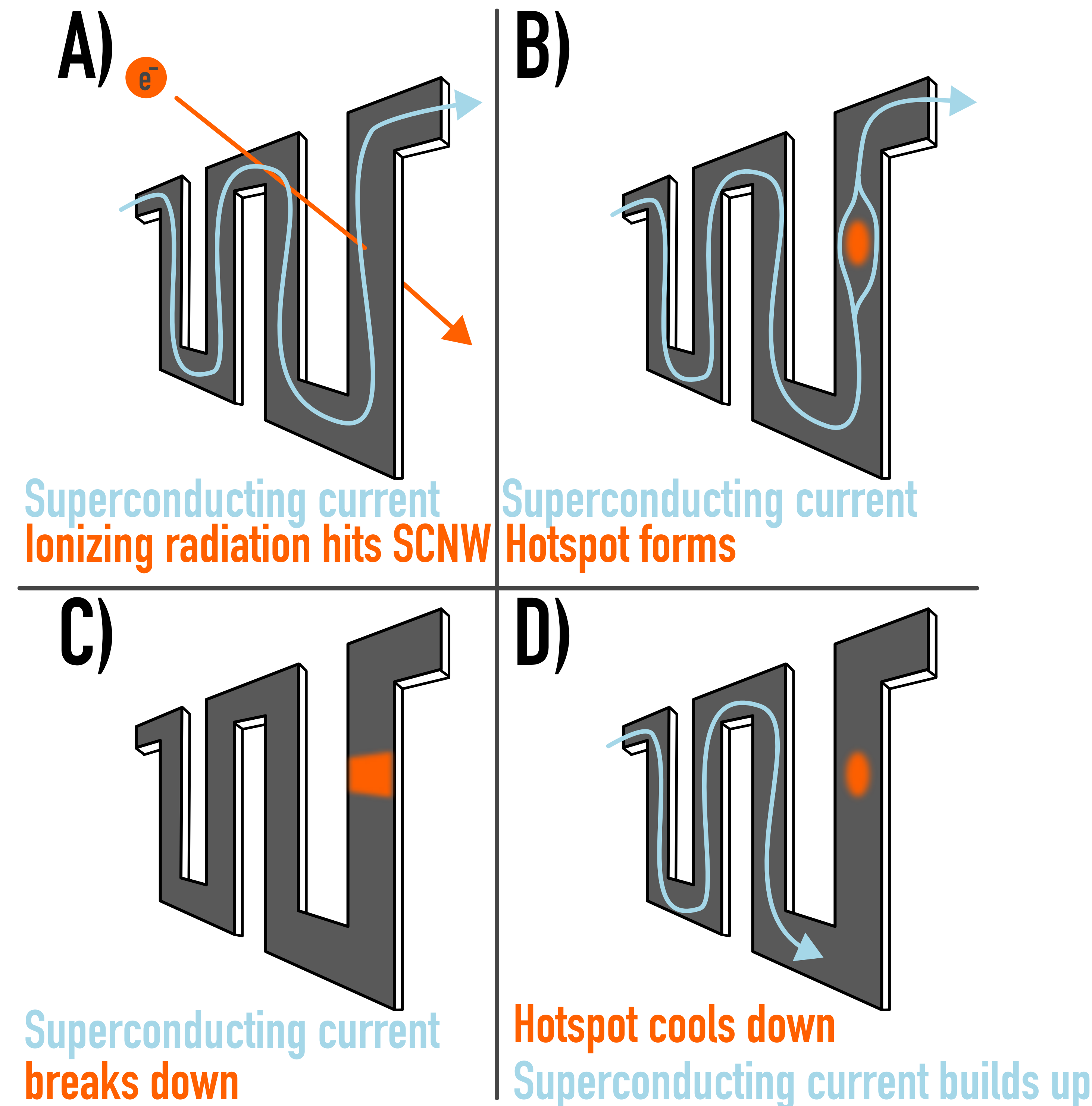

Superconducting Nanowires

- Superconducting nanowire provided from Quantum Opus, including aluminium coating
- Limited size; requires development of electron focusing system

Felix Benkel MSc

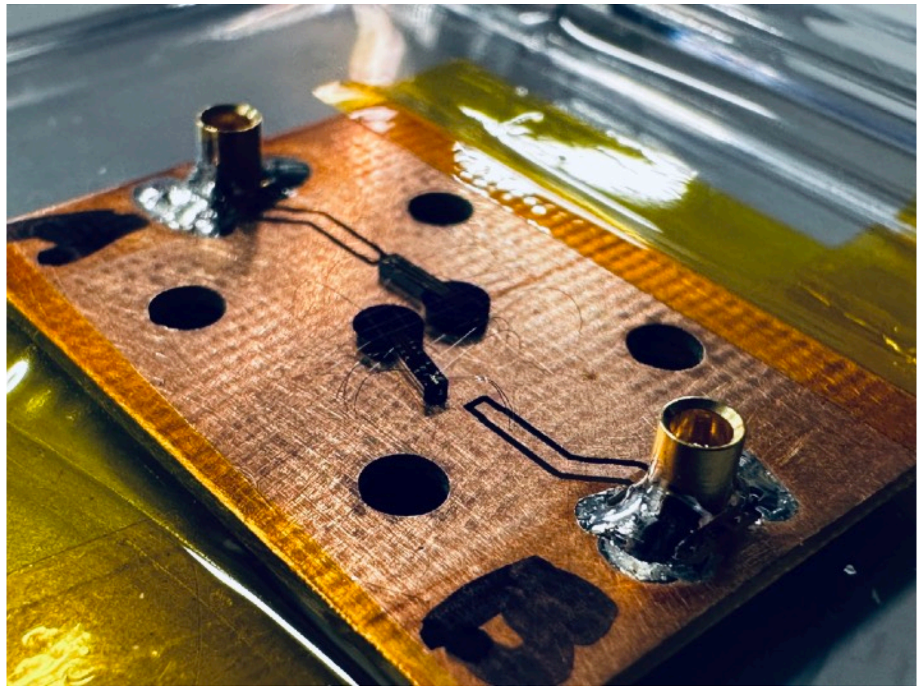

Superconducting Nanowires

- Superconducting nanowire provided from Quantum Opus, including aluminium coating
- Limited size; requires development of electron focusing system

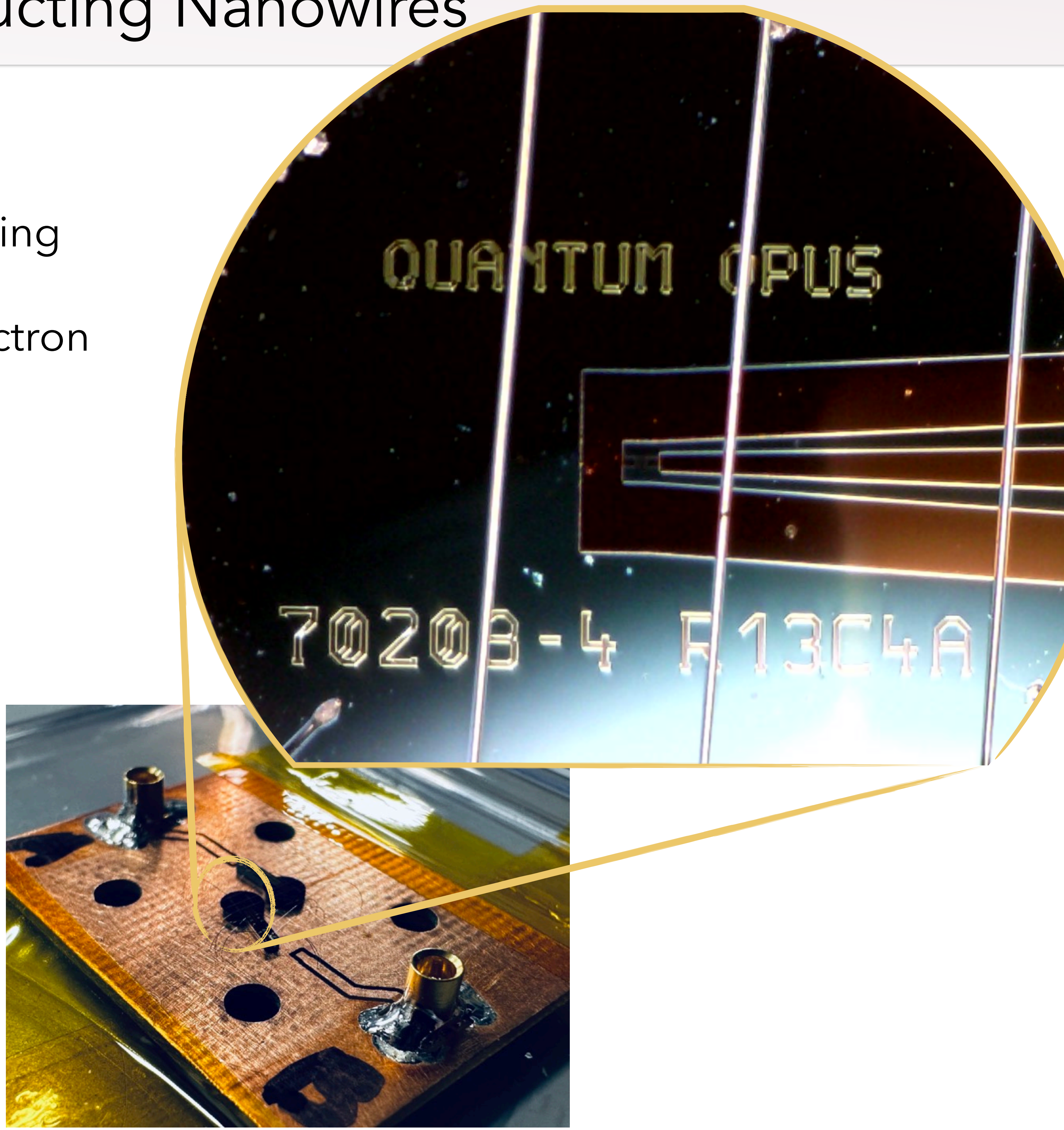

Felix Benkel MSc

Superconducting Nanowires

- Superconducting nanowire provided from Quantum Opus, including aluminium coating
- Limited size; requires development of electron focusing system

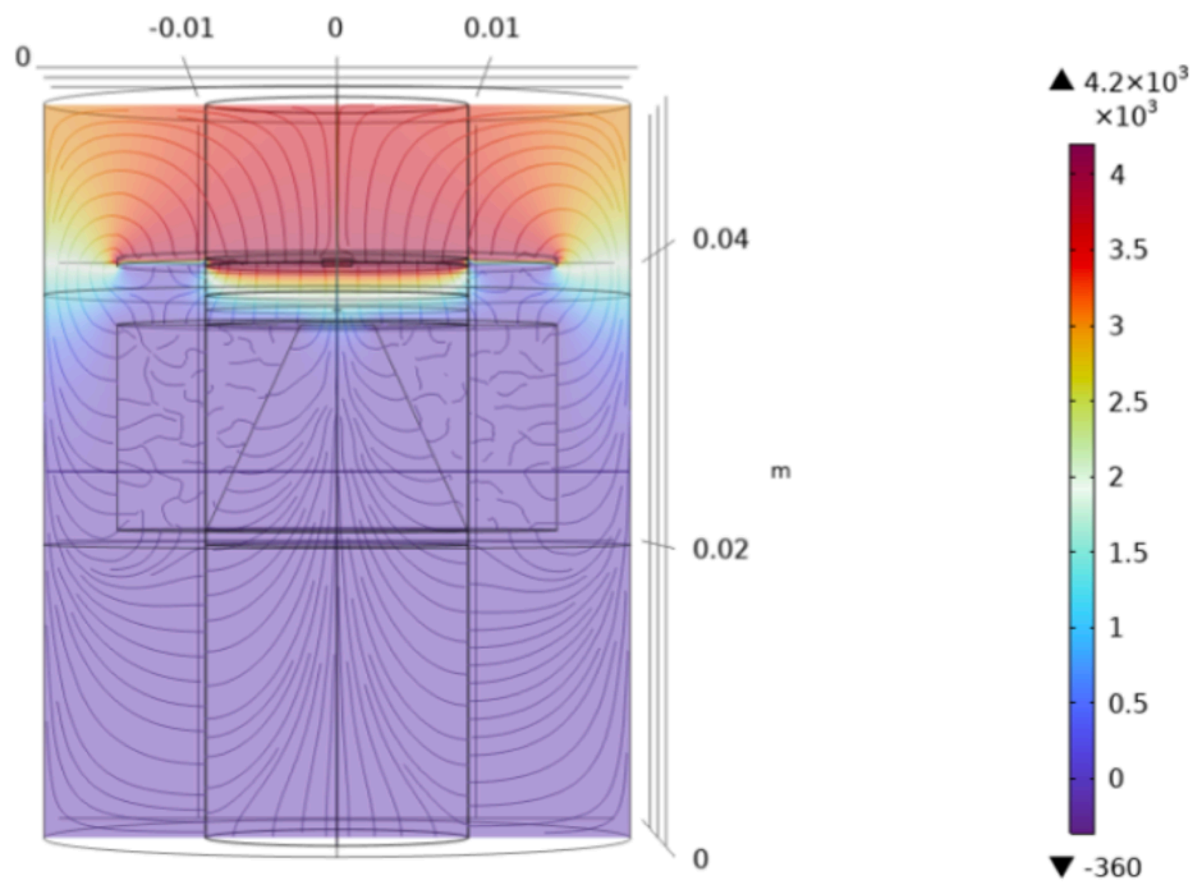

Felix Benkel MSc